Diffusion of Ozone Gas with Bubble Column in Turbulent Flow

By Pierre-André Liechti, MSc. Swiss Federal Institute of Technology Lausanne
Regensdorf, Switzerland

Co-author Prof.-Dr. Robert Hausler, École de Technologie Supérieure, University of Québec
Montréal, Canada

Co-author Étienne Bérubé, MSc.A., École de Technologie Supérieure, University of Québec,
Montréal, Canada




ISBN-13 : 978-2-9822819-0-5
Dépôt légal, Bibliothèque et Archives nationales du Québec, 2024.

01/08/24

Table of Content

1. Acknowledgement

It shall be mentioned that the authors collaborated in many projects with scientists, process-, chemical- and electrical engineers as well as other process specialists in this field. Their impact on the scientific and process engineering content addressed in this document is fundamental.

Among these People, we would like to especially express our thanks and gratitude to late Robert Cabana, late Patrick Cejka, Tony Di Schiavi, Richard Fontaine, Luc Tremblay, Gisella Gesuale and Luciano Paolini. Our thanks also go to Ozonia Infilco-Degrémont, especially François Février and Ali Erfani.

2. Preamble

The content of this essay is chemical engineering knowhow, based on science and scientific facts, on experience, observations, thoughts, and their interpretation, qualitative and quantitative understanding of physical phenomena involved and observed. The authors have been working together in a scientific–engineering collaboration for more than 30 years in the field of ozonation, combined with other treatment technologies, for water, wastewater, leachates of landfills, etc. Another background of the authors is their experience in design and operation of Wastewater Treatment Plants, particularly activated sludge systems and biological filtration. Both authors have also focused their work on optimization of diffusion systems for air, oxygen, and ozone in water, wastewater, and leachates.

Although applied to transfer from a gas phase & diffusion of ozone in wastewater, the process and associated engineering design developed in this document can be applied to any other gas, even liquid, to be diffused into any fluid, provided Full Turbulence, as defined later, exists in this fluid and the diffusion and chemistry parameters are well known, qualitatively and quantitatively. This is the case for ozone to be introduced into water or wastewater for reaction with well identified components and tasks, as will be demonstrated in this essay.

The main project that finally led to writing this document already started at the beginning of the 1990s and lasted until the end of the 2010s. Universities of the Province Québec in Canada collaborated intensively with developing and providing the scientific basis necessary for a project of such a magnitude and importance [1].

The author’s first involvement with diffusion was the improvement of the efficiency of oxygen transfer from air introduced with porous diffusers into activated sludge, with the “Counter Current Aeration” technology developed by Schreiber Kläranlagen from Germany at the end of the 1960s.

Another interesting research field of large-scale application was the use of Softwood Granular Activated Carbon as biological support for the treatment of secondary wastewater in an aerated bioreactor. The purpose of this research was to investigate the effect of the large pores existing in these particles for the support and development of biomass, as opposed to the large active surface provided by the very large number of micro pores of traditional activated carbon. This experiment was performed in the late 1970s at the wastewater treatment plant of the city of Lausanne, Switzerland.

The Author was also deeply involved in the development and implementation of the applications of the ozone and oxygen technologies for Clay-Kaolin Bleaching, in the USA and Ireland, and pulp bleaching in the USA, Canada, Japan, Austria, New Zealand, Australia and Brazil. The fundamental requirements were homogeneity and isotropy to be generated by forced turbulence for the bleaching and/or precipitation reactions with ozone and oxygen on the particulate level, Clay-Kaolin Particles and Wood Fibers, to guarantee quality and mechanical solidity of ceramics and paper. The application of ozone for pulp bleaching demanded a partial pressure of ozone of up to almost one atmosphere and was controlled in such a way as to make sure that ozone would act in its molecular form O_3. To this aim, the Author wrote a patent describing a technology for ozone gas compression without losses. This technology was applied in medium consistency (slurry with 10 % pulp) pulp bleaching with ozone. With oxygen the situation for pulp was trickier, in the sense that the reaction path of oxygen in the presence of organic matter, say lignin, involved oxygen radical species, so with the risk of damaging mechanically the fibers.

Fully turbulent, homogeneous, and isotropic plug-flow chemical process reactors were of the essence and had to be designed accordingly. The Author collaborated to achieve this aim with USA and EU suppliers of mixers for Clay-Kaolin as well as pulp slurries and compressors for ozone and oxygen. For reasons of confidentiality, it is not possible to cite references. The experience so gained shall be used in the development of the ozone and oxygen diffusion process proposed in this document.

Facts, observation, and interpretations, related to in many scientific and technical books and publications, have been read and analyzed to confirm (or contradict) and support the facts presented in this document. Descriptions, approaches, argumentation, and explanations are developed in this essay in necessary detail so to make sure that a safe and reliable Chemical Engineering Design of a Bubble Column for Ozone and Oxygen Diffusion and Reactions in a Fully Turbulent Water Flow is possible.

The thread leading through this text consists of the scrolling of the thoughts and analysis of scientific and process technical facts, as they appeared and came to mind in course of developing this subject and were identified while consulting the literature. The literature proposes many papers and essays dealing with the scientific approach to the problem of turbulence and turbulent gas-liquid bi-flow. Many mathematical methods, all based on the Navier-Stokes Equation, are presented, and developed. This essay proposes a Process Engineering Design Method with equations and correlations stemming from the well-established scientific evidence, allowing for a reliable design of an ozone diffusion system operating in a water/wastewater flow with fully turbulent field.

The proposed design method is based on basic physical chemical processes, meaning that it has a general engineering character. It can be adapted to any two-phase flow gas-water or any other liquid of low viscosity, provided that the correct values of the basic physical parameters and constants are used.

3. Natural and Forced Turbulence

In chemical reactors, hydrodynamic and hydraulic homogeneity as well as isotropy are generally fundamental requirements. Homogeneity and Isotropy entail:

1. no dead zone in clearly identified zones inside the reactor, meaning physical homogeneity in hydrodynamics and hydraulics all over these zones, in translations and rotations.

2. concentrations of reactants, chemistry, and kinetics of reactions between reactants equal in all the smallest reactor minute volume identifiable in the engineering design method, for instance a gas bubble and its direct surroundings.

As already mentioned in the Preamble, turbulence is used for the chemical treatment of kaolin and pulp slurries with ozone to provide the indispensable homogeneity and isotropy for generating a final product with the necessary homogeneous quality on the particulate level. In the treatment of these slurries, other chemicals in addition to ozone are used in similar manner. These mentioned slurries, as well as other industrial sludges and slurries, have consistencies ranging from 10 wt% of dry pulp to more than 50 wt% for clay. The consequence is a very high viscosity. Generating Natural Turbulence “NT” with a large kinetic energy of a high viscosity slurry for providing the necessary turbulence for homogeneity and isotropy is practically not possible. Therefore, Forced Turbulence “FT” is the solution to this requirement.

Turbulence is caused by mechanical means, generally within a series made of fully mixed impeller reactors, called Continuously Stirred Tank Reactors “CSTRs”.

However, it is also a fundamental requirement for guaranteeing chemical reactor homogeneity and isotropy that the dosing and distribution of the chemicals into the product to be treated also be homogeneous. Due to the high density of the slurries, slenderness and large height of such reactors are fundamental requirements, pressures at the bottom of such reactors are therefore rather high. For reasons of confidentiality, it is not possible to go more into details of such reactors in this essay.

The chemical products can be introduced into the slurry, either dissolved in a liquid, mostly water of industrial quality, or by means of a carrier gas, or both combined. With ozone, all three technologies are applicable. However, since most ozone generators operate at low pressure, less than a bar gauge, efficient compression of the ozone carrier medium is sometimes of the essence. In the case of gaseous chemical product, for example ozone, supplied with a gas (oxygen or air) as the carrier fluid, a system’s pressure up to several bars gauge is a requirement, to provide the necessary optimum volumetric gas to product ratio.

Such total dual equipment for the treatment of industrial slurries needs a high-power supply, generates heat through inter-particulate and with reactor wall friction. Moreover, abrasion and corrosion of equipment occur, leading to problems of product quality if the design is not done with the necessary correct engineering and high maintenance. The operating costs, operation and maintenance are consequently high.

The most important information to be provided by these industrial application examples of Forced Turbulence “FT” is the demonstration that the products so generated have the required high quality. Examples are high quality, mechanically and electrostatically robust papers and ceramics.

To provide quality to a consumer product, homogeneity and isotropy are fundamental requirements for any treatment reactor when safety and health of the consumers and the environment are concerned, for example disinfection and removal of pollutants from potable water and wastewater.

Water and wastewater, with a dilute solution of constituents to be treated chemically and dosed reaction chemicals, have a low viscosity. Hence Natural Turbulence “NT” can be considered. In most water and wastewater treatment cases, flows can be made turbulent with standard equipment, construction, and mechanical works. NT can be considered as Natural Intrinsic Energy. This energy is available almost for free and can therefore be used to provide homogeneity and isotropy inside a treatment reactor.

The purpose of this document is to address an Engineering Design Method for Natural Turbulence “NT” Homogeneous and Isotropic Reactors, applied to the example case of disinfection of and elimination of micropollutants from wastewater, a worldwide concern. This method is using the large information feedback from industrial applications of ozone with Induced Turbulence “IT” as presented here above.

Applying such an NT Engineering Method allows for the design of a hydrodynamically, hydraulically, and chemically well-defined bubble column chemical reactor, leading to smaller, more efficient, and less costly equipment. Other technologies, such as Packing Towers filled with Raschig Rings generating sort of macro-turbulence of the size of the packing elements are also homogeneous and isotropic. Examples of Packing Towers with Raschig Rings for potable water treatment operated or still operate in Germany and Québec, Canada.

The Author had the privilege to be involved in the design of all the examples of application of mentioned in this paragraph. The co-Author‘s scientific contribution and advice are of great benefit as far as chemistry and practical experience.

4. Introduction

Focus of research on ozone technologies is increasingly aimed at the abatement and inactivation of acute and chronic toxicity of water and wastewater.

Acute toxicity is generally caused by pathogenic microorganisms, such as viruses, prokaryotes (bacteria) and eukaryotic protists (protozoa, algae, and fungi) [2]. Most of these microorganisms are protected against lethal or unfriendly environment by a carapace, a protection wall or as spores. Acute toxicity can be the cause an epidemic and pandemic outbreak (e.g. the 1993 Milwaukee cryptosporidiosis outbreak).

Chronic toxicity is the consequence of a slow process, harmful and generally lethal in time to the human, and quite rapidly harmful to some flora (algae) existing in natural waters. Chronic toxicity is the result of the presence of a cocktail of poisonous micro-pollutants “MPs” in minute concentrations in natural waters resulting from agricultural chemicals, such as pesticides (e.g. chlorothalonil), and in treated and untreated wastewater inflows. The main sources of MPs are personal care products “PCPs”, pharmaceuticals, pesticides, drugs, and other chemicals, generally used for the protection and the integrity of the human and other useful goods for our society. However, these compounds are used in potentially harmful excess with respect to their required action dose. All these MPs are disposed of in industrially and domestically used waters or groundwaters, and so pollute natural waters. These products are generally very stable chemically and not at all or only very slowly biodegradable by nature and in a modern Wastewater Treatment Plant “WTP” fitted with extended aeration activated sludge and/or biological filtration processes. Some pesticides end up in their action as extremally stable and harmful by-products, as was discovered with chlorothalonil.

Acute and chronic toxicity can be made inactive by partial oxidation, i.e., disinfection. The relevant parameter for abatement level of acute toxicity to be achieved by partial oxidation in water and wastewater is the “CT”, meaning the average Concentration “C” of the disinfectant acting during the Time “T” on the microorganism. Pathogens must be “killed” by disinfection, their physical integrity must be harmed by destruction of their carapace, i.e., lysis, in order avoiding a possible reactivation by self-repair.

The relevant parameter for the inactivation of MPs by partial oxidation is the variable concentration over time “Cϴ” of the oxidant acting during a time “T = ϴ”. Overall kinetics, chemical and diffusional, of the reaction rate are of the essence in such processes.

Ozone is one oxidant among others able to simultaneously abate acute and chronic toxicities. Experience shows that in some cases of disinfection of wastewater with ozone, the kinetics of MPs abatement is faster than that of acute toxicity (Fig. #1) [1].

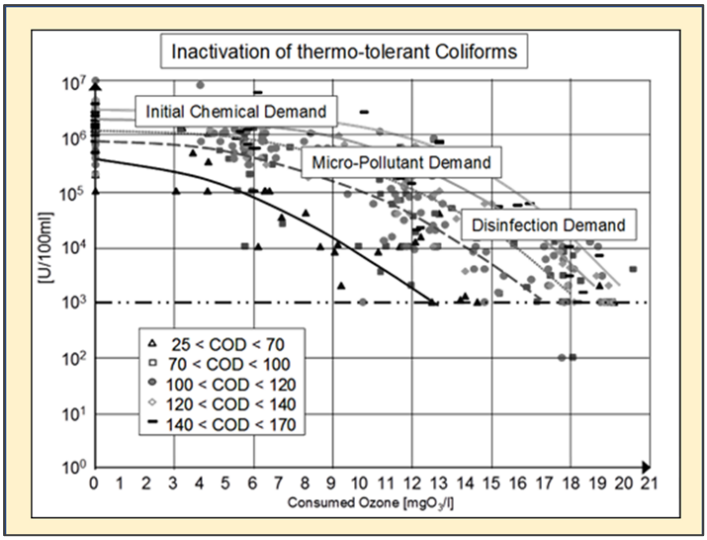

Fig. # 1 ***Domains of Action of Ozone during Disinfection***
Retrieved from Gesuale et al. [1].

Excess oxidation action on MPs can also result in the formation of Disinfection By-Products “DBPs”, which can be more toxic than the original MPs. An example of this phenomenon is seen with the upper and lower curves of Fig. #2. The influence of ozonation on chronic toxicity was evaluated with the Luminotox Method. The Luminotox Method is a rather fast method working with Photosynthetic Enzymatic Complexes “PECs” which, when stimulated by light, emit fluorescence, and express within minutes a decrease in fluorescence parameters as result of the presence of toxic compounds contamination, showed as [%] inhibition or Luminotox Signal [%]. Therefore, control and mitigation of the formation of DBPs such as bromates and more poisonous micro-pollutants can be a drawback to any disinfection technology, in particular ozone diffusion, if not designed and engineered correctly [3].

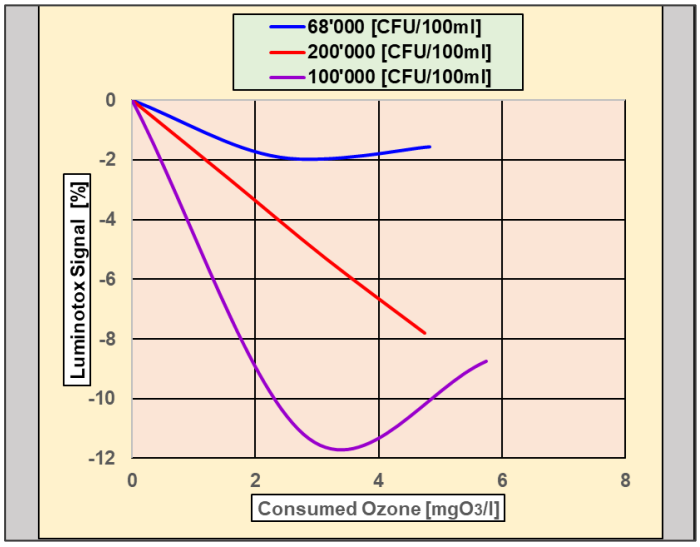

Fig. # 2 ***Chronic Toxicity Abatement measured with Luminotox***

5. Basic Considerations about Turbulent Bubbly Flow

Together with its generation, diffusion of ozone into water and wastewater is the heart of the technology. Optimization of ozone diffusion technology towards better engineering, operation performance and safety, both for energy and reaction efficiencies, is therefore of the essence.

Ozone is generated inside an Ozone Carrier Gas "O_3CG" by means of an electrical machine with a power semi-conductor electronics driven Ozone Generator "O_3G". The nature of the O_3CG (air or oxygen) as well as the concentration at which ozone is generated in the O_3CG are fundamental Design Parameters. The O_3CG is introduced and diffused into water or wastewater with a Bubble Column "BC", generated either directly with porous diffusors, or indirectly by means of an Ozone Gas Carrier Water Flow "O_3CWF".

The Hydraulic and Hydrodynamic Pattern "HHP" of a Bubbly Flow "BF", consisting of a Water/Wastewater Flow "WF" spread inside the BC to be treated with ozone, has a fundamental importance with respect to optimization of the Ozonation Reactor "O_3R". The HHP of the WF into which a BF is introduced can be, Laminar "L", Turbulent "T" or Fully Turbulent "FT" as defined as per the Moody Diagram (Fig. #3). Keeping the integrity of the HHP of the WF entering the O_3R inside the BC is of fundamental importance.

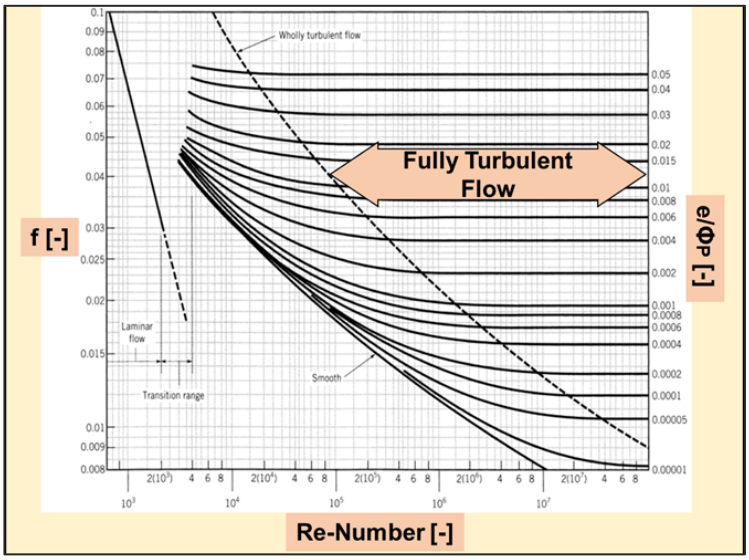

Fig. # 3 *Moody Chart*

The Moody Diagram is a chart that produces a value for the Conduit Darcy Friction Factor "f" [-] depending upon the Water/Wastewater Flow Reynold Number "Re_L" [-] and the relative Roughness "e/Φ_{hyd}" [-] of the conduit as a parameter (equation 5-1).

$$Re_L\,[-] = v^{\circ}L\,{}^{*}\phi_{hyd}/v_L \qquad \text{(Equation 5-1)}$$

where v° L [m/s] = O_3R superficial water velocity.
Φ_{hyd} [m] = conduit hydraulic diameter;
v_L [m^2/s] = kinematic viscosity of the water/wastewater.
e [m] is the absolute surface roughness of the conduit.
In fact, the Moody Diagram applies to the water/wastewater flow inside the O_3R in absence of the BC. However, its signification is also valid to a BF, under the conditions of homogeneity and isotropy, as will

be discussed later. Other HHP features are Fully Mixed “FM” and Plug- or Piston-Flow “PF”. As will be shown later in this essay, an O_3R with T- or FT-HHP can be considered as Plug-Flow Reactor “PFR” [4]. Other characteristics of fundamental importance are:

- Homogeneity meaning no preference in translations.
- Isotropy meaning no directional preference in the three dimensions “3-D” (rotation) of the BF.

According to Professor Michel Roustan of the International Ozone association IOA, the highest disinfection efficiency is achieved with a Plug-Flow Reactor “PFR” (IOA-EA3G conference, Lausanne 2018).

Following the Covid pandemic, Wastewater Disinfection has gained importance. Recent Literature provides the following information, among others. The EAWAG Institution, a department of the Federal Institutes of Technology in Zürich and Lausanne, Switzerland, as well as other similar research institutes, have proven the presence of the virion (non-active form) of the Covid Virus in treated wastewaters.

The IOA-EA3G Webinar of June 2021 presented following facts [5, 6]:

1. The Covid Virus is an enveloped virus, as opposed to non-enveloped viruses.
2. Its genetic material is double protected by an outer envelope and a nucleocapsid.
3. As far as disinfection is concerned, a simple lysis of the envelope is not sufficient.
4. To inactivate the genetic material of the virus, the nucleocapsid must be sufficiently damaged to guarantee full inactivation of the genetic material of the Covid virus.
5. Data presented at this online seminar indicate that a higher O_3-CT is needed for efficient disinfection, when compared with standard ozone disinfection of viruses.

6. Items developed in this essay

This essay investigates the engineering aspects and needs for design of an efficient and optimized O_3R consisting of a combination of a Fully Turbulent Hydraulic and Hydrodynamic Pattern “FT-HHP” and a Turbulent-HHP “T-HHP”. Designing and implementing a single FT-HHP is sometimes not completely possible, for reasons of local site conditions or works against optimization and can lead to excess construction costs.

It addresses the following items:

1. Summary of classical O_3Rs with BC.
2. Residence Time Distribution “RTD”.
3. Turbulence definition from an engineering point of view with an emphasis set on T- & FT-HHP.
4. Characteristics of a Turbulent Flow needed for the purpose of correct Engineering Design
    a. Conditions for establishment and existence of a stable T- & FT-HHP.
5. Physical representation of T- & FT-HHP.
    a. Mathematical formulas and correlations developed based on established scientific and practical research facts (no algorithms are presented).
6. Turbulent and Fully Turbulent Bubbly Flow “TBF” & “FTBF”, consisting of a BC generated inside a fully turbulent water flow (FTWF) and a turbulent WF (TWF)
    a. Conditions for generating and sustaining a homogeneous and stable BC in a FTWF and TWF.
    b. Bubble breakage and coalescence
    c. Shape stability of the bubbles inside a FTBF and TBF.
7. Effect of Turbulence Intensity “TI” on the behavior of the BC
    a. generated and homogeneously dispersed inside a FTWF and TWF
    b. the Reaction Kinetics of Ozone “O_3RK” with the reactants dispersed in a FTWF and TWF.
8. Effect of Turbulence Intensity “TI” on Diffusion Kinetics “DK” of the Ozone and the constituents of the O_3CG.

The focus of this essay is directed towards the case of Wastewater “WW”. We continue with a comprehensive description of a FTWF and a TWF. A thorough investigation, understanding and description of turbulence is deemed first as fundamental to provide the solid base for this Engineering Approach on Diffusion of Ozone Gas with Bubble Column in Turbulent Flow. Next, we present a qualitative and quantitative description of dynamic diffusion in a FTWF and a TWF, the so-called Eddy Diffusion “ED”. Then we present a physical description of a BC generated inside a FTWF and introduced into a TWF, addressing its stability under the influence of the strong TI of the FTWF and TWF where this BC is generated and installed, respectively.

Another item is the qualification and quantification of the scales of size and energy of the dynamic turbulence inside the voids in between the bubbles of the FTBF & TBF in order to characterize ozone diffusion. Then we propose a qualitative and quantitative description of the diffusion path of ozone from the inside of the ozone gas bubble into the bulk of the inter-bubble liquid where the reactions with ozone take place. This first approach assumes that the O_3CG is inert and practically non soluble in wastewater, only partially true with oxygen, but considered as acceptable when air is the O_3CG. The model which we will use is the “Surface Renewal Model” as proposed by Danckwerts [7], which fits well with T and FT hydrodynamic conditions surrounding the bubbles.

In the case of Oxygen as the O_3CG, we address the issue of the solubilization and diffusion of oxygen into the FTWF and, if in excess concentration, its negative effect on the integrity of micro-organisms. Finally, we will present results with a design program developed for such a situation based on a typical case. As suggested by Prof. Michel Roustan on occasion of the IOA Conference in Lausanne in 2018, we will verify this case with the second Damköhler Number "Da_{II}" linking the Chemical Reaction Rate "CRR" with the Diffusive Mass Transfer Rate "DMTR" [8, 9].

We will also consider the important fact, as proposed by Batchelor [10], that our system is in a statistical equilibrium. Indeed, our system is a closed statistical system in which the average values of all the physical quantities characterizing the state are independent of time in the reactor stages as defined in the design, item addressed later in this document.

The technical and scientific content of this document results mainly from a study with 3 different pilot tests on the same WW, and preliminary designs, starting 1991 and lasting until 2007, with the aim and achievement of successfully qualifying ozone against UV for the largest ever planned and under construction ozone plant for disinfection of a wastewater plant effluent.

7. Classical O_3Rs

Due to its rate and conduit size, the Water/Wastewater Flow "WF" circulating in channels and pipes of all municipal & industrial O_3Rs is basically turbulent, even fully turbulent, and the BF is not considered. The Re is in practically all cases much larger than 10 000, see Fig. # 3. O_3Rs are often made of an intake vertical chamber, the Ozone Diffusion Chamber "O_3DF", where the O_3CG is introduced and fast Ozone Reaction Kinetics "O_3RK" take place, followed by an Ozone Reaction Chamber "O_3RC" where the slower O_3RKs are completed (Fig. # 4). Such dual reactors in series can also be implemented.

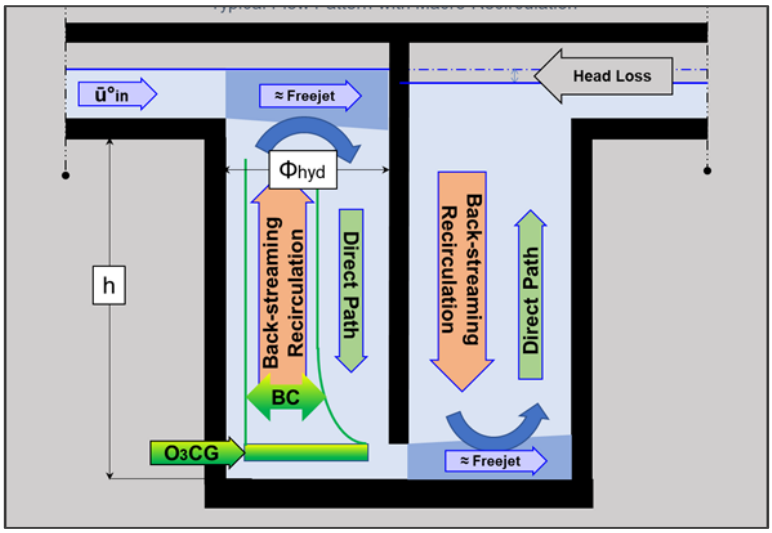

Fig. # 4 *Ozone Diffusion with single Bubble Column*

Input channel and pipe flows are always Turbulent Homogeneous and Isotropic "THI". This means the HHP of WF in an O_3R should in fact be THI, but the physical reality shows they are not :

- the change from horizontal to vertical input flow direction adds macro-turbulence into the hydrodynamic system within a very short las of time.
- this macroturbulence will prevail in the vertical reactor for a certain non-negligible time (see Eddy Decay Time later in this document).

Ignoring for the moment the BC, the horizontal inflow to this first chamber generates a sort of an asymmetric free-jet against a vertical wall, whose momentum induces strong back-streaming and macro-recirculation [11]. For achieving full homogeneity in this chamber, axial-longitudinal dispersion induced by the turbulence within the different turbulent zones needs time, dependent of their respective Re.

Not considering for the moment the influence of the BC, experience shows that the corresponding Entrance Length "EL", at the end of which homogeneity and isotropy are again achieved, is approximately equal to 10 diameters (square or circular) of the vertical chamber. This means that a chamber with a Φ_{hyd} of 2 [m] diameter should be 20 [m] deep before it becomes homogeneously T or FT, independent of the ratio of O_3R-Wetted Height "h_w" to Hydraulic Diameter Φ_{hyd} [m] (h_w/Φ_{hyd} [-]). An EL over 10 times the Φ_{hyd} [m] is necessary to obtain the homogeneity of the turbulent flow. However, this condition is rarely achieved in typical O_3Rs. However, it is also a fact that any item creating a sufficiently strong hydraulic

disturbance, such as a BC can shorten this EL, if adequately conceived with sufficient added mixing energy. Within the different flow zones, the HHPs are necessarily T or FT, except in the dead zones.

A BC not homogeneously generated at the bottom of the chamber will amplify the phenomena of macro-recirculation in the whole reactor. More so, a BC generated at the bottom of the O_3R generally does not have enough energy (expansion of the O_3CG, mixing energy) to overcome the macroturbulence induced by the horizontal inflow. Such a situation exists in BCs equipped with individual porous diffusors (Fig. # 5).

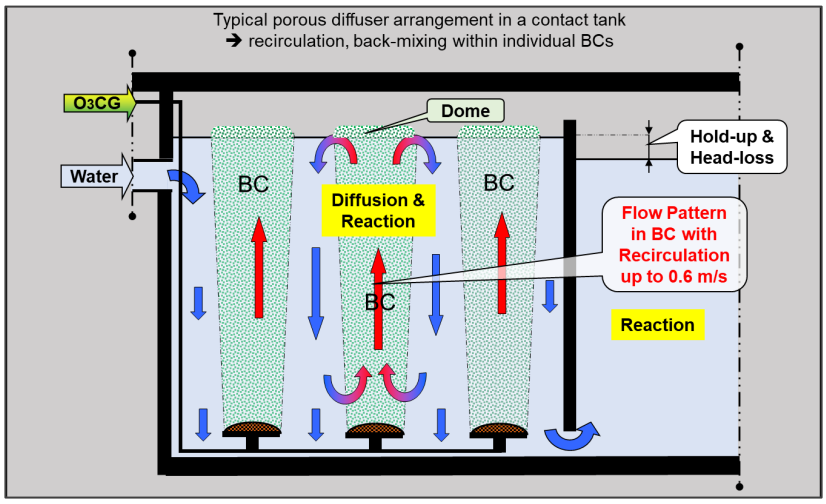

Fig. # 5 *Ozone Diffusion with individual Bubble Columns*

Due to the vertical water entrainment with friction by the vertical bubble gas flow of the individual BCs, a vertical upstream velocity of up to 0.6 [m/s] sets in, as measured experimentally. Compensation downstream recirculation takes place between the individual BCs of each single porous diffusor, in addition to the mean flow velocity. A bubble with an average Sauter diameter $\Phi_{B_{32}}$ of 3 [mm] has, in a still environment without any turbulence, a free terminal ascending velocity, or slip velocity $v°_B{}^{\infty}$, of around 0.3 [m/s]. An actual absolute ascending velocity of approximately 0.9 [m/s] sets up itself inside the individual BCs, leading to a much shorter residence time for diffusion, made evident by the dome generated at the top of the individual BC. This principle is applied in Activated Sludge Aeration systems to avoid settling of the biomass. Fig. # 6 shows two examples of O3Rs with porous diffusors, one with a modern diffusor layout (left image) and an older one (right image).

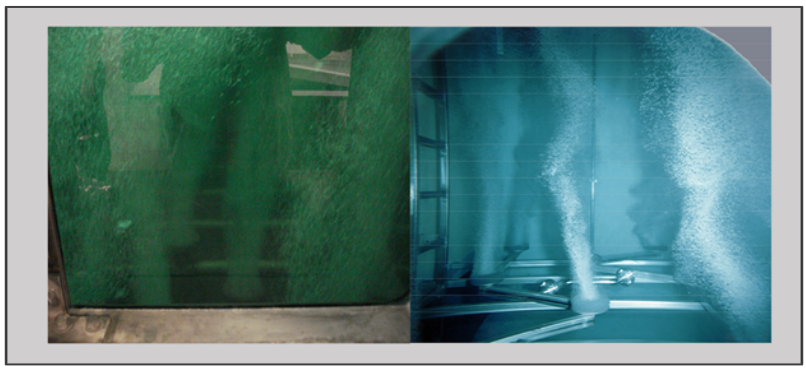

Fig. # 6 *Ozone Diffusion with Porous Diffusors*

Due to their dimensions the 2 O_3Rs presented on Fig. # 6 should be turbulent, because the influent stream is turbulent. Hence, Turbulent Dispersion Diffusion “TDD” should act on the individual BCs and disperse the bubbles radially more broadly. However, there is little evidence that this is the case, due to lack of eddies of the size necessary to disperse the bubbles radially. It can therefore be deduced that in between the individual BCs, in the bulk of the water flow, the TDD acting on dissolved components diffusing out of the bubbles, such as ozone, is slowed down by this situation. This therefore means that there is little homogeneity of ozone diffusion in these O_3Rs, even though there is some macro-recirculation between the individual BCs. Such O_3Rs are certainly neither homogeneous nor isotropic.

8. Residence Time Distribution (RTD)

Residence Time Distribution “RTD” is a fundamental parameter for the design of an efficient O_3R. Since disinfection is designed based not only on reaction kinetics and average values, but also on residence time, the shape of RTD is of the essence. Fig. # 7 is an example of RTD measured on the O_3R of a pilot plant treating wastewater (see picture on page #1 & Fig. #8 hereafter).

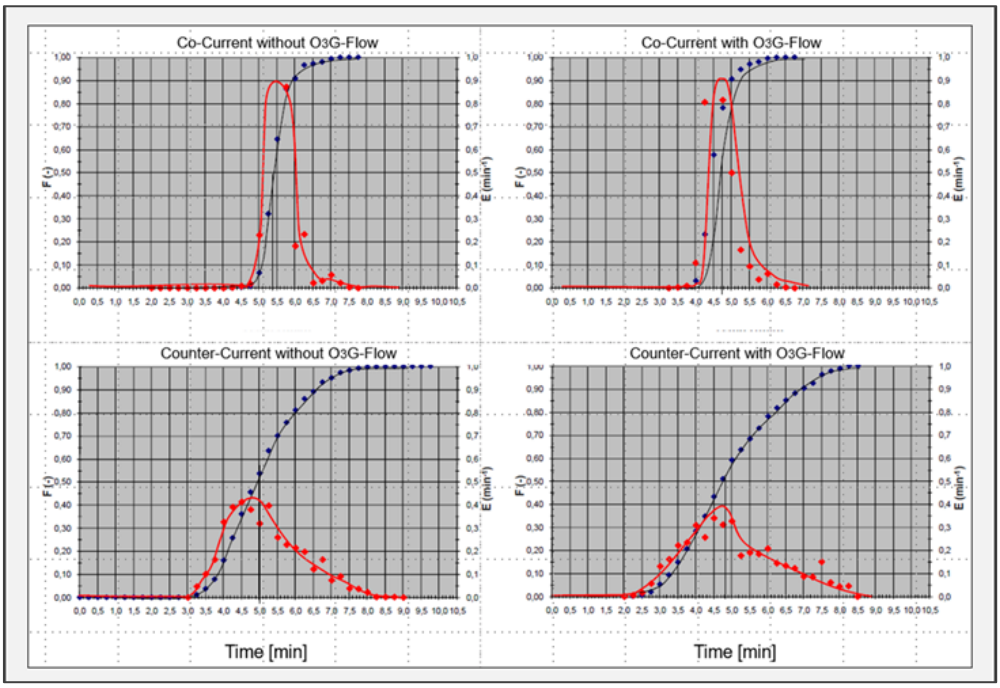

Fig. # 7 *Residence Time Distribution* (h/Φ = 47)

The system is moderately Turbulent and Homogeneous, but not fully isotropic, because it is not FT. Both Co-Current “CC” (meaning both O_3G and WW-Flow upwards) and Counter-Current “CtC” (meaning O_3G-Flow upwards and WW-Flow downwards) BC patterns were tested for RTD, with and without O_3G-Flow (Fig. # 7). In the CC-Flow, with moderate turbulent pattern and a large ratio h/Φ [-], with or without O_3G-Flow, the RTD shows a narrow form with a small standard deviation. This shape approaches that of a PF-Flow. This also shows that the O_3G-Flow has little influence on the HHP of the total two-phase gas-liquid volumetric flow, i.e., that the energy released by O_3G-Flow is not sufficient to alter the initial almost PF-pattern of WW-Flow. The large ratio h_w/Φ_h [-] >> 10 also leads to the installation of a homogeneous BF. The turbulent wake immediately upstream of the porous diffusor helps the establishment of the homogeneous BF.

The situation is different in the CtC-Flow modus. The RTD is flatter and broader, indicating a larger standard deviation, but still quite symmetrical. Again, there is no noticeable influence of the O_3G-Flow. The flatness (Kurtosis) of the RTD results from the porous O_3G-diffusor installed at the bottom of the column. The turbulent wake exists downstream of the diffusor and has therefore no influence on the O_3G distribution. In fact, the O_3G cylinder amplifies the phenomena of upwards push and macro-recirculation. Table 1 summarizes the physical and design parameters of the pilot plant described in this chapter.

Table 1 Physical parameters of the pilot plant

Characteristics of the O_3R Physical Parameter	Symbol	Value	Unit	Comment
Number of Columns	-	3	[-]	
Operation modes	-	-	-	Co- and counter-current
O_3R-Diameter	Φ_h	0.15	[m]	
O_3R- wetted Height	h_w	7.05	[m]	
Ratio height to hydraulic diameter	h_w/Φ_h	47	[-]	
Wastewater flow	$V_L°$	2.0	[m^3/h]	Primary effluent
Re-Number without O_3-Gas	Re_L	4 700	[-]	Moderately turbulent
Ratio entrance length EL to h_w	EL/ h_w	=/> 10	[-]	Turbulent flow, not fully
Entrance length	EL	≈ 1.5	[m]	EL ≈ 10 Φ_h << h_w
Normal O_3G-Flow	$V°_{GN}$	0.1	[Nm^3/h]	Normal at Standard Conditions
Standard Temperature	T_{STP}	273.15	[K]	
Standard absolute Pressure	P_{STP}	100	[kPa]	

It would be wrong to disqualify the CtC-Flow Pattern in a scale-up process to design the large size plant since in the large size plant, the diffusion system would be different and optimized. From a process engineering point of view, a CtC reactor is basically more efficient as far as mass-transfer is concerned. Scale-up is the method using data obtained from pilot tests, together with laboratory tests, for the design of the full/industrial size plant [12]. It is therefore of the essence to organize pilot testing under sufficient variable conditions for the most important parameters and interpret, qualify, and quantify the data collected accurately. This method has been applied by the authors, when necessary, in the cases mentioned in the next paragraph. The Fig # 8 presents the 3-Column pilot plant described in Table 1 and used for the experiment presented in Fig # 7.

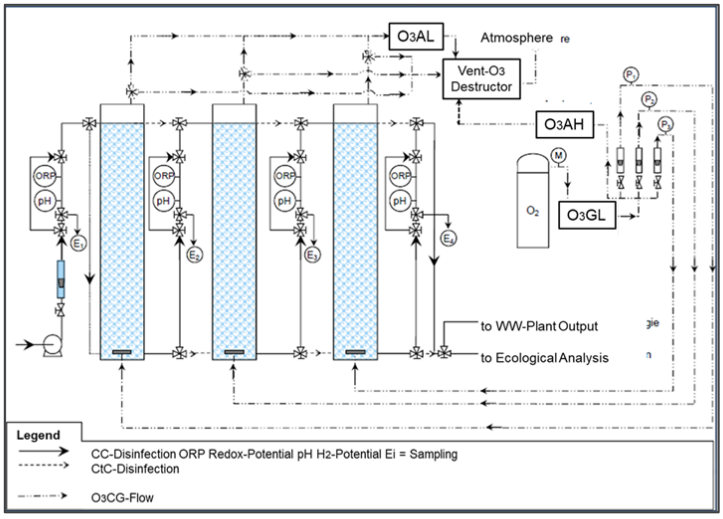

Fig. # 8 *3-Column pilot Plant*

9. Basic Experience

The authors have been confronted, within the course of their activities and work over some 30 years, with several different situations about the implementation of systems for diffusion of ozone, with oxygen and air as its carrier gas, in the field of potable water, primary and secondary wastewater and leachate treatment. In the last 20 years, their investigation and research activities, as well as design of systems, dealt mainly with disinfection and inactivation of micropollutants with ozone in primary and secondary effluents of industrial/domestic and combined wastewater treatment plants [1].

CC-BCs, in the upwards or downwards flow hydraulic pattern and CtC-BCs, with porous diffusers, hydro-injectors, radial diffusers, static mixers, perforated tubes and combinations have been evaluated in pilot plant tests. With consideration of the correct scale-up methods, these tests have generated data for the design and construction of large-scale systems. One situation of fundamental technological interest and importance was the testing of a WWTP Effluent with an ozone pilot plant made of a CC-BC inside a turbulent hydraulic-hydrodynamic downflow FTWF / TWF pattern (Fig. # 9).

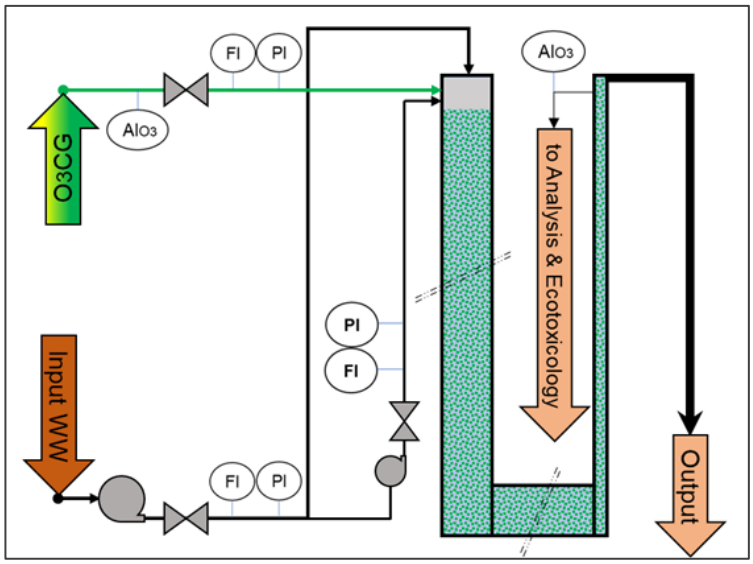

Fig. # 9 ***Fully Turbulent Pilot Plant***

The size and design of this pilot plant were selected to provide results making it possible to scale-up for the design of the much larger industrial scale system, i.e., with a scale-up ratio > 2 000 [-] [12]. Parallel to this special pilot plant testing procedure, the same water was tested with a conventional ozone pilot system consisting of BCs in series in a moderate turbulent HHP. A moderate turbulence consists of the hydrodynamic condition between laminar and fully turbulent. The moderate turbulent HHP is identified by its RTD as per Fig. #7 here above and its layout is represented on Fig. #8. Both systems gave the same results as far as the task of the ozone has been, disinfection and micropollutant inactivation.

However, the pilot plant with a combination of FTBF, respectively with TBF- and PF-patterns achieved these aims within an average water residence time of less than 60 seconds. It was completed without any residual ozone, neither in the system's off-gas, nor in the pilot plant effluent, provided no excess of the Ozone Dose c_{DO_3} [g-O_3/m^3] with respect to the Ozone Demand D_{O_3} [g-O_3/m^3] was applied.

Obviously, since the chemical kinetics were the same for both pilot systems, the so-called Turbulent Kinetic Energy “TKE” prevailing inside the FTBF/TBF-PF-O_3R was the process reason for such a fast-overall reaction kinetic. The fast kinetics are confirmed by the results communicated by Marc-Olivier Buffle in his thesis [13], where tests were conducted in a TF-PF-O_3R surrogate testing system on secondary and tertiary wastewaters of different origins and qualities. TKE is the energy which drives the so-called Eddy Diffusivity “D_E”, which is much faster compared to Molecular Diffusion “D_m”. From a process engineering point of view, this offers the advantage of designing a hydraulically and hydrodynamically well-defined system. Moreover, it can present an economical advantage because ozone systems can be more easily adapted to the restrictive conditions of the local plant site and also reduced in size. The size reduction may also result in an ozone dose reduction and therefore its costs.

This essay proposes a system design for ozone diffusion under well-defined hydraulic and hydrodynamic conditions, which also contributes to mitigation and control of Disinfection By-Products “DBP” formation, such as bromate.

10. Turbulent and Fully Turbulent Water Flow TWF / FTWF

The use of turbulence for the design of an O_3R requires a sufficient clear understanding of the physical phenomena involved. The format of this section is a scrolling obtained from consulting the literature. The purpose of this section is not to present a complete theory of turbulent flows. However, we present the physical status of a turbulent water flow with sufficient details so to describe a broad, safe, and solid comprehensive basis to be used for the engineering design of an O_3R with turbulent flow.

The basic references are Grassmann [14], Pope [15], Batchelor [10], Tavoularis [16], Fox et al. [17], Hinze [18], Laufer [9] and other authors. Reading out these references shows agreement of how to qualify and quantify turbulence for simple systems, such as shear free turbulence in free-jets or wakes and shear turbulence in tubes and pipes, i.e., the confined systems.

This section addresses and describes the physical facts, mathematical functions and experimentally verified correlations as they exist today, established with dimensional analysis which are the basis. These mathematical descriptions are applicable for precise, reliable and safe engineering relating to the design of ozone diffusion in a FTWF/TWF. Turbulence, physically a stochastic process which cannot be precisely described with linear differential equations, is today still under scientific investigation. The Navier-Stokes equations, statistics, as well as auto- and 2-point-correlations are the basis for a mathematical analysis of its behavior. Correlations are necessary for mathematically solving the problem.

Fundamentally, we are in this essay considering a flow confined inside a vertical conduit, cylindrical or square, with down-flow and/or up-flow hydraulic pattern. Moreover, the free-jet flow is addressed later in this essay. Ozone diffusion is implemented in such geometrical constructs. These are simple forms of a T- and/or FT-System for which results issued from available experimental and analytical research apply very well. The Reynold Number Re_L [-] characterizes the HHP of the water flow (Fig. # 10). Physically Re_L [-] stands for the ratio of the inertial forces to the opposing viscous forces acting on the water/wastewater flow.

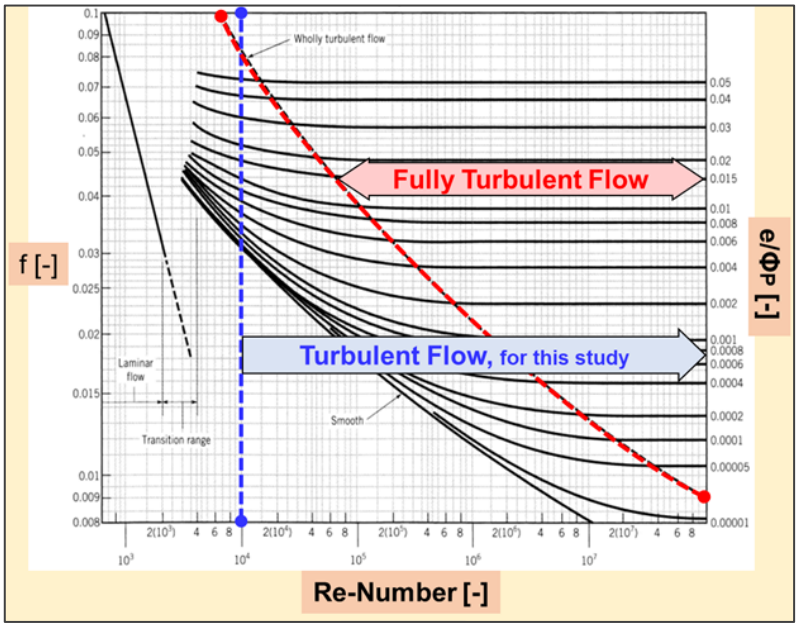

Fig. # 10 ***Moody Diagram***

Considering the Moody diagram, two areas are of importance for the technology addressed in this essay:

Turbulent Water/Wastewater Flow "TWF":

- A Flow is considered Turbulent "T" when its Re_L > 3'000 to 4'000 [-];
- Reynold's experiment proved that as soon as the flow is turbulent, axial dispersion acts at once and quite fast on an ink filament introduced into the medium [19];
- This fact is the fundamental basis for turbulent diffusion.

Fully Turbulent Water/Wastewater Flow "FTWF":

- A TF is generally declared as Fully Turbulent "FT" when its Darcy Friction Factor "f" is constant, independent from Re_L [-] for a given Pipe Wall Relative Roughness e/Φ_P [-]. e [mm] is the roughness of the surface of the pipe, ΦP [mm] is the diameter of the pipe and for a square conduit, ΦP [mm] is the hydraulic diameter Φhyd [mm].
- This definition applies in this paper, as per Fig. #10.

The difference between TWF and FTWF addresses the homogeneity and isotropy of their HHP. A FTWF is considered to have full homogeneity and isotropy. For a TWF we mention the Kolmogorov hypothesis [15] which proposes "*that Real Turbulent flows are practically locally Homogeneous and Isotropic and thus Universal on Small Scales regardless of their inhomogeneities and anisotropy on large scales"*. As will be shown later, Turbulent Diffusion is implemented by Small Scale Turbulent Motions. Hence, we can assume that the HHP of a TWF is homogeneous and isotropic. More so, for this study we assume that ReL > 10'000 [-] and that T-HHP and FT-HHP is 3-dimensional "3-D" i.e., axial-radial-angular. For cylindrical ducts/conduits with turbulence at high enough Re_L [-], the system behaves 2-dimensional 2-D axial-radial because of rotational axis-symmetry.

During this study, we will address both Turbulent and Fully Turbulent Patterns "T" and "FT" as T, and hint towards the differences where necessary. These assumptions have been experimentally proven for simple systems, such as a turbulent flow in straight pipes, vertical or horizontal, supported also by the observations made by the authors in the pilot plant made of a combination of FTWF and TWF (Fig. # 9, p. 16). More about these issues will be presented in the Section 12 "Methodology for Building a Homogeneous BC in a FTBF".

A TWF with an enough high Re_L=/> 50'000 [-] can be considered as being hydraulically piston or plug-flow "PF" for engineering design. Any pilot plant for ozone diffusion system can be designed with a quite large Re_L> 10'000 [-]. Hence, scale-up from the data obtained with piloting to the large-scale system should not present a major difficulty, essentially for simple systems. An industrial/large-size system designed with any correct scale-up method based on pilot testing data will necessarily have a larger Re_L [-] meaning more isotropy, homogeneity and PF HHP. These conditions result in an improved ozone diffusion.

One basic condition is that the molecular viscous shear processes along the wall of the conduit take place in a layer whose thickness is much smaller than the dimensions confining the system under consideration. For engineering needs, this layer has been defined qualitatively and quantitatively under the concept "Law of the Wall" [4]. According to this law, the "Wall Layer" consists of three sublayers, the

viscous layer (along the wall), the buffer and the turbulence building log-law inner layers, which make the hydraulic/hydrodynamic link between the system's confining wall region and the bulk of the TWF. The total thickness "δ" of these three layers is of the order of a 1 to 3 millimeters in the case of TWF in pipe (Fig. # 11). Outside this layer, the mean axial velocity profile of a turbulent water/wastewater flow can be assumed to be practically flat, and therefore PF when Re_L> 10'000 [-].

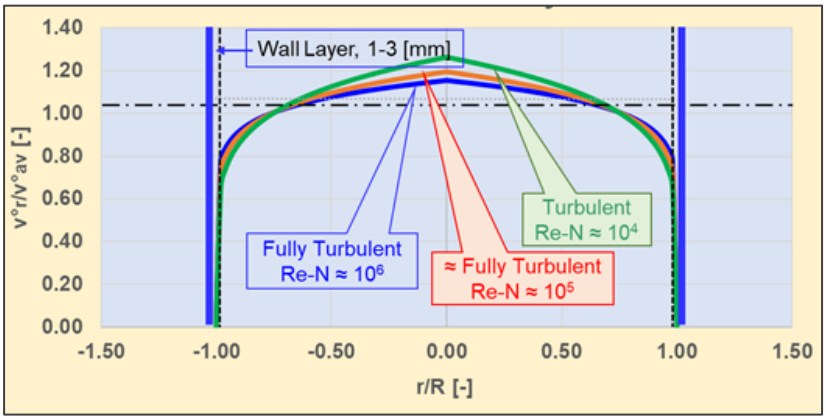

Fig. # 11 ***Turbulent Mean Axial Velocity Profile***
Retrieved from Fox et al. [17]

As will be presented later in this section, turbulence can physically be described to consist of 3-D elongated vortices, in the immediate neighborhood of the conduit wall, being stretched due to viscosity's shear stress, and 3-D Eddies, associated to spheres of different sizes in the bulk of the TWF. Based on multiple experiments with pipe flows at a sufficient high Re_L > 10'000 [-], in the region of the flow outside the Wall Layer i.e., in the bulk of the flow, the largest eddies are sufficiently small that the hydrodynamic conditions can be considered not only homogeneous, but also isotropic. This means that the existing turbulent conditions are statistically uniform in all translations and orientations (Fig. # 12).

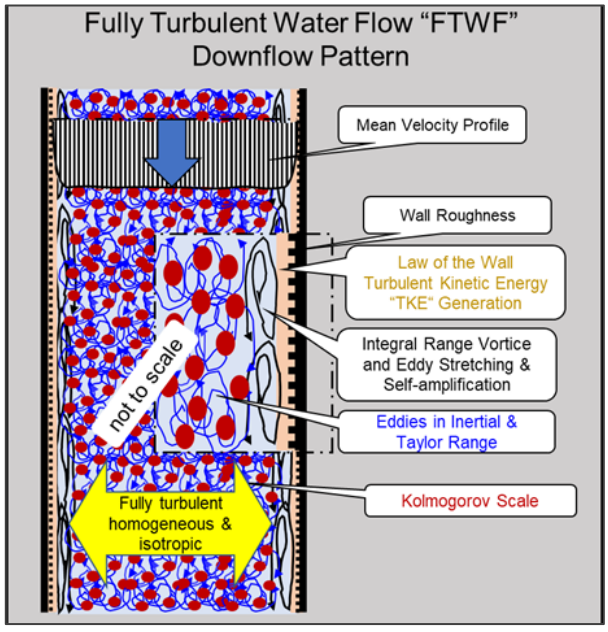

Fig. # 12 ***Homogeneous Isotropic Flow***

In the field of engineering, these Eddies (i.e., 3-D rotating bodies) can also be associated with equivalent spheres. Homogeneous and Isotropic Turbulence “HIT” prevails in these eddies. The flatter the turbulent average velocity profile is, corresponding to a larger Re, the more the HHP is homogeneous and isotropic on a larger scale. To illustrate this, Fig. #13 is a photograph of the shallow border of a FT-River where the three above defined flow regions are clearly to be seen (river width 30 [m]).

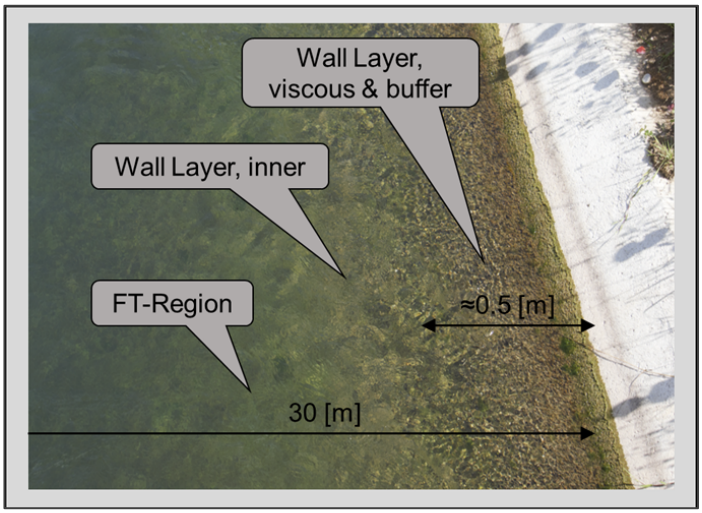

Fig. # 13 ***River Flow Pattern***

In a closed system such as in a vertical conduit, the same pattern exists, although on another scale. Indeed, the pattern is qualitatively similar because this pattern results from the Wall Layer, i.e., wall friction head loss. In a laminar flow the wall friction losses are directly transformed into heat in the bulk of the flow, due to the kinematic viscosity v [m^2/s] of the water. As already addressed, turbulence is initiated when the shearing forces resulting from the inertia of the water flow surpass the cohesion forces of the water resulting from its kinematic viscosity v [m^2/s].

The inertial forces of the mean flow near the wall of the conduit combined with the non-slip condition along the wall (i.e., flow velocity equal to zero at the wall) tear off the cohesion of the water which can no longer be kept by its viscosity. Tearing off is induced by a strong axial stress created by the inertia of the main flow as opposed to the viscous homogenizing forces i.e., high Re_L [-]. A steep gradient of the mean flow velocity is created. Near wall streaks and elongated vortices inside the wall layer, which cannot be but anisotropic, and are beginning and intermediate forms of turbulence, are generated. Head losses generated along the wall of the conduit are not directly dissipated as heat, but almost completely transformed first into Turbulent Kinetic Energy “TKE” carried by eddies of variable sizes homogeneously and isotropic spread inside the bulk turbulent flow, i.e., outside the wall layer. These eddies will be ultimately dissipated as heat by viscosity.

An analysis of the Navier Stokes equations (including the continuity equation), more precisely of the Reynold Averaged Navier Stokes “RANS” equations which introduce the statistical physical concept of Reynold stress for qualifying and quantifying turbulence, fundamentally describes the dynamics of a T- & FT-flow of a fluid. Thorough mathematical analysis of the RANS equations has evidenced the physical reality of the path of turbulent energy, such as :

- its generation (head losses along the wall of the conduit);
- its transformation into TKE with near wall elongated vortices, carried by the largest eddies.
- its transport towards the bulk of the flow by the largest eddies,
- its cascading inertial dissipation by turbulence transfer from larger to smaller eddies in the bulk of the flow,
- its viscous dissipation into heat (Fig. # 12, here above).

The application of the Fourier Transform to the TKE equations allows to qualify and quantify the transport of this kinetic energy by vorticity, associated with eddies. Such eddies can for example be observed downstream in the wake of the pillar of a bridge over a river (von Karman vortex street). These eddies or vortices rotate and move within the turbulence field of the mean water flow. They carry a linear and rotational momentum with mass and therefore energy. Through embedment and contacting with each other, they transport and exchange mass as well as energy and spread it inside the bulk of the TWF. Hence, turbulence is useful energy for diffusion. With a good understanding of the physical phenomena of turbulence, its intrinsic energy added to the longitudinal kinetic energy of the mean flow and part of the total energy of the hydraulic and hydrodynamic system under consideration can be used for improving the ozone diffusion process.

In a TWF the head loss, or energy, generated by the wall friction is radially gradually transformed by means of Eddy Viscosity v_E [m^2/s] into TKE within the wall layer, along the conduit. In the case of a turbulent pipe flow, axis-symmetry can be assumed, the turbulence pattern is explained as 2-dimensional "2-D", meaning axial and radial. However, vorticity so generated is still 3-D, meaning eddies behaves dynamically 3-D and therefore satisfies isotropy. Some heat losses are generated inside the viscous sublayer, but their amount is negligible, given its small thickness compared to the dimensions of the system. Generation of 3-D swirling eddies, with an outer average diameter Φ_E [m], carrying this energy as specific TKE [m^2/s^2] is the result of this process. However, one must realize that TKE is generated along the walls of the conduit and is further dispersed into the bulk of the flow. This means that a gradient of TKE exists within the TF extending from the systems wall into the bulk of the flow. This gradient plays a fundamental role for the construction of a homogeneous BC inside a TWF or FTWF.

What is today not completely understood as per the communications in the literature is how the friction energy generated along the wall is transferred to the initial vortices [20]. Also, the method of transport of the energy by the eddies into the bulk of the water flow is also not completely scientifically and technically cleared. Is this process mainly carried by vortices/eddy stretching (elongation), or by shear self-amplification (shear instability), or by both? Latest literature suggests both phenomena are more-or-less equally involved. What is today's evidence is that the wall friction energy is almost completely injected into eddies as kinetic energy. As will be addressed later in this section, these not completely scientifically cleared aspects of TKE Generation shall not hinder us to develop an engineering method for reliable and safe design of diffusion of a gas such as ozone and/or oxygen into a water or wastewater flow.

These first Eddies cannot survive with their initial energy content, shape, and size, since ultimately this energy will be dissipated as heat. This process is irreversible and leads to an entropy increase of the hydraulic and hydrodynamic system. The eddies undergo stretching, convolution, swirling and mechanical shear stress [21]. Moreover, the eddies are subject to the natural irreversible TKE Dissipation "TKED" [m^2/s^3], they become smaller and smaller and less energetic and ultimately disappear as heat

due to the kinematic viscosity ν_L [m^2/s] of the water/wastewater. The evolution of the vorticity, mathematically describing the local spinning motion in all directions of the eddies which plays a major role in the inertial transfer of TKE, is characterized by its enstrophy Ω [s^{-2}]. The enstrophy is defined as the square of the vorticity. Citing the literature in continuum mechanics, e.g. Batchelor [10], vorticity is a pseudovector field that describes the local spinning motion of a continuum near some point. Enstrophy is therefore a qualitative and quantitative parameter representing the action for the eddies. Some authors relate the enstrophy to the TKED, $\Omega = \varepsilon/\nu_L$ (based on average or RMS values). This makes sense since TKE is mainly carried by eddies.

Turbulence is made visible by the presence of regularly disposed small capillary waves (not generated by the wind) on the surface of a quiet river. These waves are nothing else but the dome of the eddies just underneath the water surface (Fig. # 14).

Fig. # 14 ***River Surface Capillary Waves***

Fig. #13 and fig. #14 are representative of turbulence, although this turbulent flow has one free surface and is not entirely confined as opposed to turbulent flow in pipes. The turbulent system evolves towards thermodynamic equilibrium and maximum entropy, which is total thermal dissipation. The result of this turbulence dissipation process is that all sizes of eddies exist simultaneously and are therefore embedded, meshed, and physically linked all together. Smaller eddies exist inside eddies of larger size and are being dispersed inside the water flow. This process is physically possible because eddies have a decay time, lasting from [s] for the largest eddies to [ms] for the smallest eddies able to exist in a turbulent system. Breakdowns into smaller eddies occur continuously and rapidly, as will be addressed later in this document.

Fig. #14 also makes clear that there appears to be some repeating patterns, some kind of larger zone homogeneity, called intermittency. This is a hint to the important concept of universality, which will be addressed in section 11 “**Mathematical Proof of the Universal Law of Turbulence**”.

Eddies are moving within the turbulent field. An eddy energy calculation analysis shows that the energy of the eddies is rotational, meaning vorticity and enstrophy, and translational. Hence, within a reference frame attached to the mean water flow, TKE [m^2/s^2] can therefore be mainly considered as being made approximately of 50 [%] rotational and 50 [%] translational energy (within the mean flow). Science has identified the so-called Turbulent Energy Cascade “TEC” (Fig. # 15).

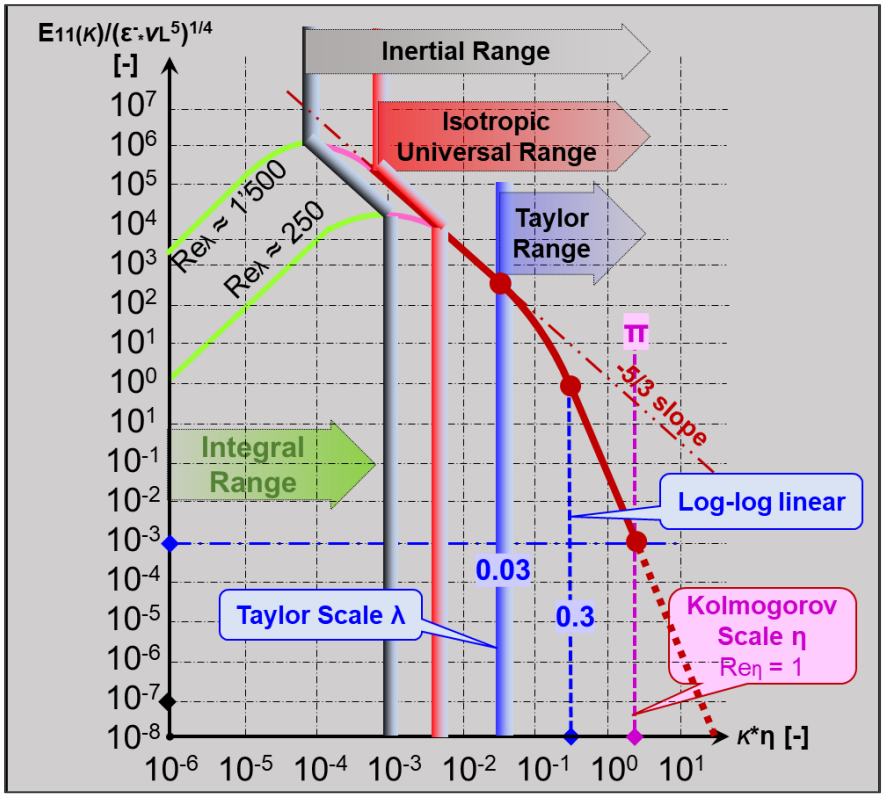

Fig. # 15 *Turbulent Energy Flow Cascade*
Adapted from Pope [15] with experimental data

Fig. # 15 quantifies the length scales, presented normalized hereafter. It is today accepted that for geometrically simple wall enclosed conduits TKE is dissipated along the Turbulent Energy Cascade "TEC". The TEC is characterized by domains and length scales, called hereafter scales (Table 2).

Table 2 Turbulent Energy Cascade Domains and Scales

Domain / Length Scale	Symbol	Unit	Comment
Largest Eddy	l_0	[m]	Limited by the size of the turbulent flow conduit
Integral Range	ITR	[-]	Range of the generated TKE carrying Eddies
Inertial Range	INR	[-]	Mechanical Turbulent Energy dissipation
Taylor Range	TLR	[-]	Mechanical and viscous Turbulent Energy dissipation
Kolmogorov Scale	KS	[-]	Mostly viscous Turbulent Energy dissipation to heat
Batchelor Scale	BS	[-]	Smallest identifiable scale
Isotropic Universal Range	IUR	[-]	Isotropy and Homogeneity prevail

TKE is transferred from the largest Eddies l_0 [m] of the Integral Range "ITR" to always smaller eddies along the Inertial Range "INR". TKE is then transferred to the Taylor Range "TLR ", characterized for engineering design by the parameters presented in Table 3. Finally, the Kolmogorov Scale "KS" is characterized for engineering design by the parameters presented in Table 4.

Table 3 Taylor Range TLR Scale

Parameter	Symbol	Unit	Comment
Universal TLR Scale	λ	[m]	Universal Law of Turbulence Beginning of viscous Turbulent Energy Dissipation
TLR Scale Reynold Number	Re_λ	[-]	Reference Number for Engineering Design

Table 4 Kolmogorov Scale "KS"

Parameter	Symbol	Unit	Comment
KS Scale	η	[m]	Viscous Turbulent Energy Dissipation
KS Reynold Number	Re_η	[-]	$Re_\eta = 1$ [-]

An Isotropic Universal Range "IUR" is identified within the INR addressed later in Section 11 "**Mathematical Proof of the Universal Law of Turbulence**". The rate of transfer and dissipation of turbulent energy is qualified and quantified by the mass specific Turbulent Energy Dissipation Rate "TEDR" ε [m^2/s^3]. ε [m^2/s^3] is practically equal to the specific wall friction losses generation rate, neglecting the heat losses inside the wall layer.

In ITR, TKE is generated from wall head losses and transported away from the wall by the largest energy-carrying eddies. In INR, TKE is transferred from larger to smaller eddies by convolution, stretching, dispersion and transfer of momentum, but practically without viscous losses. In INR, the enstrophy remains constant because of conservation of rotational momentum.

Within TLR, dissipation of TKE into heat by kinematic viscosity starts to take place simultaneously with a decaying TKE transfer among eddies, which become smaller down to KS and loose TKE. KS is the scale from where dissipation of TKE by kinematic viscosity prevails, transforming TKE directly into heat. In TLR, the enstrophy decreases because of loss of TKE. The length at which the TLR begins, the upper TLR Length "λ", will be called the TLR Length. The smallest length scale which can be defined is the Batchelor Scale "BS" l_{BS} [m]. BS, whose length scale l_{BS} [m] is much smaller than η [m], describes the size of a droplet of scalar, for example O_3, that will diffuse by molecular diffusion during the same time it takes for the energy in an eddy of size Kolmogorov η [m] to dissipate into heat by kinematic viscosity [22]. Between KS, BS and within BS, TKE is finally entirely dissipated into heat. Contrary to all the other scales and ranges that are determined by dimensional analysis and constants, estimated with correlations, and verified experimentally, η, the Scale of KS, is defined essentially based on measurable and well-defined physical parameters i.e., kinematic viscosity *v* [m^2/s], and specific TEDR ε [m^2/s^3]. The characteristic parameters are summarized in Table 5.

Table 5 Summary of the characteristic parameters of TLR, KS and BS for engineering design

Parameter	Symbol	Unit	Equation / Correlation / Comment
TEDR	ε	[m^2/s^3]	= $\Delta p * V°_L / M_L$
	Δp	[Pa]	Friction Head Loss, Wall, and Bubble Column
	$V°_L$	[m^3/s]	Water / Wastewater Flow
	M_L	[kg]	Mass of Water / Wastewater in O_3R
TLR Scale	λ	[m]	= π*η/0.03 Universal Law of Turbulence
	$Re_λ$	[-]	= $λ * u°_λ / v_L$
	$u°_λ$	[m/s]	= $0.95*(ε*λ)^{1/3}$ Orbital Velocity of Eddy with diameter λ [23]
	vL	[m^2/s]	Kinematic Viscosity of Water / Wastewater
KS Scale	η	[m]	= $(vL^3/ε)^{1/4}$ ➔ Dimensional Analysis [21]
	$Re_η$	[-]	= 1
BS Scale	l_{BS}	[m]	= $(vL * Dm^2/ε)^{1/4}$ [22]
	Dm	[m^2/s]	Molecular Diffusion of O_3 or O_2 in Water / Wastewater
	Re_{BS}	[-]	= 0

Applying the Fourier Transform to TKE transforms it into a series of frequencies. The turbulent eddies carrying the TEDR Process can be associated with a rotation frequency and mathematically defined by a corresponding sine wavelength and sine wavenumber. Each eddy, part of the of the full spectrum of turbulence and TEDR, is identified by its mass specific wavenumber $κ$ [m^{-1}] and its TKE defined as $E_κ$ [m^2/s^2]. Eddies with their specific TKE $E_κ$ [m^2/s^2] are scaled and physically identified with the parameters described in Table 6.

Table 6 Eddy Physical Parameters

Parameter	Symbol	Unit	Comment
Eddy Sine Wave Number	$κ$	[m^{-1}]	Defined by Fourier Transform
Eddy Sine Wavelength	$l_{Eκ}$	[m]	Defined by Fourier Transform
Eddy specific TKE	E_K	[m^2/s^2]	TKE carried by eddy with wavenumber
Outer Spherical Diameter	$Φ_{Eκ}$	[m]	Associated to a sphere
Orbital Velocity	$u°_{Eκ}$	[m/s]	At surface of the equivalent sphere
Re-Number	$Re_{Eκ}$	[-]	At surface of the equivalent sphere
Decay Time	$τ_{Eκ}$	[s]	Lifetime of Eddy of size $Φ_{Eκ}$

Based on the Fourier Transform applied within the IUR, the physical parameters of eddies can be defined mathematically as presented in Table 7.

Table 7 Correlations and Equations of the Physical Parameters of Eddies

Parameter	Symbol	Unit	Correlation / Equation
Diameter of Eddy	ΦE_k	[m]	$= 2\pi/lE_k$
Wavelength of Eddy	lE_κ	[m]	$= 2*\Phi E_k$
Wavenumber of Eddy	κ	[m^{-1}]	$= \pi/\Phi E_k$
Normalized Eddy Wavenumber	κ_N	[-]	$= \kappa*\eta$
Wavenumber Specific Energy:	$E_\kappa(\kappa)$	[m^3/s^2]	$= C*\varepsilon^{2/3}*\kappa^{-5/3}$ ➔ C = 1.5 Kolmogorov Constant [15]
Normalized Wavenumber Specific Energy	$E_\kappa(\kappa)_N$	[-]	$= E11(\kappa)/(\varepsilon*\nu_L{}^5)^{1/4}$
Wavenumber of TLR	κ_λ	[m^{-1}]	$= \pi/\lambda$
Wavenumber of KS	κ_η	m^{-1}]	$= \pi/\eta$
Eddy Orbital Velocity	$u°E_\kappa$	[m/s]	$= 0.95*(\varepsilon*\Phi E_\kappa)^{1/3}$ [23]
Turnaround Time	τ_{TEk}	[s]	$= \pi*\Phi E_k/u°E_\kappa$
Eddy Decay Time	$\tau_{DE\kappa}$	[s]	$\approx 1.5*\tau_{TEk}$ valid in IUR [21]
Re of Eddy	$Re_{E\kappa}$	[-]	$= \Phi E*u°_{E\kappa}/\nu_L$

These correlations stand for the spectrum of energy distribution per the system's mass and wavenumber κ [m^{-1}] across all the various length scales situated within IUR and the beginning of TR . It is common to represent the TEC on a graph with $E_\kappa(\kappa)$ [m^3/s^2] on the ordinate and κ [m^{-1}] on the abscissa, both parameters normalized dimensionless with ε [m^2/s^3] and ν_L [m^2/s], respectively with η [m], as represented on Fig. # 15, p.24, $E_\kappa(\kappa)_N = E11(\kappa)/(\varepsilon*\nu L^5)^{1/4}$ [-] and $\kappa_N = \kappa*\eta$ [-]. These correlations are valid for the one-dimensional axial energy spectrum in direction of main flow. Eddies rotate in all directions; hence this precision must be made, but since the turbulent hydrodynamic system we are concerned with is isotropic (IUR), it can be assumed that this representation is qualitatively and quantitively valid in all directions. The total normalized energy spectrum $E_\kappa(\kappa)_{Ntot}$ [-] equals $\approx 2*E\kappa(\kappa)N$ [-], according to Pope [15].

Most experiments with TWF of different fluids, mainly water and air, and geometrically simple T-systems (i.e., shear-free such as downstream of a grid, in a free jet and/or with shear as confined in open channel or pipe) have produced the same normalized -5/3 slope characteristic curve for the IUR to TLR and the curve from TLR down to KS ranges. This is a remarkable fact, since it shows that the full range of the turbulence spectrum including IUR & TLR down to KS can be described as Universal**,** as presented in the next section, with the condition that the turbulence is isotropic. This is the case within IUR down to KS. This domain, corresponding to the IUR, is also called the "Taylor Frozen Flow Hypothesis" [2].

11. Mathematical Proof of the Universal Law of Turbulence

By exploiting randomness, three mathematicians have proved an elegant law that underlies the chaotic motion of turbulent systems [24, 25]. “We see Batchelor’s law all over the place,” said Jacob Bedrossian, a mathematician at the University of Maryland, College Park and co-author of the proof with Alex Blumenthal and Samuel Punshon-Smith. He added that “by proving this law, we get a better understanding of just how universal it is.” This demonstration hints towards the evidence that turbulence is a deterministic phenomenon which depends only upon a chain of previous happenings, essentially upon the initial conditions, and presents a recurrent character, i.e., a continuous repetition of similar physical features.

Based on the above results, the modeling of a turbulent system, for example a two-phase bubbly flow, with pilot plant testing allows for a better understanding of the behavior of the bubbles in such a turbulent dynamic system. Moreover, it provides an understanding about the dissipation of the turbulent energy, provided that the initial, kinematic, dynamic, and turbulent conditions are similar to that of the large-scale turbulent system. Scale-up for the design of the large-scale turbulent system is so provided. We have therefore a solid basis for developing an engineering method for the design of an ozone diffusion system under fully turbulent conditions, with oxygen or air as carrier gas. Particularly of the essence is the Normalized Taylor Scale identified with κ_λ*η [-] (Table 8).

Table 8 Universal Normalized Taylor Scale Data

Parameter	Symbol	Unit	Value	Commentary
Normalized Taylor Scale	κ_λ*η	[-]	0.03	Universality, value +/- 10 [%]
Corresponding Re-Number	Re_λ	[-]	≥ 250	Condition for universality

Most of the ozonation reactors we are generally dealing with satisfy to these universality conditions and can be engineered and designed based on the above conditions (Table 8). Also, to be mentioned is that the turbulence range characteristic curve is log-log linear, with a -5/3 slope, when κ*η > 0.3 [-]. This means that for any eddy with $Re_{\Phi E}$ [-] < Re_λ = 250 [-], increasing viscous losses must be taken into consideration. We will see later in this document that the largest eddies existing inside TBF will have an associated diameter Φ_E [mm] smaller than λ [mm]. Physically, this means that in this range, the dissipation of HIT is independent of the confining system and its forces acting on the water which generated this turbulence. The question to be answered is whether or not the TF in the voids surrounding the bubbles can be considered as isotropic and universal.

The dissipation of TKE behaves free of outside impact, based only the fluid’s own physical characteristics, i.e., its kinematic viscosity v_L [m^2/s] and energy dissipation rate ε [m^2/s^3], which is basically equal to the Head Loss Generation Rate “HLGR”. Citing Batchelor [10],“*the motion associated with the Equilibrium Range of Wavenumbers is uniquely determined statistically by the parameters* ε [m^2/s^3] and v_L [m^2/s]*”*. All surfaces of quiet rivers present the same features observed on Fig. # 14, so confirming this characteristic of universality mentioned earlier. This region of universality of the energy cascade is of great interest and provides a solid basis for turbulent diffusion engineering and design. We will see later that the size of the largest eddies which can exist in a typical ozone diffusion BC homogeneously distributed inside a FTWF will in most cases fall into the κ*η-Taylor Subrange. This means that the design

for most of the ozone diffusion bubble columns can be made based on three initial, clearly qualitatively & quantitively defined parameters and correlations, namely,

$$\varepsilon\ [m^2/s^3],\ v_L\ [m^2/s]\ \&\ \kappa_\lambda{*}\eta\ [-] = 0.03, \text{ with } \eta\ [-] = (v_L{}^3/\varepsilon)^{1/4}$$

under the fundamental condition that the introduction of the gas flow into the turbulent water/wastewater flow does not perturb its universality**.** Under normal conditions, as in confined straight pipe flow, smaller eddies can basically not coalesce and form larger eddies, except if for some reason hydraulic energy is added to the system. Similarly to the entropy of a thermodynamic system which increases, the enstrophy showing curl-inertial dissipation effects towards equilibrium of a T-Flow is constant in an isolated system, if no addition of energy coming from outside of the T-System occurs.

The above description of turbulence reflects the research made by many scientists, such as Danckwerts [7], Reynold, Taylor, Batchelor [10], von Karman, Hinze [18] and Kolmogorov, to name only some of them. All their ideas and development of theory and physical reality are summarized in Pope [15]. As will be shown further in this essay, Eddy Diffusion “ED” quantified by the eddy diffusivity coefficient D_E [m^2/s] is a very much faster physical process than molecular diffusivity quantified by its coefficient D_m [m^2/s]. It is therefore of the essence for good engineering to evaluate qualitatively and quantitatively properly where each physical process prevails.

Considering the Fig. # 15, the universality, only valid for geometrical simple systems, can be used for the design of a T-System such as confined in a vertical straight pipe. Hence, using the correlations resulting from this description of turbulence, we propose a mean for enabling a good engineering approach to ED in a TWF. A correct estimation of the specific TKE Dissipation Rate ε [m^2/s^3] and the Kolmogorov Scale Wave Number κ_η [m^{-1}], equal to π/η [m^{-1}], which are the fundamental parameters for such a design, is of the essence. The correlations hereafter make it possible to quantify with good precision the physical phenomena forming HIT. Dimension- and time- scales, as well as energy- and power-spectra can therefore be figured out mathematically, providing design engineers with the necessary tools for an accurate and safe design of such systems. Important is that all the different correlations and formulas to be found in the scientific literature are convergent, supplying practically equal values, hence applicable for a TWF.

For the completion of this paragraph, a summary of the mathematical expressions and correlations allowing for an accurate-conservative and safe diffusion system design in a TBF (Table 9, Table 10 and Table 11). Since TKE generation and TKE dissipation rates are the motors in a TWF, the correlations proposed here after, based on TKE, provide a consistent approach. Total TKE k [m^2/s^2] is practically equal to the total specific friction energy produced in the system, in fact that minus the negligible viscous losses in the viscous wall sublayer.

Table 9 Turbulent Kinetic Energy TKE Identification

Parameter	Symbol	Unit	Correlation / Equation	Comment
TKE	k	[m^2/s^2]	$\approx \int E_\kappa(\kappa)*d\kappa$ $= \sum[E_\kappa(\kappa)+E_\kappa(\kappa+\Delta\kappa)]/2*\Delta\kappa$ $\approx \sum E_\kappa(\kappa)*\Delta\kappa$	Applicable when $\sum CSTR = 110$. See section 17 “***System Design***”. Valid for ITR, INR, ISR,TR to KS.
	$E_\kappa(\kappa)$	[m^3/s^2]		Wavenumber Specific TKE
	$d\kappa$	[m^{-1}]		Wavenumber Increment

The specific TKE/RKE Dissipation Rate ε [m^2/s^3] is practically equal to the conduit wall friction energy generation rate, in fact equal to that minus the negligible viscous sublayer dissipation rate.

Table 10 Turbulent Kinetic Energy Dissipation Rate TEDR

Parameter	Symbol	Unit	Correlation / Equation	Comment
TEDR	ε	[m^2/s^3]	= $\Delta p * V°_L/M$	TKE Dissipation Rate
	Δp	[Pa]		Total wall and BC friction head loss in the conduit[1]
	$V°_L$	[m^3/s]		Water /Wastewater volumetric flow rate
	M	[kg]		Mass of Water/Wastewater in the Ozone Diffusion Reactor O_3R

[1]In a BC, Δp must also include the friction losses caused by the slip velocity of the bubbles within the mean water flow and added turbulence in their wake as well as the additional head loss due to water/gas double-flow.

Table 11 Other Mathematical Equations and Correlations

Parameter	Symbol	Unit	Correlation / Equation	Comment
Re- Number of O_3R	Re	[-]	= $\Phi_{hyd} * v°_L/\nu_L$	Only Water/ Waste Flow
	Φ_{hyd}	[m]	-	O_3R Hydraulic Diameter
	$v°_L$	[m/s]	-	Average Water/Wastewater Velocity in O_3R
	ν_L	[m^2/s]	-	Kinematic Viscosity of the Water/Wastewater
TKE of Wavenumber κ	$E_\kappa(\kappa)$	[m^3/s^2]	= $1.5 * f_{ITR} * \varepsilon^{2/3} * \kappa^{-5/3} * f_{TLR}$	Pope [15] and Bakker [21]
	f_{ITR}	[-]	= 1	Correcting factor of TKE for the INR
	f_{TLR}	[-]	= $1.23 * e^{-5.2\kappa_{TLR}*\eta}$	Correction factor of TKE in TLR
Eddy-			-	Pope [15]
Diameter	$\Phi_{E\kappa}$	[m]	-	Fourier Transform
Wavenumber	K	[m^{-1}]	= $\pi/\Phi_{E\kappa}$	Fourier Transform
Time Scale	$\tau_{E\kappa}$	[s]	= $1.053 * \varepsilon^{-1/3} * \Phi_{E\kappa}^{2/3}$	Bakker [21]
Orbital Velocity	$u°_{E\kappa}$	[m/s]	= $0.95 * (\varepsilon * \Phi_{E\kappa})^{1/3}$	Bakker [21]
Turnaround Time	$\tau_{TE\kappa}$	[s]	= $\pi * \Phi E / u°_{E\kappa}$	
Total Lifetime	τ	[s]	= k/ε	

Parameter	Symbol	Unit	Correlation / Equation	Comment
Lifetime in IR	τ_{IR}	[s]	$\approx \tau/10$	
Decay Time	$\tau_{DE\kappa}$	[s]	$\approx 1.5^* \tau_{E\kappa}$	
Re-Number	$Re_{E\kappa}$	[-]	$= u^\circ_{E\kappa} * \Phi_{E\kappa}/\nu$	
Kolmogorov Scales-				Pope [15]
Length	η	[m]	$= (\nu_L^3/\varepsilon)^{1/4}$	
Time	Θ_η	[s]	$= (\nu/\varepsilon)^{1/4}$	
Velocity	u°_η	[m/s]	$= (\nu^*\varepsilon)^{1/4}$	
Taylor Scale	λ	[m]	$= \eta/0.03 = 33.3^*\eta$	Pope [15]

*The articles by McDonough [26] and Trettel [27] have also been consulted for the writing of this table.

12. Methodology for Building a Homogeneous and Isotropic "BC" in a "TWF/FTWF"

Addressing a Bubbly Flow "BF", the design parameters Re, v°, *v*, ρ, η, ε and $E_{\kappa}(\kappa)$ must be calculated based on the total flow of both fluids constituting it, the O_3-Gas, and the water/wastewater. One condition, which is of the essence, is that the process system introducing the O_3-Gas into the water/wastewater flow shall not disturb its homogeneous and isotropic State. When compared with the single water/wastewater flow entering the system, which is the basis for the first calculation step, the BF introduces energy added to the original TKE. This energy is generated by the friction losses along the bubbles rising with their bubble terminal ascending velocity $v°_B^{\infty}$ [m/s] or slip velocity with respect to the water. This includes the TKE added to the system by turbulences generated in the wake of the bubbles and the increased wall friction losses due to the increased flow velocity of the gas-water/wastewater bi-flow induced by the dynamic gas hold-up α_{gdyn} [%] in the bubble column.

As an introduction, we cite here out of Hinze [18] :

> "*Smaller eddies corresponding to higher wavenumbers are excited by the transfer of energy by inertial forces from the larger eddies. It may be assumed that, in contrast with the larger eddies, these much smaller eddies are independent of the external conditions producing the forces that generate the initial largest eddies. This assumption is supported by experimental evidence, that even in anisotropic turbulent flow, the high wavenumber range of turbulence is close to isotropy"*.

Another basic fact proven through observations is that the biggest eddies of the Integral Range "ITR" cannot be larger in size than the confinement main dimension of thew system, i.e., the cross-section of the conduit and, in the case of an established stable bubble column, the size of the liquid bulk volume in between the bubbles. We will see later that the eddies responsible for Eddy Diffusion D_E [m^2/s] are generally situated inside the Taylor Range "TLR" i.e., inside the isotropic universal range. Theory and experience also show that the larger the Re-Number of the mean flow is, the broader the isotropic universal range extends over the water flow.

The above assumption for simple diffusion systems justifies the hypothesis that the turbulent conditions in the liquid between the bubbles of a BC homogeneously distributed inside a TWF/FTWF are hydrodynamically and hydraulically isotropic and therefore necessarily homogeneous. These conditions help the engineering design of an ozone diffusion system (Fig. # 12, p.20). Hence, we will also, in our further approach to Eddy Diffusion D_E [m^2/s], make no longer any difference between a TWF and FTWF, qualifying it simply as TWF. More so, we consider that the translational energy of smaller eddies enveloped by larger eddies contributes as well to eddy diffusion.

The topic of this section addresses the generation and the stability of a BC and the size of its bubbles inside a TWF. In order to be efficient for diffusion of ozone and its reactions with the constituents of the water or wastewater, a BC must be homogeneously built up and distributed as effectively and rapidly as possible inside a TWF. A BC inside a TWF is named hereafter as a Turbulent Bubbly Flow "TBF". The basic conditions for a reliable engineering for the design of an ozone diffusion system under turbulent homogeneous and isotropic conditions are :

- that the Equivalent Sauter Diameter Φ_{B32} [mm] of the bubbles

    - stays constant and stable, within a narrow standard deviation of its statistic Gaussian Distribution.
    - or diminishes homogeneously and steadily because of the solubilization of the O_3CG.
- that the Number of Bubbles #B [-] in the BC stays constant
    - unless the bubbles are in course of the diffusion process completely solubilized into the liquid.
- that there should be no breakage nor coalescence of bubbles, and that constant and well-defined hydraulic & hydrodynamic conditions prevail inside the TBF.

The equivalent Sauter diameter Φ_{B32} [mm] = $\Sigma n_i*\Phi_{Bi}^3/\Sigma n_i*\Phi_{Bi}^2$ in a TBF needs to be qualified by the standard deviation σ_{PDF} [-] of the probability distribution function PDF of Φ_{Bi} [mm]. We assume, based on the approach developed in the literature [28-30], that in a TBF a homogeneous and isotropic turbulent force field surrounds the bubbles. We can therefore also assume that these forces acting on the O_3CG leading to the formation of the BC in the TBF will act homogeneously and isotropic in all directions. These same forces will provide to the bubbles an average (ignoring dynamic surface effects) shape almost spherical because they will not affect the average value of the surface tension. Hence, the result should be a PDF with an almost normal (symmetric) Gaussian Distribution Function "GDF" with skewness = 0.

The same reasoning leads to the assumption that the GDF should be narrow with its standard deviation σ_G [mm] quite small. Considering an initial Φ_{B32} = 3 [mm], observations into the bulk of the TBF of the fully turbulent pilot system (Fig. # 9, p. 16 and Fig. #22, p.43) have shown that the variable Φ_B [mm] is approximately constant in narrow vertical sectors, with estimations of a first vertical range at the beginning of the TBF $\Delta\Phi_B$ = +/- 0.5 [mm], leading to the first σ_G = 0.20 [mm] with GDF (before solubilization of the O_3G starts to be noticeable). These observations also showed that the upwards movement of the bubbles was mostly along a straight path, with little wobbling and spiral movement, a strong sign of the homogeneous and isotropic pattern of the turbulent forces acting on them. Again, these observations can be explained by the isotropy and homogeneity of the dynamic system. However, some horizontal movement of bubbles, without coalescence, was seen immediately behind the transparent tube wall, indicating the presence of the larger eddies of the ITR where TKE is generated. This behavior can be considered as characteristic for a TBF in wastewater where the organic matter adsorbed to bubble surface is physically attached to both the bubble and the wastewater. This adsorbed organic matter stabilizes the bubbles.

Ozone (O_3) is always generated inside a carrier gas "O_3CG". The O_3CG was originally dried air, but in modern times, high purity gaseous oxygen is used, with some nitrogen (up to 5 % by volume) and argon, when generated by an adsorption-desorption cycle of nitrogen on a molecular sieve system. The achievable ozone concentration c_{O3G} [wt%] can amount to up to 12–15 [wt%], corresponding to 8–10 [vol.%], in oxygen gas. Given this rather low c_{O3G} [wt%], low partial pressure and low solubility of ozone, an efficient diffusion of O_3 into the water or wastewater is of the essence for best O_3-Reaction.

The construction of an efficient TBF requires energy because the ozone carrier gas "O_3CG" must be diffused as homogeneously as possible as bubbles inside the TWF, meaning that bubble surface energy must be generated, quantified as surface tension σ [N/m] or surface energy [Nm/m^2]. The O_3CG is transported by continuously flowing inside the ozone generator "O_3G" and the downstream pipe leading to the ozonation reactor "O_3R". Its surface energy with respect to water is equal to zero in a dry system.

As soon as gas is being bubbled into a liquid, Bubble Surface Energy “BSE” is created, from practically zero to the value corresponding to the Gas-Liquide Interface Area “GLIA” of the TBF.

Turbulent Kinetic Energy “TKE” is the source of BSE generation through action of the eddies of the TWF on the O_3CG. TKE is generated from friction losses along a liquid contact surface inside the O_3R conduit. Hence a large conduit liquid contact surface area is of the essence. This TKE-generating contact surface can be:

1. the wall of the conduit itself with its roughness.
2. the surface created with fittings placed inside the conduit, such as inside a static mixer, creating a homogeneous volumetric distribution of the surface that generates TKE inside the conduit.
3. some other means increasing the head-loss inside the conduit, such as in the Venturi of a hydro-injector, creating a strong increase of water/wastewater velocity v°L [m/s], thus large $v°L^2$ [m^2/s^2];
4. in a narrow pipe with a high Darcy friction factor f [-], by adding roughness to the conduit surface.

Above mentioned methods are appropriate for the construction of a homogeneous TBF. Direct BC generation inside the O_3R can be made with porous diffusors. However, diffusors are at risk of clogging (in wastewater) and do not meet the engineering layout requirement for a TBF. Also, using the TKE generated by the wall friction losses inside the O_3R is generally not strong enough for building a homogeneous TBF.

In a standard O_3R-conduit without built-in fittings and operated with a typical superficial water $v°_L < 1.0$ [m/s], there is necessarily a gradient of TKE flow generated from the wall surface towards its central axis. TKE is physically present as eddies of many sizes which are energetically activated by momentum eddy diffusivity, the eddies closer to O_3R wall transferring their TKE mainly to the radially situated neighbor ones within a continuous diffusion process. In a normally set up turbulent fluid, this transfer of TKE is constant along the radial and somehow also axial path, so that all eddies are continuously carrying TKE and exchanging momentum with each other. If for some reason this process is interrupted because certain eddies in the transfer path have lost their TKE, for example while contributing to splitting bubbles (i.e., increasing BSE), they must be reactivated.

Momentum eddy diffusivity acts to reactivate these partially idled eddies. Momentum Eddy Diffusivity D_{EM} [m^2/s] is the driving force for transfer of TKE from the wall of the O_3R conduit to its axis. D_{EM} [m^2/s] is not infinitely fast, it depends upon the Re-number Re_L [-] of the main water flow. Fig. # 16.1, constructed with information from Beckwith [31], gives values for $D_{EM} = (1.0\text{-}1.6)*10^{-4}$ [m^2/s] in the range of typical Re values of the main water flow inside a pilot O_3R. Since this Re-dependence is qualified as linear, the representative blue line can be extended towards larger Re_L-values, typical for large-size/Industrial O_3Rs.

Fig. # 16.2 [31] shows the radial profile of D_{EM} [m^2/s], with a maximum around 20 to 40 % of conduit radius from the wall and a drop to zero towards the central axis of the conduit. An average value is found at 70 % of maximum, which can be explained by the hydraulic/hydrodynamic axial-radial symmetry of the water/wastewater flow.

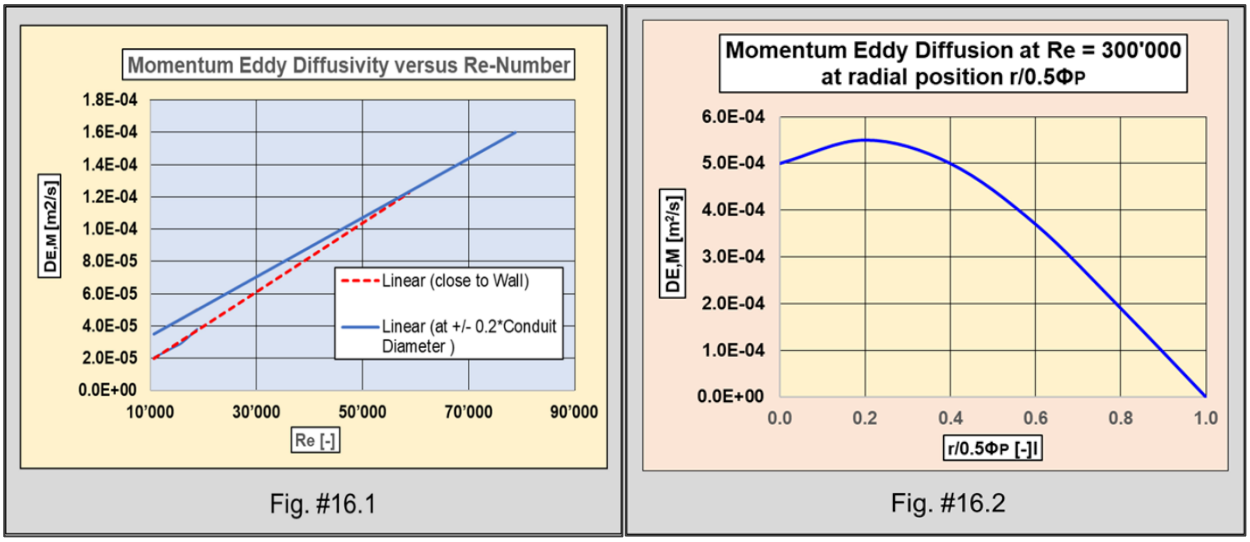

Fig. # 16 ***Momentum Eddy Diffusivity***

Compared with the D_{Emax} = 9.22*10^{-7} [m^2/s] of our example presented hereafter, this value is approximately 1 000 times faster. However, the temporal dynamic action within a TBF can nevertheless not be ignored and slows down the process of a fully homogeneous BC Formation. The process of D_{EM} [m^2/s] is not infinitely fast, because bubble splitting also needs time, of the order of 0.05–0.10 [s] if ε [m^2/s^3] is strong enough to create bubble splitting.

When considering this quantitative information, it is obvious that the direct generation of a TBF inside an O_3R needs time so that D_{EM} [m^2/s] can contribute to build-up and homogenize the TBF. This fact is of particular importance for the construction and stability maintenance of a homogeneous TBF. Eddies with enough TKE contribute to a continuous splitting, generally binary as was observed in turbulent pilot systems and presented in the literature [28-30] , process of bubbles in the generation of a BC, to always smaller sized bubbles, until balance from an energetical point between TKE and BSE, i.e., stable number and size of the bubbles of the TBF is established. An eddy which has contributed to this process loses most of its TKE which has been transformed into BSE. This eddy must be energetically reactivated through D_{EM} [m^2/s] from fresh eddies generated at the conduit wall. Because of the radial distribution of D_{EM} [m^2/s], this process requires sufficient Residence Time Θ_{Res} [s] and TKE in the BC-generating reactor. A sufficient residence time and TKE allows both for homogeneity of BC distribution in the reactor and homogeneity of bubble size, identified with their average Sauter Diameter Φ_{B32} [mm].

Two processes are crucial for the generation of a stable BC in a homogeneous TBF: the splitting of larger bubbles and the coalescence of smaller bubbles, both through the action of TKE. As already mentioned, TKE must supply at least equal, in fact more energy than the BSE added to the final BC. From a dynamic-physical point of view and according to authors in the field [28-30], a Critical Bubble Capillary Diameter ΦB [m] can be defined, corresponding to the minimum TKE dissipation rate εcrit [m2/s3] necessary for an eddy to deform the bubble surface against its confinement energy exerted by the bubble BSE, before bubble splitting can start (Table 12).

Table 12 Bubble Breakage Equations / Correlations

Parameter	Symbol	Unit	Correlation / Equation	Comment
Bubble Surface Restoring Pressure	$p_\sigma(\Phi B)$	[N/m^2]	= $\sigma L * S_B/V_B = 6*\sigma_L/\Phi_B$	V_B = Volume of Bubble S_B = Surface of Bubble
Bubble Surface Deforming Stress	$p_D(\Phi B)$	[N/m^2]	= $4.1*\rho*(\varepsilon_{crit}*\Phi_B)^{2/3}$	Batchelor [10]
Bubble Critical Diameter	Φ_{Bcrit}	[mm]	= $1'260*(\sigma_L/\rho_L)^{3/5}*\varepsilon_{crit}^{-2/5}$	$p_\sigma(\Phi_B) = p_D(\Phi_B)$ Fig. #17
Condition for Breakage	-	-	$p_D(\Phi_B) > p_\sigma(\Phi_B)$	-
Critical TEDR for Breakage of $\Phi B32$ = 4 [mm]	ε_{crit}	[m^2/s^3]	> 1.2	Φ_{B32} from 4 [mm] to 2x3 [mm]
Critical Weber Number	We_{crit}	[-]	= $\rho_L*u°_T{}^2*\Phi_B/\sigma_L$	$u°_T \approx 2*(\varepsilon_{crit}*\Phi_B)^{2/3}$
Bubble Breakage Probability Time Scale	Θ_{BB}	[s]	= $4*\Phi_B*(8.2*(\varepsilon*\Phi_B)^{2/3}-12*\sigma/(\rho*\Phi_B))^{-1}$	Batchelor [10] & experiments Fig. #18

Bubble splitting can take place if $p_D(\Phi_B) > p_\sigma(\Phi_B)$. The correlations/equations presented in Table 12, set up essentially on physical parameters and dimensional analysis, are a correct basis for a reliable engineering design of an O_3R with eddy diffusion. Fig. # 17 shows the dependence of Φ_{Bcrit} [mm] with corresponding critical ε_{crit} [m^2/s^3], where we identify the fact that a sharp increase of TKE Dissipation "TKED" Rate $\varepsilon > \varepsilon_{crit}$ [m^2/s^3] is necessary for generating bubbles with $\Phi_{B32} < 5$ [mm].

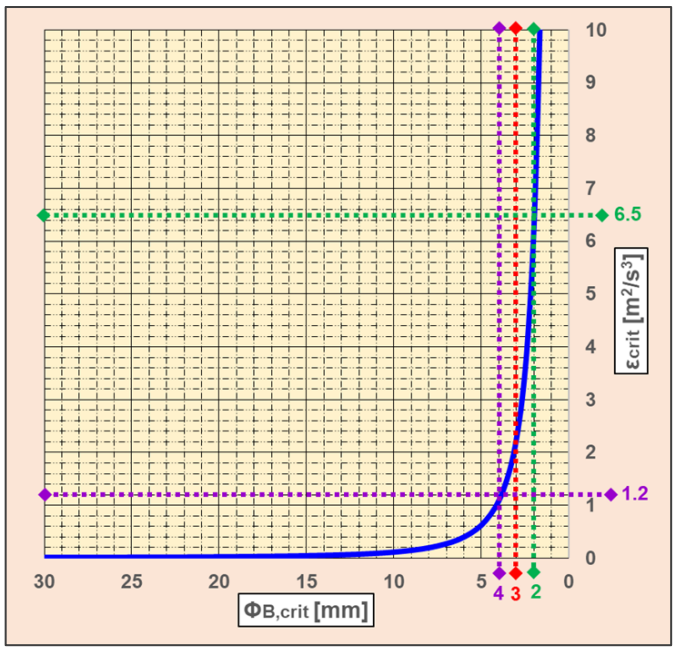

Fig. # 17 ***Critical Turbulent Kinetic Energy Rate***

For a binary splitting of a bubble with Φ_B = 4 [mm] to 2 bubbles with $\Phi_{B32} \approx 3$ [mm], $\varepsilon > \varepsilon crit = 1.2$ [m^2/s^3] is necessary (Table 12 & Fig. # 17). For a binary splitting of a bubble with Φ_B = 2 [mm], $\varepsilon > \varepsilon crit = 6.5$ [m^2/s^3] is necessary. The value of $\varepsilon > \varepsilon crit = 1.2$ [m^2/s^3] for the direct generation of a bubble with Φ_B = 3 [mm] is seldom achieved within the TBF acting inside an O_3R. This also explains and justifies the choice of Φ_{B32} = 3 [mm] as minimum/optimum bubble diameter for most of the BCs selected for ozone diffusion and other applications such as aeration systems for activated sludge.

According to Kamp et al. [32], bubble breakage can only take place if the We-Number $We_{crit} > 4.5$. [-]. This correlation can be considered as equivalent to correlation for Φ_{Bcrit}. Bubble Breakage "BB" is not immediate, it takes the time Θ_{BB} [s] in addition to the time needed by D_{EM}. The correlation for Θ_{BB} [s] is proposed by these authors [28-30]. Θ_{BB} [s] has been established by postulating, similarly to mechanical processes, that the probability of bubble breakage is proportional to the difference between the acting forces. Fig # 18 shows the time-lag Θ_{BB} [$s*10^{-3}$] profile for binary splitting of a first bubble with Φ_{B32} = 30 [mm] down to the minimum Φ_{B32} = 3 [mm]. This process is possible with ε_{BB} = 15.0 [m^2/s^3], that is an achievable value inside a free jet (see Fig. # 19, p. 38). Θ_{BB} [s] diminishes steadily down to $\Phi B32$ = 3 [mm], but then increases rapidly for $\Phi_{B32} < 3$ [mm] (Fig. # 18). Again, this observation is in accordance with what is presented on Fig. # 17. We realize that the cumulative time for splitting a bubble down to Φ_{B32} = 3 [mm] amounts to a nonnegligible laps of time.

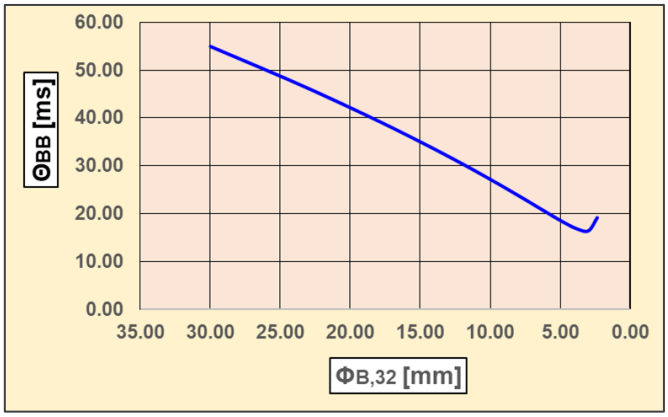

Fig. # 18 ***Temporal Binary Splitting of Bubble***

We also realize that the value of ε_{BB} = 1.2 [m^2/s^3], i.e., the minimum energy needed for bubble destabilization before binary breakage from $\Phi_{B32} \approx 4$ [mm] down to Φ_{B32} = 3 [mm] is much larger than ε_{BC} = 0.0046 [m^2/s^3], which is the actual TKED rate acting inside the TBF of our example presented later in this essay, value that is characteristic for TBF. Hence, it is evident that a homogeneous BC with Φ_{B32} = 3 [mm] cannot be achieved in the TBF of our example, which can be regarded with respect to the operation parameters as representative for typical cases. For devices able to generate bubbles with Φ_B =/< 3 [mm] to be achieved in a BC, sufficient time and a much larger internal friction head-loss will be needed so to generate the necessary $\varepsilon_{BBact} >> 1.2$ [m^2/s^3].

The conclusion is that a Homogeneous Turbulent Bubble Column "HTBC" must be generated inside an O_3R with a separate system, BC-builder, and injection with free-jet into the O_3R, aiming at a

homogeneous TBF. Such BC-builder can be a combination-series of a hydro-injector, a turbulent pipe (hindering bubble coalescence) and a free-jet. Some other systems, for example a vertical chute of multiple water/wastewater jets impinging in a closed ozone gas room on the free surface of the water/wastewater flow to be treated, can also create an initial TBF wherein the kinetic energy of the impinging water jet is almost entirely transformed into BSE. A hydro-injector is a technology which builds a Gas-Liquid Interface area, i.e., a TBF, by mixing the O_3G by aspiration into a partial vacuum generated in a contact chamber by a sharp increase in the velocity of the water/wastewater flow through an inflow orifice. The O_3G-water/wastewater bi-flux is then discharged into the O_3R at its operating pressure. In some cases, the pressure of the O_3G off the generator must be adjusted to that required by the output of the hydro-ejector, which is basically the pressure inside the O_3R. The ozone carrier gas driving water flow $V°_{DW}$ [m^3/s] needed to mix and possibly compress the O_3G is defined by its volumetric ratio to the actual ozone gas volumetric flow at operating temperature T & pressure P ($V°_{O3G}$ [m^3/s]) and the systems pressure. The consequence is head loss inside the hydro-injector resulting into a large TKED Rate ε_{HI} [m^2/s^3]. This ε_{HI} [m^2/s^3] has generally a value of several hundreds, leading to generation of bubbles with $\Phi_B < 3$ [mm]. Generally, a turbulent pipe is needed between the hydro-injector and the O_3R.

A free-jet, mono- or duo-flux (water and gas), builds itself up when a large velocity water flow discharges from a nozzle into a much slower moving water flow [33, 34]. The free-jet, in our case a gas-water bi-flux, is a shear free anisotropic turbulent flow which constructs the BC inside the O_3R down to equilibrium in the wastewater flow $V°_L$ [m^3/s] (Fig. #19). Basically, bubble coalescence takes place inside the free-jet downstream at $x/\Phi_{FJ} \approx 20$ [-] where ε_{FJ} [m^2/s^3] starts to lose value rapidly (Fig. # 20). This fact could be observed under very variable flow conditions in the turbulent pilot represented on Fig. # 8 (p.15). Equilibrium between Φ_{B32} [mm] and $\varepsilon_{BB} < \varepsilon_{crit}$ [m^2/s^3] is reached at the end of the free-jet.

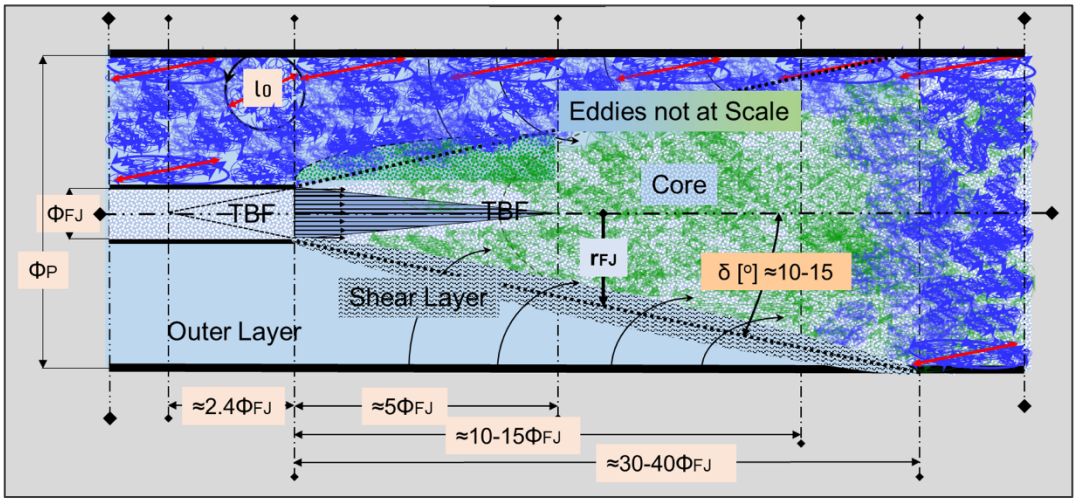

Fig. # 19 ***Free-Jet Build-up***

This equilibrium depends upon the dynamic gas hold-up in the bubble column α_{Gdyn} [%], defined hereafter. The operation parameter α_{Gdyn} [%] sets the size of the largest eddies which can exist inside the homogeneous BC in between the bubbles. Large eddies may lead to bubble coalescence and therefore α_{Gdyn} [%] must be selected optimally. Experience shows achieved stable Φ_{B32} = 3 to 5 [mm] with α_{Gdyn} = 3 to 5 [%]. Initial Turbulent Energy Production & Dissipation P_{FJ} & $\varepsilon_{FJ,i}$ are large, as compared with ε_{FJ} in the O_3R of example, but decay rapidly (Fig. # 20). The residence time in the free-jet is short.

Ultimately, this equilibrium is given by the barrier set by the sharp increase of the energy needed to split bubbles with diameters Φ_{B32} < 3 – 5 [mm] (Fig. # 17 & Fig. # 18). We name such systems BC-Builders.

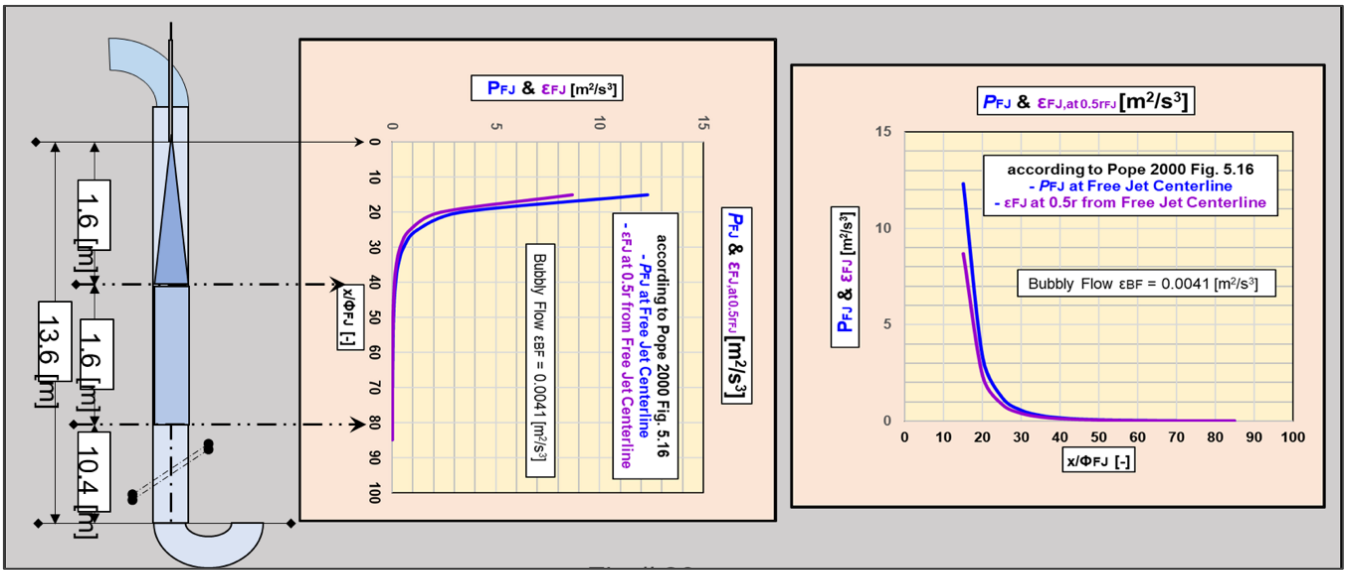

Fig. # 20 ***Free-Jet Characteristics***

BC-Builders are for example static mixers, hydro-injectors (Venturi gas injector), high-flow velocity tubes. These systems can be all combined longitudinally or radially with free-jet of initial diameter Φ_{FJ} [m], with an axial or radial discharging of the bi-flux into a broader O_3R with a hydraulic diameter Φ_{hyd} >> Φ_{FJ} [m]. These devices are designed on a much smaller dimension scale when compared with a typical PF-O_3R. They run with a combination of a Driving Volumetric Water Flow $V°_{DW}$ [m^3/s] chosen for best efficient operation in relation to the Volumetric Gas Flow $V°_{O3G}$ [m^3/s] to be bubbled into the O_3R, at optimally selected operating pressure and temperature "PT" conditions. A typical value of the volumetric flows ratio $V°_{DW}/V°_{O3G}$ [-] = 2.0. Characteristic values of ε [m^2/s^3] are 100-300 [m^2/s^3] for static mixers and hydro-injectors, generated with large head loss surface (flow division or radial mixing internals) in static mixer and high flow velocity in hydro-injector. The value of ε for a high-flow velocity tube is 10-30 [m^2/s^3]. Their Re-Number is of the same order of magnitude as Re of O_3R.

A free-jet is free of external shear forces and well-documented in the literature, qualitatively as well as mathematically with correlations [15]. The turbulence of a free-jet is non-isotropic [18] which means, quoting Batchelor [10] that "there is no direct effect of any fixed boundaries on the turbulence in the flow". The free-jet generates intrinsically its own TKE, but it merges into an O_3R with a HIT water flow. An axial free-jet (Fig. # 19), as opposed to a radial free-jet, establishes itself in the main flow direction at the outlet of a hydro-injector, a static mixer, or a high-flow velocity tube. The free-jet TKED rate varies from order of magnitude $\varepsilon_{FJmax} \approx 100$ [m^2/s^3] down to ε_{BC} [m^2/s^3] of the O_3R. It makes the hydraulic/hydrodynamic liaison between the BC-Builder and the O_3R. It fully discharges at its end homogeneously and isotropic distributed eddies (and bubbles) with their length, velocity, and time scales at a characteristic downstream distance of 22-27Φ_{FJ} from its beginning into the O_3R (Fig. # 19). The result is a homogeneous and isotropic TBF. A free-jet imposes its TBF to the main flow, meaning that the confinement for TKE scales is given by the volume of the liquid bulk existing between the bubbles.

The TKE of the free-jet is generally not entirely dissipated at 22-27Φ_{FJ} downstream distance. As per Fig. # 20 the full dissipation of the free-jet can take up to 80Φ_{FJ} downstream. This means that after full merge of both fluxes, the resulting TKE is carried by the O_3R TBF. The value of the cone angle δ [°] depends upon the difference of density between the two-phase gas-liquid free-jet and the receiving main flow.

With the here above recommended Liquid-Gas Volumetric Flows Ratio $V°_{DW}/V°_{O3G}$ = 2.0 [-] for a Hydro-Injector, δ ≈ 13 [°] corresponds to a total length of ≈ $23\Phi_{FJ}$ [34]. Since there are no external forces acting on the free-jet, its flow of momentum remains constant. Its mean flow kinetic energy lost is transformed almost entirely into TKE, as per Fig. # 2 0. At the end of the free-jet, its final TKE is established and transferred to the main flow. Fig. # 20 uses the values of the example presented hereafter and shows the ratio between the free-jet TEDR $\varepsilon_{FJ}/\varepsilon_{BC}$ [-], established with data from the literature [15], applied on the left side to the example treated in section 13 "**Turbulence in the voids between the bubbles of a TBF"** hereafter.

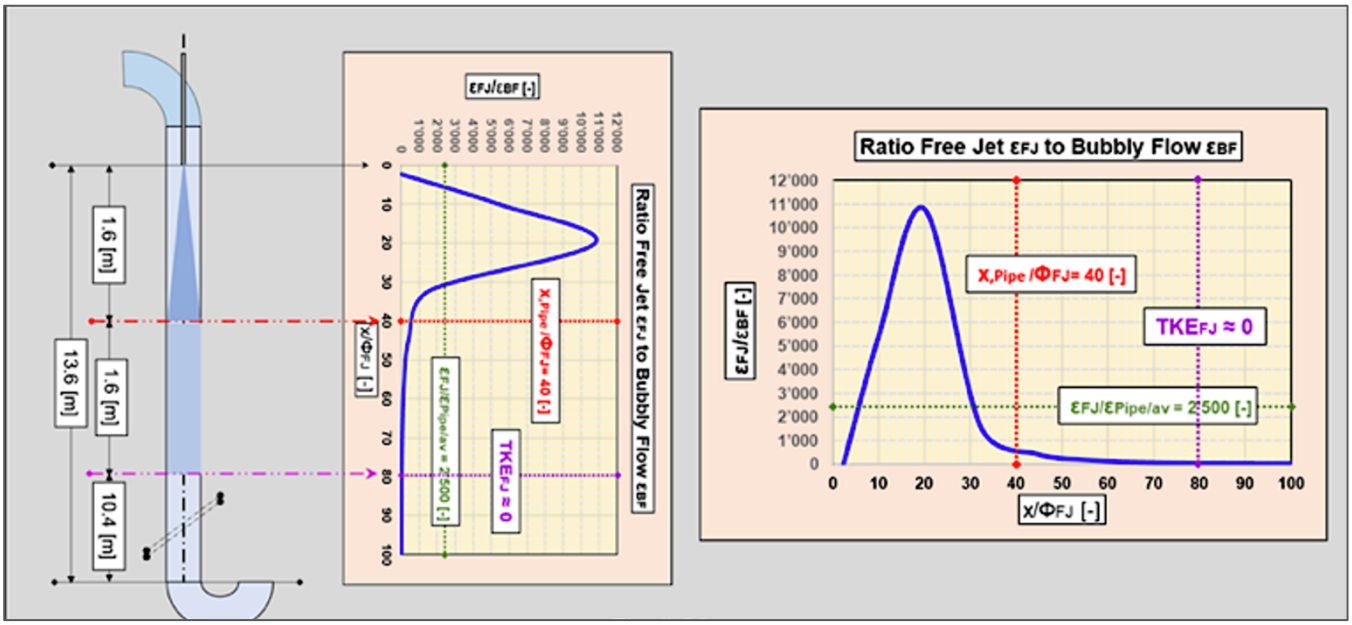

Fig. # 20 Free-Jet Characteristics

As already mentioned, ε_{FJ} [m^2/s^3] is much larger than ε_{BC} [m^2/s^3]. This is caused by the dynamic activation energy Δ. Since the free-jet and the main flow are flowing in the same direction, such a gas-water bi-flux O_3R must be designed with hydraulic pattern co-current downstream or upstream. Co-current "CC" means that both volumetric flows $V°_{DW}$ & $V°_{O3G}$ [m^3/s] go in the same direction. Counter-current "CtC" means that the volumetric flows $V°_{DW}$ & $V°_{O3G}$ [m^3/s] go in opposite directions. $V°_{DW}$ [m^3/s] downwards and $V°_{O3G}$ [m^3/s] upwards out of physical necessity. However, the slip velocity $v°_B^{\infty}$ [m/s] of bubbles in the water is always upstream. $v°_B^{\infty}$ [m/s] of a bubble with Φ_{B32} ≈ 3.0 [mm] equals in wastewater $v°_B^{\infty}$ approximately 0.25 [m/s], verified experimentally in TBF i.e., swarm of bubbles (see Fig. 21 constructed based on general information available in the literature). In a permanent downstream bi-pattern, a main flow superficial velocity $v°_W$ > 0.3 [m/s] is required under any operation situation. If this cannot be achieved with the system design, a combination of downstream-upstream operation mode with two injection systems can be engineered, as per the example presented hereafter.

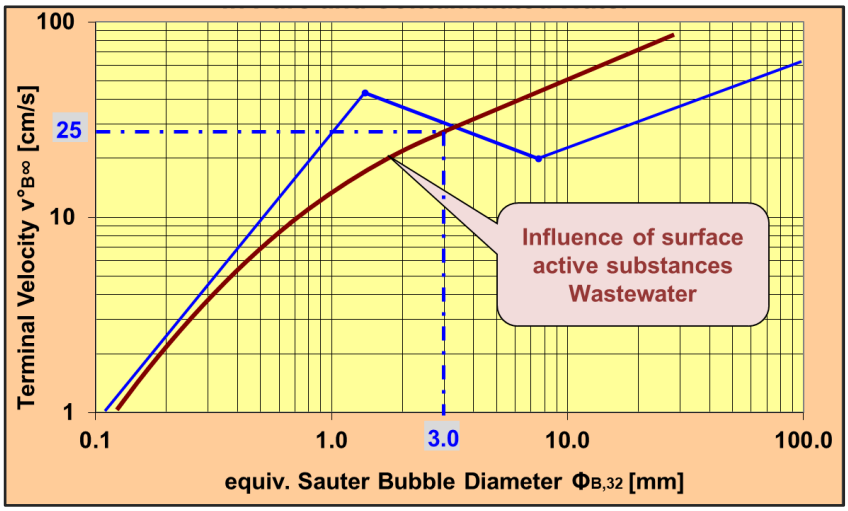

Fig. # 21 ***Bubble Slip Velocity / Terminal Rising Velocity in pure and contaminated water.***

A radial free-jet system, consisting of several free-jets with appropriate semi-radial-tangential design situated along the perimeter of the O_3R conduit can also be implemented, as presented in the example hereafter. Such an arrangement allows for a CtC Gas-Liquid bi-flow pattern. Due to the high value of ε_{BB} [m^2/s^3] in the free jet (but short residence time), diffusion of ozone and reaction will take place in the free-jet-generating system, which will not be considered and will lead to a conservative design. The dynamic gas retention or hold-up α_{Gdyn} [%], based on superficial velocities and bubble split velocity, and their directions, shall be considered. It will be larger in the down-flow mode and smaller in the up-flow mode as compared with static hold-up, based on instantaneous volumes or volumetric flows. The value of α_{Gdyn} [%] has a direct impact on the distance d_{BB} [mm] between the bubbles in the bi-flux, hence on the equivalent diameter Φ_E [mm] of the largest eddies and therefore on their TKE.

The CC-DF hydraulic mode needs special attention in design, because of the risk of gas embolism when DF $v°_{W/WW}$ starts to approach $v°_{B}\infty$, resulting in an obstruction to the free O_3G-Flow in the O_3R and leading to theoretically infinite α_{Gdyn} (Table 13). In such a case, a combination of CC-DF and CtC-DF must be implemented in the Design, see Paragraph 16 System Design with Overall Chemical Reaction in a TBF.

Table 13 Co-Current/Counter-Current Hydraulic Modes & Dynamic Gas Retention

Parameter	Symbol	Unit	Correlation / Equation	Comment
Co-Current	CC	-	-	$V°_{O3G}$ & $V°_{W/WW}$ same directions
Counter-Current	CtC	-	-	$V°_{O3G}$ & $V°_{W/WW}$ opposite directions
Hold-up	α_{Gdyn}	[%]	$= v°_G /(v°_W+v°_B{}^{\infty})*100$	Dynamic Hold-up
O_3G	$v°_G$	[m/s]	$= V°_{O3G}/S_{O3R}$	Superficial $V°_{O3G}$ Velocity at O_3R Temperature T and Pressure P
W/WW	$v°_{W/WW}$	[m/s]	$= v°_{W/WW} /S_{O3R}$	Superficial $V°_{W/WW}$ Velocity
Bubble	$v°_{B}\infty$	[m/s]	$= f(\Phi_{B32})$	Fig. # 21

Parameter	Symbol	Unit	Correlation / Equation	Comment
Reference	$v°_{W/WW}$	[m/s]	> 0 < 0	W/WW-Flow Up-Flow “UF” W/WW-Flow Down-Flow “DF”
	$v°_{B\infty}$	[m/s]	always > 0	Buoyancy Absolute Terminal Bubble Slip or ascending Velocity
Hydraulic Modes	CC-DF	-	$- v°_{W/WW} > v°_{B}{}^{\infty}$ $v°_{G} < 0$ $- v°_{W/WW} = v°_{B}{}^{\infty}$	$V°_{O3G}$ carried DF by $V°_{W/WW}$ Gas Embolism, $\alpha_{Gdyn} \rightarrow \infty$
	CtC-DF	-	$- v°_{W/WW} < v°_{B}{}^{\infty}$ $v°_{G} > 0$	Typical for Porous Diffusors
	CC-UF	-	$v°_{G} > 0$ / $v°_{W/WW} > 0$	Typical for Porous Diffusors

In a homogeneous and isotropic TBF, some authors claim to have determined some turbulence suppression as compared to a normal TWF. All measurements and observations which were made with TWF in transparent pipes, as defined in this essay and that are described in the literature, show that the production of TKE, taking place mainly inside the Integral Range “ITR”, is entirely confined within the inner layer of the wall layer. The wall layer makes the transition to the homogeneous and isotropic turbulent outer layer, as is the case with the bulk of the TWF. Considering the size of the eddies within the Integral Range “ITR” where TKE is generated, it means that these eddies must be oblong and narrow, even streaks according to some literature, due to stretching by the bulk mean FT flow (see Fig. #12 at p.20). This stretching by the mean flow is a stress acting on the large eddies leading to their first splitting towards the Inertial Range “INR”. Once the TBF is installed inside the TWF at the end of the free jet, the non-slip condition along the wall of the pipe still applies. The fact that the TKE of the free jet is much larger than the TKE of main flow means that it will impose its bi-flux structure existing at its end to the BC in the main flow. The size of the largest eddies in a TBF, Φ_{Emax} [mm] defined hereafter, is given by the size of the water bulk volume existing in between the bubbles, INR, it depends therefore upon the value of the gas hold-up

Coalescence of bubbles shall be addressed [32, 35-39]. In a homogeneous stable BC, there is an equilibrium between the stress $p_D(\Phi_B)$ [Pa] exerted by the TKED Rate ε [m^2/s^3] on the surface of a bubble and the BSE restoring pressure $p\sigma_L(\Phi_B)$ [Pa]. The smaller Φ_{B32}, the larger the size Φ_E of the eddies in the water or wastewater bulk around the bubbles. Hence, smaller bubbles can easily be taken into the inside swirling mouvement of these eddies. This phenomena can lead to coalescence of bubbles with the consequence of a lowering of the systems Gibbs surface energy, i.e., towards equilibrium.

Since there is no change of local volumetric flow of the O_3CG, the released energy is mainly a back-gain of TKE. However, if the BC is homogeneously distributed and isotropic inside a HIT waterflow, each bubble is statistically pushed-pulled by the surrounding eddies in all directions with zero resulting force (right picture on Fig. # 22 and Fig. # 23 hereafter). The left picture of Fig. # 21 shows the free-jet with its surrounding side turbulence building its TKE.

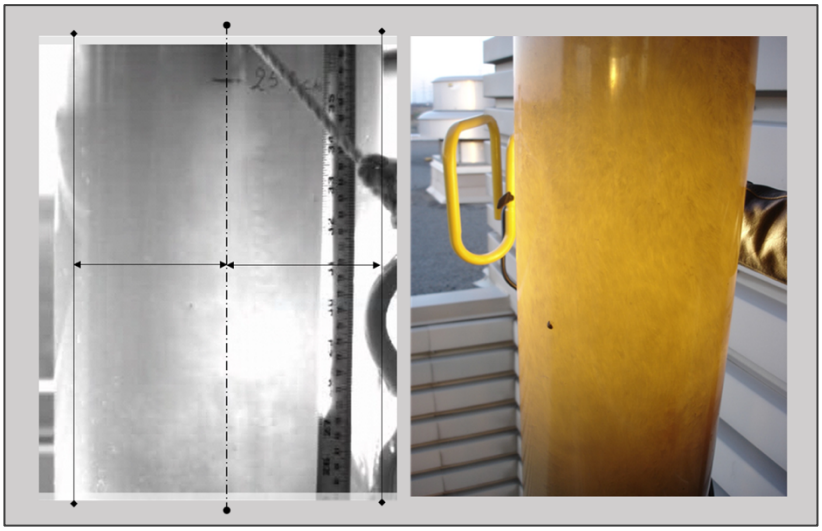

Fig. # 21 ***Free jet (left) and Turbulent Homogeneous Bubble Column (right)***

In particular in BCs with hold-up $\alpha_{G,kin}$ > 1 [%], which is charateristic in O_3R BCs, the surrounding eddies are too small. They therefore do not have enough energy to displace rising bubbles with $\Phi_{B32} \approx 3$ [mm] and their added mass, more so since this added mass is turbulent, being part of the surrounding turbulent eddies. The above assumptions are confirmed by observations, as showed also by Fig. #6 repeated here, showing individual BCs generated with porous diffusors in two potable water treatment plants.

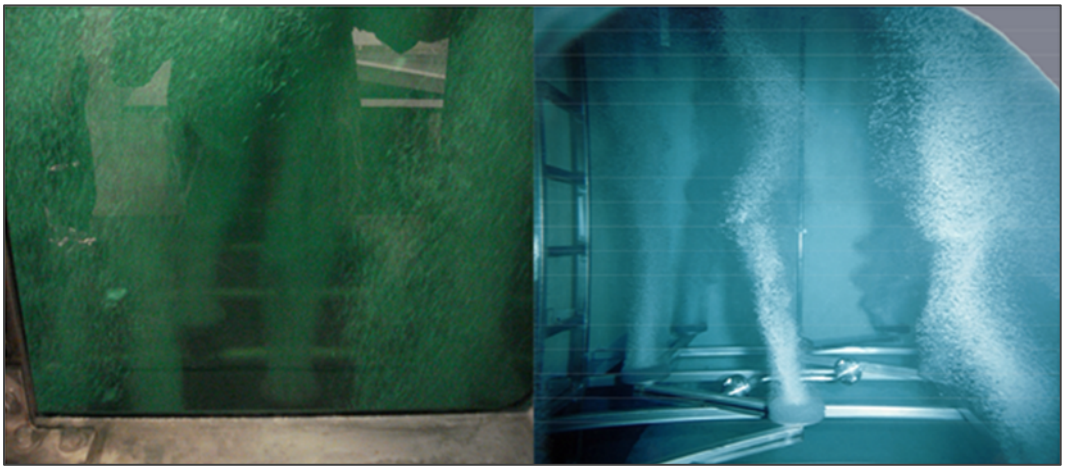

Fig. #6 Ozone Reactor with Porous Diffusors

These BCs, with $\Phi_{B32} \approx 3$ [mm] are released into a surrounded TWF. The diameter of the largest eddies in the liquid bulk separating the bubbles within the BCs equals approximately $2*\Phi_{B32} \approx 6$ [mm]. No coalescence can be observed. However the vertically divergent cylinder of each BC hints to some bubble dispersion (macro-diffusion), in accordance with the rate value of the order of $D_B \approx 0.2*10^{-3}$ m^2/s, as published in the literature. We can also see the influence of some macro-turbulence. The process of bubble coalescence is physically more complex to be addressed and described mathematically with correlations. Several physical parameters are to be qualified and quantified, among others:

- buoyancy;
- differential bubble slip velocity, hence different bubble diameter;

- turbulent wake of head bubble, which can be neglected in a BC with constant Φ_{B32} [mm] and with narrow standard deviation of the bubble size gaussian distribution;
- velocity of collision of both bubbles;
    - immediate bouncing away from each other after collision or not, depends upon the surrounding eddies.
    - In a HIT-TBF these velocities equal zero since the resulting sum of the push-pull actions of the surrounding eddies on the bubbles equals statistically zero.
- contact time between colliding bubbles;
    - the contact time must be larger than the drainage time necessary to eliminate the capillary action between the contacting surface of the bubbles for coalescence to take place.
- film drainage time between two colliding bubbles needed to thin and expell the capillary contact film;
- repulsive electrical surface charge of the bubbles in WW applications, due to adsorbed DOM, generally negative, similarly to colloids (NOM) in surface water, can be assimilated to a Zeta-Potential;
- bubble-surrounding eddies must be large and have enough TKE.

In a HIT-BC, one can assume that statistically the distribution of the bubbles in TBF is a 3-D Gaussian. We can consider, for design purposes, that the volume distribution of the bubbles in a TBF is tetrahedral. It has been observed in the fully turbulent pilot plant (Fig. # 8, p.6), under variable flow conditions, i.e., under variable turbulence intensity, that in a stable-built HIT TBF bubbles are agitated along the wall of the O_3R under the influence of the larger eddies of the ITR. In that case, breakage was observed, but no coalescence could be seen. Obviously, conditions for coalescence are not, or difficult, to be satisfied, at least in wastewater because partly of the negative electrical charge existing at the surface of the bubbles. For two bubbles to coalesce, they must first be transported by surrounding neighbor eddies rotating in opposite directions (Fig. # 22). This is statistically rather improbable in a HIT TBF.

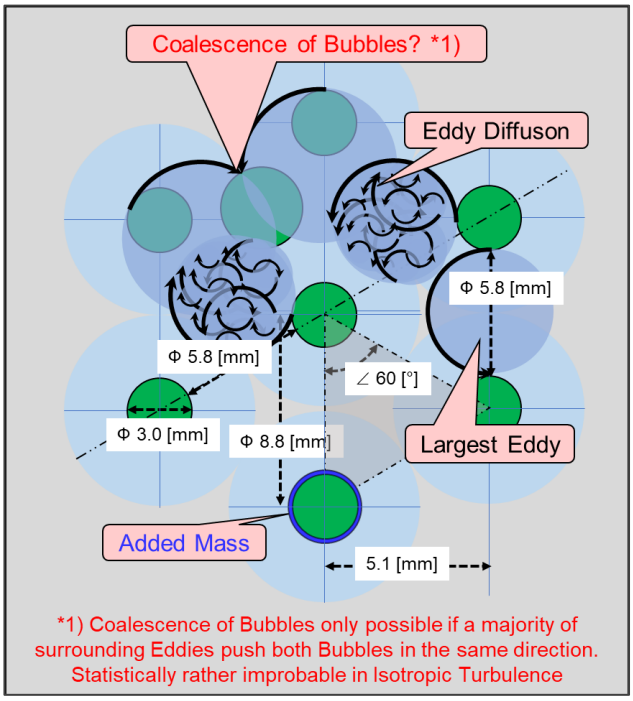

Fig. # 22 *Bubble Coalescence*

13. Turbulence in the voids between the bubbles of a TBF

We assume that homogeneous and isotropic turbulence “HIT” exists in the liquid situated in the voids between the bubbles of the TBF Bubble Column. This is an acceptable assumption since, as will be presented hereafter, the eddy with the size Kolmogorov “KS” is much smaller than the smallest scale of the inter-bubble liquid bulk. We assume that this turbulence is continuously regenerated and contributing fully to Eddy Diffusion D_E [m^2/s], because an HIT-BC has been completely constructed in the main flow inside the BC-Building stage with hydro-injector and free-jet in the intake of the O_3R. Of the essence is the largest possible size of an active inter-bubble eddy. The bubbles under the effect of buoyancy move vertically with their slip velocity $v°_B{}^{\infty}$ [m/s] inside the HIT TBF. The surrounding eddies larger than the smallest distance between neighbor bubbles should therefore stretch the bubbles, which would result in surface energy. This cannot be in a stable HIT TBF because the energy of the TEDR of the surrounding eddies is too weak based on the arguments developed in section 11 here above. The mean force-action on the surface of the bubble of each surrounding eddy is statistically equal in all directions. Observation shows that in a HIT TBF, the shape of the bubbles stays practically solid, almost spherical.

Eddy stretching close to the O_3R confining wall is the beginning of TKE dissipation cascade leading to the generation of smaller eddies, hence we assume that this stretching leads to splitting. Since the entropy of the turbulent system cannot decrease without addition of some energy to the system by an outside action, eddy coalescence cannot take place in the voids between the bubbles. We assume therefore that the largest possible eddy cannot have a diameter Φ_{Emax} [mm] larger than the smallest distance d_{BB} [mm] between 2 neighbor bubbles (Fig. # 23).

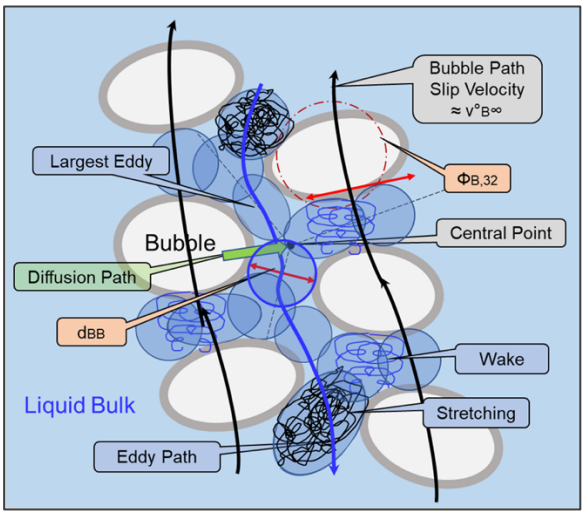

Fig. # 23 *Bubbles, Eddies and Diffusion Path Swarm*

From the point of view of sound engineering design this assumption is conservative, since, as will be described in the next chapter the value of eddy diffusivity, E_D [m^2/s] depends directly on the value of the diameter Φ_{Emax} [m] of the largest eddy of the HIT TBF. The width of this passage depends upon the Gas Hold-up $\alpha_{G,kin}$ [%] in the HIT TBF, is typically of the order of d_{BB} = 5 to 7 [mm] with $\Phi_{B32} \approx 3$ [mm] in a stable HIT TBF. All bubbles contribute also with their wake turbulence to eddy diffusion into the water bulk between them. The average diffusion distance d_{Diff} [m] for design is the one separating the central point of the liquid Bulk from the surface of the bubbles, based on a homogeneous bubble distribution

(Fig. # 23 & Fig. # 24). The diffusion areas of all surrounding bubbles overlap in the region of the central point.

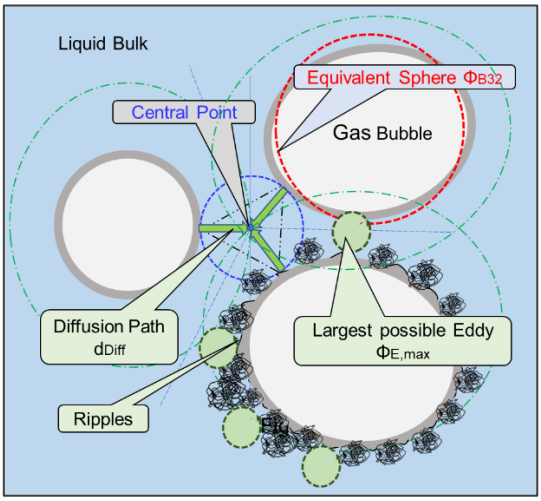

Fig. # 24 *Eddy Diffusion Path*

This raises the question about the friction head-loss created by the BC rising with the overall slip velocity v_B^{∞} = 0.25 [m/s] for Φ_{B32} = 3.0 [mm] in a TBF and TKE generated in the wake of the bubbles. As already said, in a TBF, the bubbles are pushed-pulled by the surrounding eddies in all directions with zero resulting force. This is also true for the surface deformation action of the surrounding eddies. It is therefore reasonable to assume that the bubbles will keep an average rigid shape and that this shape will not be very much different from a sphere, as confirmed by observations. The surrounding eddies will however generate ripples on the surface of the bubbles (Fig. # 24), meaning an energy demand.

These ripples will contribute to turbulent diffusion at the immediate surface of the bubbles, defined and calculated as per Glaeser and Brauer [40]. More so, it can be assumed, that the Re-Number to be considered is not the Re_B [-] of the bubble/sphere based on its Slip Velocity v_B^{∞} = 0.25 [m/s] in a laminar/quiet water flow, but the Re_L [-] imposed by the TBF on the bubbles, since all bubbles are surrounded by this turbulence. We always will have Re_L > 10'000 [-] in a TBF. Hence, we can take the gas bubble friction coefficient in water/wastewater $\xi_B = C_D$ = 2.5 [-] (Fig. # 25).

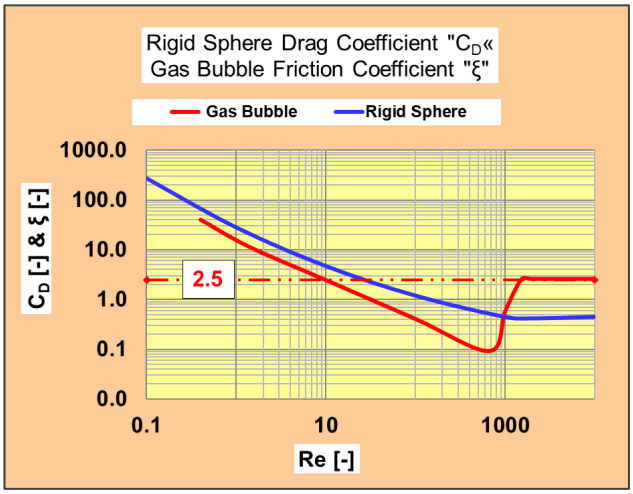

Fig. # 25 *Gas Bubble Friction Coefficient*

As a parenthesis about head-loss in a TBF, and not to be forgotten, is the fact that in a CC Downstream Bi-flux, the O_3G is being compressed by the water flow, assumed isothermally. Herewith a summary of waterheads to be taken into consideration, added to the TKE Head loss, i.e., compression energy of the O_3G, TBF additional head-loss, friction, and wake and gas hold-up, as well in the free jet as in the O_3R. These waterheads are necessary to correctly determine the water surface level and total energy line upstream the O_3R.

Similar with a free jet, the turbulence in the wake of a bubble is non-isotropic and shear free [18]. Based on measurements conducted on BCs, authors [18, 41-43] propose simple correlations for the determination of the pseudo-TKE “TKEw” generated in the wake of the bubbles with the HIT TBF. The turbulence induced by the wake of the bubbles in a BC is included in the TBF head-loss, which also contributes to the generation of TKE. This wake turbulence also contributes to homogenization of the dissolved ozone. More so, it compensates for dilution due to the spherical diffusion pattern out of the bubble, as will be addressed later in this document. The measurements show that the TKE self-generated in the wake has a low value in comparison with the TKE of the TBF.

The next question is, what turbulent range and scales shall be considered for quantifying the Eddy Diffusion D_E [m^2/s]?

We propose the following approach. Calculations show that for most cases of a HIT BC in a TBF the size of the largest eddy will fall into the Taylor Range “TR”. HIT within the Inertial and Taylor Ranges, down to the Kolmogorov Scale, is therefore considered for Eddy Diffusion D_E. This means that only part of the TKE will be dissipated as TKE carried by the smaller eddies, the rest of TKE being simultaneously dissipated as heat.

In the core of a HIT TWF reasoning, it says that since all eddies are considered being homogeneously embedded with and within each other, D_E [m^2/s] to be chosen shall be that corresponding to the largest eddy which exists in this TWF. However, in a HIT TBF with a homogeneous BC there is a domain restriction given by the presence of bubbles. Therefore, since all eddies contribute to diffusion, we will in this conservative design approach select an average Eddy Size Φ_{EDiff} [m] between Φ_{Emax} [m] and Φ_{Emin} [m], corresponding to the KS-Scale, and only its fraction of turbulent energy still existing as TKE for the quantification of D_{Eav} [m^2/s].

14. Mass Transfer Coefficient

The corresponding mass transfer coefficient k_{mtE} [m/s] will be determined with the surface renewal model, proposed by Danckwerts, in a well-mixed semi-infinite slab, by applying as diffusion coefficient D_E [m^2/s] (Fig. # 26) [7, 44]. The penetration model, with consideration that the whole water/wastewater bulk in the voids between the bubbles is HIT, could also be considered, leading to values of D_E [m^2/s] approx. 12% larger. However, we consider the surface renewal model as more accurate because the eddies acting at the gas to liquid Interface at the water/wastewater side represent a real surface renewal. Homogeneous and isotropic turbulence in the water/wastewater bulk in between the bubbles justifies the use of this model. This model assumes the presence of two regions:

1. A bubble to liquid interface region where small liquid contact elements, i.e., in our case smaller turbulent eddies, are saturated with ozone by their own D_E [m^2/s]. These smaller eddies are swept away from the interface into the bulk of the inter-bubble liquid by the larger eddies.
2. The fully turbulent region which consists of eddies of several sizes within the universal range.

The use of this model is also justified by the physical fact that the relevant parameters can be given a value, as presented in Table 14. More so, D_E [m^2/s] selected for design is an average value resulting from the full range of eddies active in the water bulk in between the bubbles and hitting them, contributing to diffusion, Fig. # 26. Considering a turbulent homogeneous and isotropic diffusion field, it can be assumed that the surface of the bubbles is statistically swept by eddies of all sizes existing in this field.

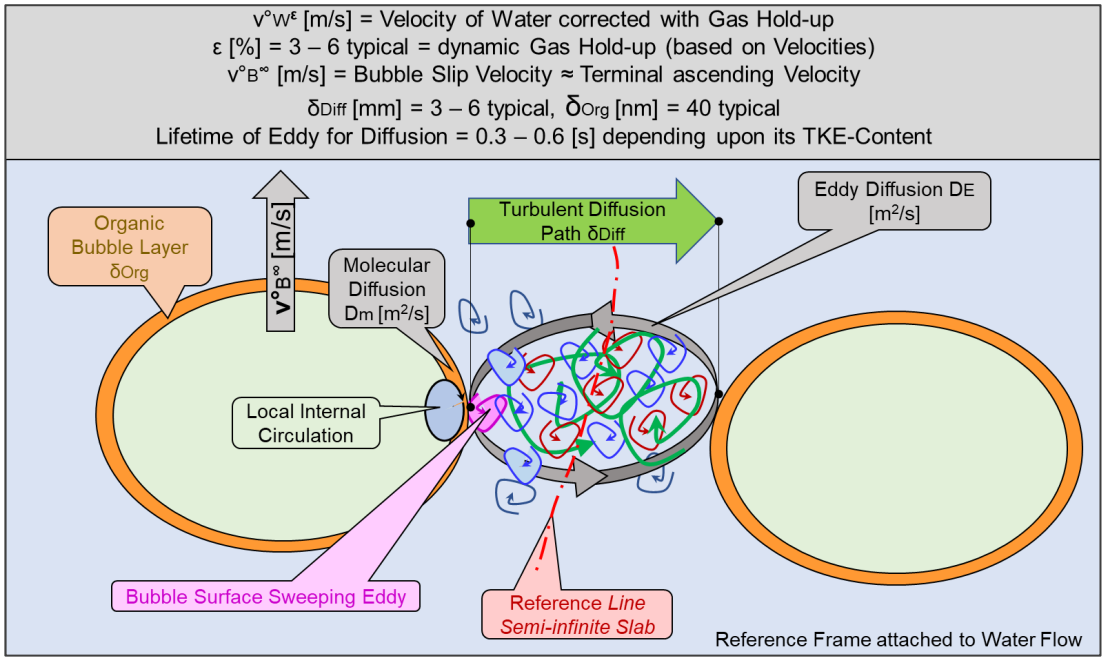

Fig. # 26 *Danckwerts Surface Renewal Model*

One can argue that the Law of the Wall should apply between the surface of a bubble and eddies sweeping it, i.e., the non-slip condition. This condition applies to a solid fixed non-moving surface, swept by water flowing freely with a much lower density, such as in a pipe. However, considering the densities of gas and water involved, the opposite situation exists. As already mentioned, the surface layer of the bubble will be locally hit, pushed & pulled by the sweeping eddies, leading to bubble surface waves and

deformation, bubble internal circulations and turbulence according to Glaeser and Brauer [40], as well as local displacement of surface-active substance, similar to the Marangoni effect.

Table 14 Main Parameters applicable to the Surface renewal Model by Danckwerts

Parameter	Symbol	Unit	Correlation / Equation	Comment
Mass Transfer Rate	$R°$	[g/m^{2}s]	= k*[c*-c°]	Higbie / Danckwerts Models [7]
Reactant Concentration	c*	[g(m^3]	-	At the Liquid Side of Gas to Water/Wastewater Interface
Reactant Concentration	c°	[g(m^3]	-	In the Bulk of the Water/Wastewater HIT Full Mix Phase
Mas Transfer Coefficient	k_{mtE}	[m/s]	$=(D_E*s)^{0.5}$	Eddy Mass Transfer Coefficient [7]
Eddy Diffusion Coefficient	D_E	[m^2/s]	$\approx/= 0.02\Phi_{E*}(\varepsilon_*\Phi_{E\kappa})^{1/3}$	See Section 16 Eddy Diffusion DE
Surface Replacement Rate	s	[s^{-1}]	$= v°_B{}^{\infty}/\Phi_{B32}$	Stable Bubble Size Stable Turbulent Bubbly Flow TBF Stable Slip Velocity
Bubble Slip Velocity	$v°_B{}^{\infty}$	[m/s]	= 0.25	Wastewater Fig. #21
Bubble Sauter Diameter	Φ_{B32}	[m]	= 0.003	System Design Choice

As a final point, turbulence suppression by a BC, suggested in some literature, can be ignored because this suppression takes mainly place in the narrow region along the systems wall and the sublayer (Law of the Wall).

15. Diffusion from a single ozone gas bubble towards the bulk of water

The full diffusion path for ozone starts in the gas phase i.e., inside the bubbles. In wastewater, unlike in potable water, the gas bubbles are generally coated by a film of organic material, which is a barrier towards diffusion (Fig. # 26, repeated hereafter). This is qualitatively and quantitatively non-negligible for the correct calculation of diffusion from a gas bubble towards the surrounding liquid. We try to quantify this fact by considering as surrogate organic the protection wall of a "Gram-Positive" bacteria made of Peptidoglycan as representative example for such an analysis. We select a layer thickness of 40 [nm], as per Gaudy [2].

Measurements show that the molecular Diffusivity of Ozone D_{mO3} [m^2/s] in such a polymer can be taken with a value equal to 60% of $D_{mO3} = 1.74*10^{-9}$ [m^2/s] in water, which is approximately $1.0*10^{-9}$ [m^2/s]. The corresponding $k_{mt} = 0.026$ [m/s], based on the film model [7]. We can also assume that the resistance to diffusion inside the bubble is negligible, since there is internal gas circulation as argued about in the precedent section. Hence, the resistance to diffusion of ozone from the bubble out into the bulk of the liquid will be made by two components in series, in the bubble coating layer and in the turbulent liquid.

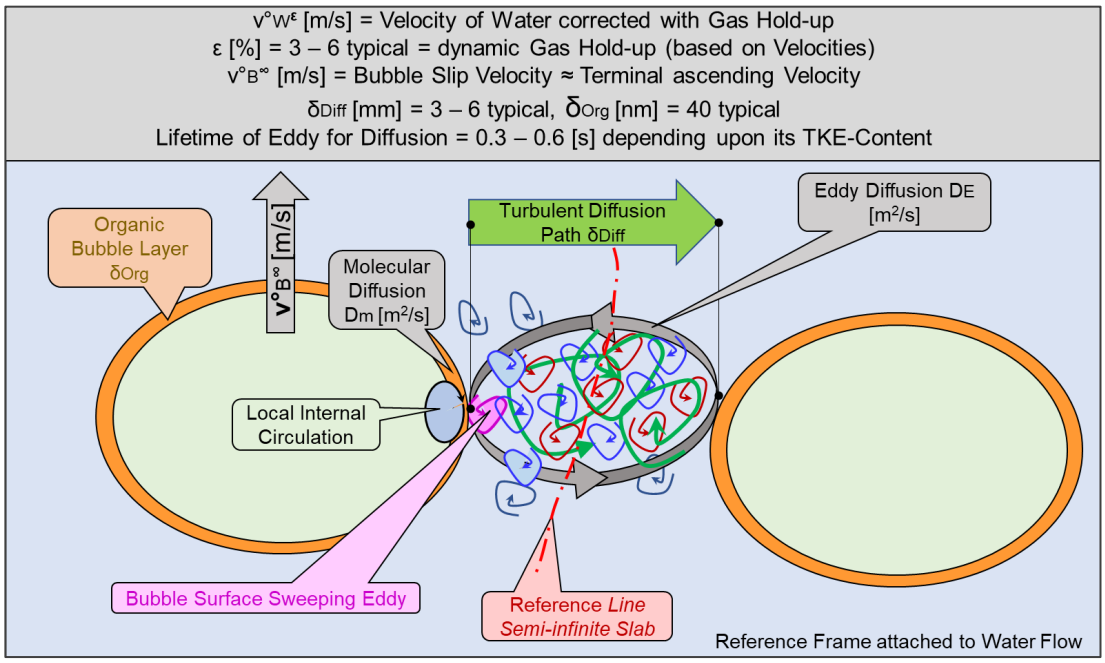

Fig. # 27 *Danckwerts Surface Renewal Model*

16. Eddy Diffusion D_E

This section reports information stemming from the following basic references, among them Sherwood et al. [45], Treybal [46], Levenspiel [47], Danckwerts [7], Kolmogorov [21], Kraume [48], Glaeser and Brauer [40] and others [10, 18, 23, 26, 49].

Diffusivity, D_m & D_E [m^2/s], is defined as the velocity of displacement of a particle in a medium multiplied by a defined resulting minute linear distance travelled between two points by this particle through the action of its velocity vector range. Diffusion is the effect of diffusivity on the travelling in time of this particle in its solvent medium under the presence of a gradient of concentration of this particle in this medium and the effect of a certain agitation in this medium. The agitation can be caused by thermal molecular agitation, hence Molecular Diffusion D_m [m^2/s] and/or induced by axial-longitudinal and radial turbulence inside a pipe, hence identified in this essay as Eddy Diffusivity D_E [m^2/s] caused by eddies, as named, and described in section 10 "**Turbulent and Fully Turbulent Water Flow TWF / FTWF**", here above. D_m [m^2/s] is independent of position in the diffusion space and depends only upon the system's temperature and viscosity. D_E [m^2/s], to the contrary, is independent upon the system's temperature, but depends upon the local scales of turbulent agitation inside the diffusion system. It is therefore position-dependent; hence its strength is affected by the size and the velocity of the eddies of local TKE.

Eddy Diffusion D_E [m^2/s] acts directional in a homogenous system, for example axial-longitudinal or radial, and all-directional in a homogeneous and isotropic system. In the case of a HIT-TBF, D_E [m^2/s] acts in all directions of the TBF (a) within an eddy and (b) from eddy to a neighboring eddy, i.e., 3-D. In a HIT environment D_E [m^2/s] depends only upon the system's TEDR and the size of the locally acting eddies in the diffusion space. $D_{E\kappa}$ [m^2/s], referencing D_E [m^2/s] to the size of eddy with wavenumber κ [m^{-1}], is defined and quantified based on following statistical approach [23]. Consider a patch of scalar material in solution in water and spreading under the effect of diffusion (Fig. # 27). The concentration of material in this initial patch is not homogeneous. Inside this patch $D_{E\kappa}$ [m^2/s] of eddies smaller than the patch size can contribute over a short time to concentration peaks, but statistically mainly to material dilution. Inside this patch D_m [m^2/s] contributes to smoothen the local and much smaller-scale heterogeneity and concentration peaks, proving its importance in the whole diffusion process. Physical contact with neighbor eddies, i.e., within the Turbulent Energy Cascade "TEC", tears eddies apart and enhances this phenomenon by transferring dissolved material from eddy to eddy.

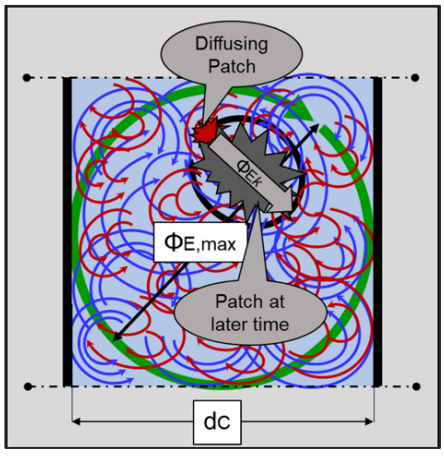

Fig. # 27 ***Turbulent Diffusion Patch [22]***

From an engineering design for an HIT diffusion system point of view, eddy diffusivity can be defined based on the following approach, with hint to the references mentioned above, based both on dimensional analysis and diffuse spreading.

One half-turn of eddy with diameter $\Phi_{E\kappa}$ [m] moves a small chunk of this first patch one eddy diameter $\Phi_{E\kappa}$ [m] to its new furthest away position, simultaneously stretching and diluting the scalar patch. During the same laps of time, eddy diffusivity $D_{E\kappa}$ [m^2/s] of smaller and larger eddies inside and surrounding the eddy-displacing chunks within this patch, contributes to increasing the patch size and to diminishing its average scalar concentration. Its peaks are simultaneously smoothed through molecular diffusivity D_m [m^2/s]. The patch size growth is considered being equal to the average displacement of a particle under the action of $D_{E\kappa}$ [m^2/s], according to the Random Walk Analogy [22, 23]. Based on the Random Walk Analogy, the increased size $\Phi_{P\kappa}$ [m] of the patch (equivalent diameter) under influence of diffusion is estimated to correspond to 95 % of a Gaussian Concentration Distribution (as verified experimentally) with the following parameters and assumptions:

- σ_{PDF} [m] is the standard deviation of a Gaussian concentration distribution in a patch of size $\Phi_{P\kappa}$[m]
- During the half-turn of an eddy with wavenumber κ [m^{-1}], a patch particle is carried a distance $\Phi_{E\kappa}$ [m] away, stretching simultaneously in all directions more or less equally, meaning that $\Phi_{P\kappa}$ [m] = $\Phi_{E\kappa}$ [m]
- Turnaround time of an eddy with a wavenumber $\Theta_{E\kappa}$ [s] is the time it takes for an eddy to make one complete turn on itself.
- $u°_{E\kappa}$ [m/s] is the eddy orbital velocity, defined based on physical parameters, corrected with a constant stemming from laboratory experiments.

Physically, since the half-turnaround time $0.5\tau_{TE\kappa}$ of this eddy equals approx. 30 [%] of its decay time $\tau_{DE\kappa}$, see section 11 "**Mathematical Proof of the Universal Law of Turbulence**", $D_{E\kappa}$ [m^2/s] has the time to fully act. Summarizing the above assumed facts, the correlations and formulas hereunder are the basis for the development of a design method of a BC for diffusion of ozone, and oxygen, in a TWF (Table 15).

Table 15 Main Parameters applicable to Eddy Diffusion

Parameter	Symbol	Unit	Correlation / Equation	Comment
Eddy Diffusivity	$D_{E\kappa}$	[m^2/s]	$\approx/= 0.02(\varepsilon_* \Phi_{E\kappa})^{1/3}$ $\approx/= 1/16\pi*\Phi_{E\kappa}* u°_{E\kappa}$	Random Walk Analogy [22, 23]
Scalar Patch Diameter	$\Phi_{P\kappa}$	[m]	$= 4\ \sigma_{PDF} = \Phi_{E\kappa}$	Random Walk Analogy
Standard Deviation	σ_{PDF}	[m]	$= \sqrt{(2\ D_{E\kappa}*\Theta_{E\kappa}/2)}$	Random Walk Analogy
Eddy Diameter	$\Phi_{E\kappa}$	[m]	-	Wave Number κ
Eddy Turnaround Time	$\tau_{TE\kappa}$	[s]	$= \pi* \Phi_{E\kappa}/u°E\kappa$	

Parameter	Symbol	Unit	Correlation / Equation	Comment
Eddy Orbital Velocity	$u°_{EK}$	[m/s]	$\approx/= 0.95(\varepsilon*\Phi_{EK})^{1/3}$	Kolmogorov Experiments [21]
TEDR	ε	[m^2/s^3]	-	TEDR "Turbulent Energy Dissipation Rate"

Important is to realize that eddies are associated to spheres in a homogeneous and isotropic system. So, the above description of D_E must be understood as acting in all-directions inside the 3-dimensionnal environment. In a TF, the above correlations show that the largest eddy diffusion D_{Emax} [m^2/s] happens with the largest possible Φ_{Emax} [m], which corresponds to the largest systems confinement distance d_C [m], of the order of scale ≈ Φ_P [m] or Φ_{hyd} [m] of the conduit. In a homogeneous TBF, the largest eddy diffusion D_{Emax} [m^2/s] corresponds to d_{BB} [m] (Fig. # 23, p.45). This fact shows that D_{Emax} [m^2/s] is much smaller in a BC as compared with the Pipe without BC.

At this point and from a chemical engineering point of view, it is necessary to have a good quantitative idea about dimensional scales (Fig. # 28) of the distances between particles and reactants under consideration and the different turbulence ranges and scales, with the assumption that the system is completely homogeneous and isotropic HIT, as discussed in the earlier sections.

Item	Reactor	ITR	INR	TLR	FC	KS	DOC	BS	MPs/Br^-	O3
Scale	ΦHyd	Φ0	ΦIN	Φλ	FC↔FC	Φη	DOC↔ DOC	ΦBS	Br^-↔Br	O3↔O3
Distance [mm]	585	~90	~57	13	0.27	0.13	≈0.02	0.0053	≈0.0005	≈0.00005

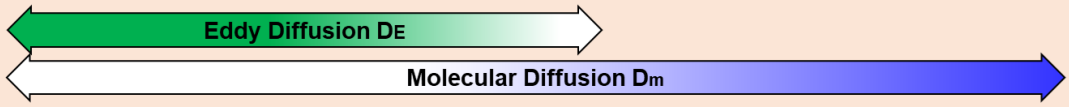

- #FC Counts = 5E+06 [-/100ml] ΦE-C 0.0012
- DOC = 10 [g/m^3], ΦDOC = 0.0005 [mm] average, # DOC particles = 1.02E+14
- MP Bromide B^- = 0.5 [g/m^3] ΦMP <<0.0012
- O3-Res. = 0.4 [g/m^3] ΦO3 <<0.0012
- ITR = Integral Range, INR = Inertial Range, TLR = Taylor Range, KS = Kolmogorov Scale, BS = Batchelor Scale

Fig. # 28 ***Scales for Diffusion and Chemical Reaction***

Fig. #29 illustrates this situation with the following comments:

1. D_E [m^2/s] prevails down to KS;
2. D_m [m^2/s] predominantly takes over from KS down to BS;

- D_E [m^2/s] is much faster than D_m [m^2/s], as per example in section 17 hereafter, with D_{mO3}= $1.74*10^{-9}$ [m^2/s] and D_{Eav} = $1.07*10^{-6}$ [m^2/s] corresponding to an average eddy size within the BC with Φ_{Eav} = 2.5 [mm], D_{Eav} ≈ 600 times faster than D_{mO3}.

3. DOC is within D_m [m^2/s] action range;

4. The concentrations of dissolved reactants such as MPs and O_3 are entirely within the range of D_m [m^2/s] action range, meaning that D_m [m^2/s] plays the final role for the overall reaction kinetics,
5. Microorganisms are carried by the D_E [m^2/s] action range down to KS and mainly by Dm [m^2/s] within KS.

Based on example of section 17 **"System Design with Overall Chemical Reaction in a TBF"** hereafter, a calculation shows that each microorganism will be surrounded by approximately $1.0*10^{11}$ O_3 molecules. Assuming "unrealistic" total absence of HIT, therefore $D_E = 0$ [m^2/s], and initial dissolved O_3 $c_{O3L} = 0$ [g-O_3/m^3] inside the KS-Scale, this situation would result in a maximum distance equal to $\Phi_{\eta max} = 0.13$ [mm], for c_{O3L} [g-O_3/m^3] to be transported from outside KS by action of $D_{mO3} = 1.74*10^{-9}$ [m^2/s] within KS. Applying the integrated "erf" form of Fick's second law of diffusion, such a layer would be saturated within a laps time of about 1 [s], see Fig. #33 in section 17 hereafter. Hence, D_m [m^2/s] has plenty of time to contribute to disinfection. Applying the proposed method of calculations suggests for KS $D_E \approx 3.1*10^{-9}$ [m^2/s], i.e., $\approx 2* D_{mO3} = 1.74*10^{-9}$ [m^2/s]. This result is qualitatively correct, quantitatively not very precise, but this fact does not affect this engineering design method. This number is negligible as compared with the average value $D_{Eav} = 1.45*10^{-6}$ [m^2/s]. This reality emphasizes the importance of D_m [m^2/s] for ironing out concentration peaks in the complete process of diffusion within an HIT environment and efficient disinfection. It also shows that the corresponding time scale does not slow it down, due to fact that the distance scales are short as compared with those applying to D_E [m^2/s].

Another fact shall be considered. Unlike D_m [m^2/s], D_E [m^2/s] is independent upon the quality of the material in solution in the solvent. It acts equally on all molecules and particles (provided they are much smaller than $\Phi_{E\kappa}$ [m]) present in the whole O_3R, i.e., O_3DC and in O_3RC. Hence, this fact shall be taken into consideration for the method of design of a FTBF Diffusion System. Micro-organisms will be transported by D_E [m^2/s], therefore enhancing disinfection.

Another point must be discussed regarding the Kolmogorov size patch. The size η [m] is a mathematical construct, which could be identified experimentally. However, a patch of this size is not physically frozen, it can be distorted if hit by neighbor eddies and/or torn apart. Thus, eddy diffusivity D_E [m^2/s] can still act on it, down to the Batchelor Scale l_{BS} [m] defined in section 8 here above within which only D_m [m^2/s] acts.

Within the process approach followed so far, the Re_L [-] of the main water flow deals as design parameter only as far as it must be large enough (<10 000), allowing for installation of a T/FT hydrodynamic pattern. It is not directly involved in any of the equations and correlations serving as basis for the design of a homogeneous isotropic TBF. The main parameters are the energy of the eddies $E_\kappa(\kappa)$ [m^3/s^2] between the largest size Φ_{Emax} [m] and the Kolmogorov scale η [m] and its dissipation rate TEDR ε [m^2/s^3]/[J/skg].

Several correlations presented in the literature are proposed for an approximate design approach for eddy diffusion D_E [m^2/s] in a tube with true turbulent flow, in absence of BC, which is the first item addressed in this document, based on parameters and dimensionless numbers such as the Reynold Number Re [-] and the Schmidt Number Sc [-] and summarized with the Sherwood Number Sh [-] used for a turbulent flow Table 16. Hereafter the correlation proposed by Cussler [44].

Table 16 Sherwood Number and Eddy Diffusivity Coefficient applied to a Fully Turbulent Flowing Pipe

Parameter	Symbol	Unit	Correlation / Equation	Comment
Reynold Number	Re	[-]	$= v°_L * \Phi_{O3R} / \nu_L$	$v°_L$ [m/s] = Water/Wastewater Flow Φ_{O3R} [m] = Ozone Reactor Diameter • Reference Length Scale ν_L [m^2/s] = Kinematic Viscosity
Schmid Number	Sc	[-]	$= \nu_L / D_m$	D_m [m^2/s] = Molecular Diffusion Coefficient
Sherwood Number	Sh	[-]	$= k * \Phi_{O3R} / D_m = D_E / D_m$ $= 0.026 * Re^{0.8} * Sc^{1/3}$	See Cussler Table 8.3-3 [44] k [m/s] = Turbulent Mass Transfer Coefficient
Eddy Diffusivity Coefficient	D_E	[m^2/s]	$= Sh * D_m$	Sh [-] is a multiplier relating D_E to D_m

These correlations do not take into consideration the action of a bubble column in a turbulent flow. The most extensive study on the influence of the Bubble's induced turbulence in the vicinity of its water side surface on mass transfer in a water laminar HHP found in the literature is presented by Glaeser and Brauer [40]. For a bubble with Φ_{B32} = 3.0 [mm] the average D_E/D_m = 5.6 [-]. D_E [m^2/s] extends some 3 [mm] into the liquid bulk form the bubble surface. This study clearly proves the negligible influence of the bubble induced turbulence in a TBF.

17. System Design with Overall Chemical Reaction in a TBF

When addressing on hydraulic and hydrodynamic grounds a bubbly flow “BF”, the parameters Re, v°, *v*, ρ, η, ε and $E_{\kappa}(\kappa)$ must be calculated based on both fluid flows $V°_L + V°_G$ [m^3/s] constituting it, the ozone-gas O_3G and the water/wastewater WW, at actual operating conditions T & P in the O_3R. Compared with the single water/wastewater flow entering the system, which is the basis for the first calculating step, the BF introduces added energy to the original TKE

This additional energy is generated by the friction losses along the bubbles rising with their bubble terminal ascending velocity or slip velocity with respect to the water $v°_B\infty$ [m/s]. It includes the TKE added to the system by turbulences generated in the wake of the bubbles as well as the increased wall friction losses due to the increases in the flow velocity of the gas-water/wastewater bi-flow. These increases in the flow velocity are induced by the dynamic gas hold-up α_{Gdyn} [%] in the bubble column, up to 10 [%].

Before addressing the details of the calculation method for system design, we clarify a few basic chemical reaction aspects involving Ozone Molecules “O_3” and OH°-Radicals “OH°”, based on Elovitz and von Gunten [50], Elovitz et al. [51]. It is common knowledge that, in the presence of Dissolved Organic Matter “DOM”, quantified by its Dissolved Organic Carbon “DOC”-value, but not qualifying its type, the action and disappearance of O_3s is combined with simultaneous generation and disappearance of OH°s.

The R_{ct} concept is used in this system design. Citing von Sonntag and von Gunten [50-52] :

- “R_{ct} is defined as the ratio of the exposures of OH° and O_3, R_{ct} [-] = $\int[OH°]dt/ \int[O_3]dt$".
- The effects of reaction pH, temperature, carbonate alkalinity, and DOM shall be taken into consideration.
- In addition to the water quality parameters already discussed, ozonation can also be affected by the nature and concentration of the DOM in the source water.
- DOM influences the ozonation process principally through direct reactions with molecular O_3 and OH°.

In the secondary effluent of a typical mixed municipal-industrial Secondary/tertiary Wastewater “SWW”, meaning biologically treated, experience [50, 51] shows that the quality of DOM is more or less a constant. Citing Maizel and Remucal [53], DOM of Secondary Wastewater “SWW” (and tertiary) is “more aromatic than untreated wastewater, with distinct molecular compositions”. We can therefore continue in this essay by considering a standard DOM quality “DOM_{sww}” and so provide some general validity to the proposed method of system design.

The “Micropol” Workshop Group of the EAWAG performed in Switzerland a comprehensive study about the elimination of micropollutants with ozone and activated carbon in WWTP-SWWs, which provided fundamental data partly used in this study. The EAWAG is the Swiss Federal Institute of Aquatic Research of the Federal Institute of Technology ETH, managed by the Swiss Federal Government, and where the Author worked with as representative of the International Ozone Association IOA.

The example describes an O_3R which could be implemented for the elimination of micropollutants of a typical in flow and quality SWW effluent in Switzerland (Fig. # 29). One basic condition for the design of such an O_3R is to avoid any hydraulically dead sites, and meshed items, where accumulation of solid matter in the SWW effluent could accumulate or lead to any kind of plugging. This means that the use of classical static mixer and porous dome gas diffusors is not recommended, as per the Authors experience.

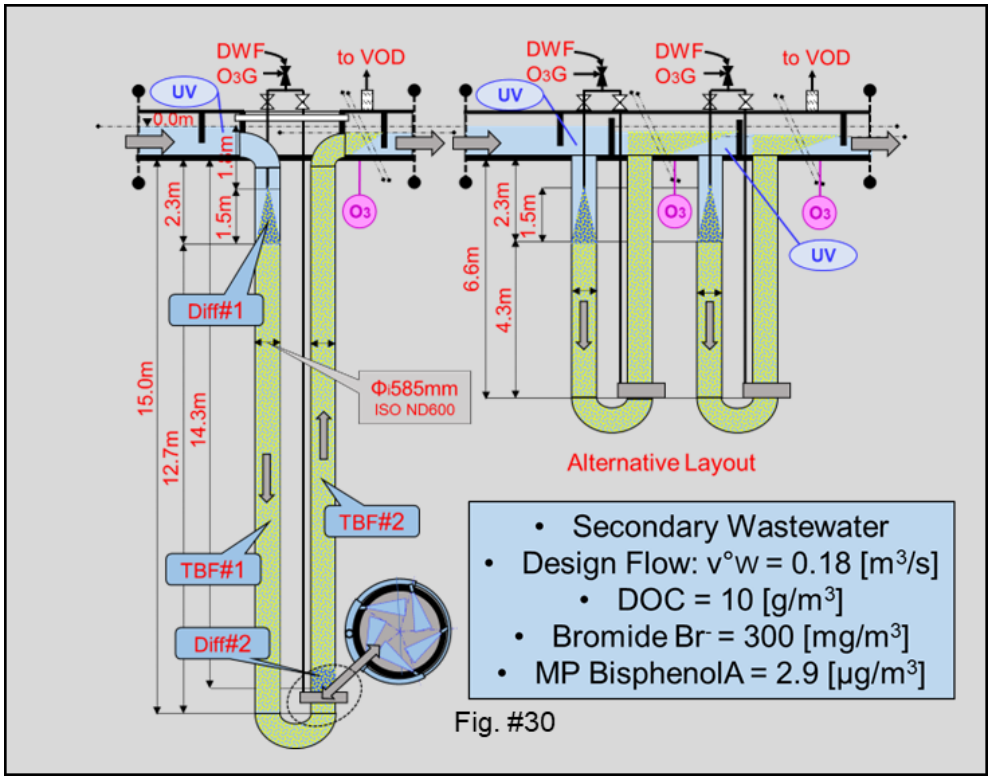

Fig. # 29 ***Secondary Wastewater Ozonation Turbulent Reactor***

For example, if in a WTP phosphorous elimination is performed simultaneous in the secondary sedimentation tank with Ferric Chloride, excess Fe^{3+} will rapidly be precipitated by O_3 already inside the BC-Builder and, combined with the hardness of the WW, lead continuously to irreversible deposits on its surface. Porous diffusors and static mixers should therefore not be considered for BC-Builder in SWW.

The basis and task to design is to consider a hydrodynamically well-defined physical-chemical process reactor, entailing that this O_3R shall be plug-flow “PF”, i.e., Fully Turbulent “FT”. The design method by the authors takes into account the following considerations:

- The energy spectrum of turbulence has been calculated in a stepwise mathematical process with 110 increments of eddy diameter Φ_E [mm], whose values have been adapted so to have smooth continuity in $\Delta\ \Phi_E$ [mm] negative increments.
- The turbulent homogeneous and isotropic TBF-O_3R is considered as equivalent to 52 Completely Stirred Tank Reactors CSTR or Sectors in series, $\#_{CSTR} = 52$, for diffusion and chemical reactions, respectively.
- The size and height of these CSTRs is much smaller than any CSTR considered in the design of all industrial isotropic and turbulent chemical reactors known to the authors.

Since the O_3R is a Plug Flow Reactor “PFR”, the design approach can be considered as follows:

- 52 CSTRs (sectors) for the calculation of the average ozone concentration c_{O_3L} [g/m^3] in each sector and the same for the carrier gas oxygen c_{O_2L} [g/m^3].

- The definition of a CSTR claims that the water/wastewater flow and all its constituents and reactants are stationary with each other, meaning that they have the same residence time, in the CSTR. This not true for the bubbles in the TBF, which move flow upwards with their Slip Velocity $v°_{B\infty}$ [m/s].
- In co-current mode downstream $v°_{B\infty}$ [m/s] increases the residence time of the bubbles in the CSTR sectors.
- In co-current mode upstream v°B∞ [m/s] reduces the residence time of the bubbles in the CSTR sectors.
- Accordingly, a correction factor must be introduced when calculating the mass transfer of O_3 and O_2 into the water/wastewater.
- For design, 52 continuous plug flow reactors “PFR” are considered for chemical reactions, with average c_{O3L} [g/m^3] and c_{O2L} [g/m^3], since the reactants in the WW are already present. This distinction is important from the point of view of chemical reaction conversion performance.
- Reality is, each reaction case, diffusion and chemical, physically takes place in PFR.

A Kinetic Performance (efficiency) “PERF” Factor k_{Perf} [-] is applied to describe chemical reaction processes, considering the Ratio of Residence Time Θ_{ResPFR} [s], Diffusion and Reaction Rates $k_{D/R}$ [s^{-1}]. For example, the ozone and oxygen diffusion k_{Perf} = 0.405 [-] with CSTR (Table 17). Also, ozone chemical reactions with COD have a k_{Perf} = 0.913 [-] assuming PFR. More examples are presented in Table 17.

Table 17 Chemical Reaction Processes and Performance Parameters

Process	Reactor Type	Parameter	Symbol	Unit	Value	Comment
O_3 & O_2 Diffusion	CSTR	Performance	k_{Perf}	[-]	= 0.405	
O_3 Reaction with COD	PFR	Performance	k_{Perf}	[-]	= 0.913	
O_3 Reaction with Bromide	PFR	OH°-Exposure	R_{CT}	[-]	= 10^{-6}	as recommended by Buffle [13] $\Theta_{ResPFR} \approx 1$ [s],
Exposure to O_3 & OH°	PFR	OH°-Exposure	R_{CT}	[-]	= 10^{-6}	
BPA Elimination	PFR	OH°-Exposure	R_{CT}	[-]	= 10^{-6}	
O_3 & O_2 Diffusion	CSTR	Performance	α	[-]	= 1.0	Secondary Effluent as per Henkel [49]
O_3 & O_2 Solubility	CSTR	Performance	β	[-]	= 1.0	

The value of the R_{CT} [-] has been selected to be equal to the value of 10^{-6} [-], see Table 17. The reasoning is as follows :

- According to Buffle [13] the R_{CT}-value is dependent upon the residence time in the O_3R.
- It varies linearly from 10^{-6} [-] to approx. 10^{-8} [-] for a flow residence time in a PFR, with the corresponding CSTR $\Theta_{ResCSTR}$ [s] falling between initially 1 [s] and 100 [s], see Fig. #32 hereafter.
- The design described in this document suggests a $\Theta_{ResCSTR}$ < 1 [s].
- The staging of O_3-supply to each sector of the O_3R means that the residence time of the proportion of the WW-fraction affected by O_3 is variable and becomes shorter with the downflow position/reference number of the sector.
- This means that the value of the corresponding R_{CT} [-] of the sector increases with its downflow position, as per Fig. # 32 & Fig. # 33.

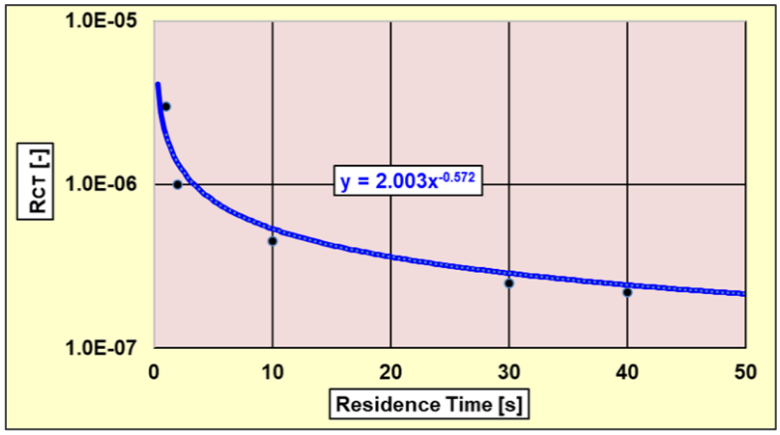

Fig. # 30 ***Municipal Secondary Wastewater typical R_{CT}-values***

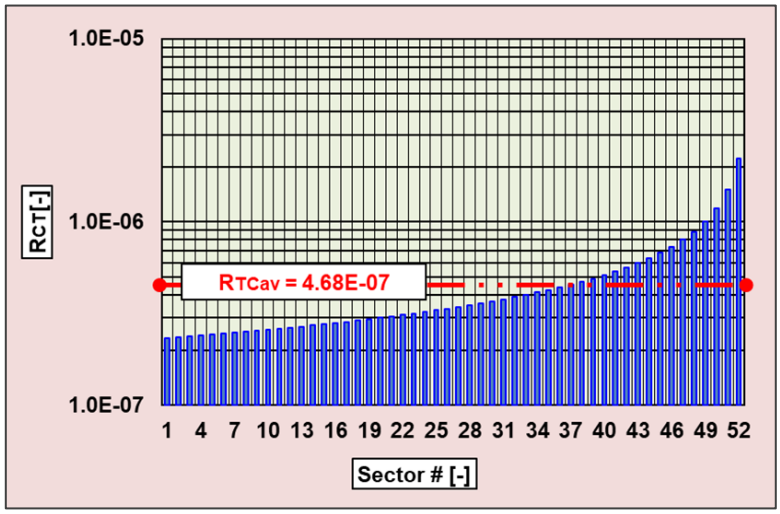

Fig. # 31 ***R_{CT} per Sector***

For the elimination of BPA, calculations considering both reactions with O_3 and OH° are made with R_{CT} = 10^{-6} [-] [13] , which is an average value within the whole O_3R. The correcting factors for diffusion rate α and solubility β of ozone and oxygen in secondary wastewater SWW are α = β = 1.0 [-] as recommended by Henkel [49]. All reactants, ozone, and Dissolved Organic Carbon (DOC), Bromide

(Br^-) and Bisphenol A (BPA) as representative micro-pollutants (MP), are distributed radially homogeneously with axial gradient in each sector (PFR). The completion of chemical reactions considers in each of the 52 reactors :

- an average ozone concentration c_{O3L} [g/m^3] in each CSTR;
- the actual continuously variable pollutant concentration in each continuous PFR;
- the chemistry as per Fig. # 32.

All calculations of a sector are made with the end values of the preceding sector. This approach is conservative, as compared to the true average values in each sector. All relevant concentrations and chemical reaction rate constants are collected from data retrieved from the literature, see Hoigné [54], Von Sonntag and Von Gunten [52] and Buffle [13]. Since the hydraulic & hydrodynamic system or TBF is homogeneous and isotropic, the basic unit for design program can be a single bubble with its surrounding liquid bulk, valid if the wall layer effects are negligible as far as bulk diffusion and chemical reactions are concerned, which is the case in this example (wall layer thickness δ < 1.0 [mm]).

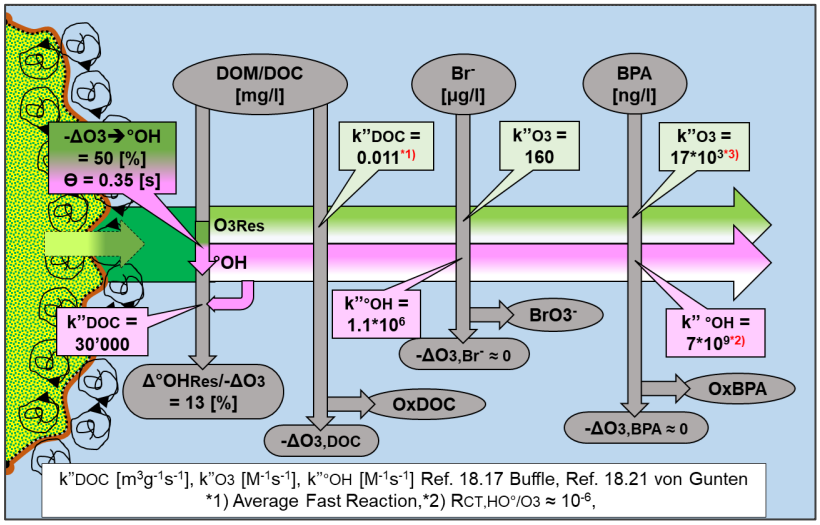

Fig. # 32 *Chemical Reaction Process*

The basic system design parameters, based on Author's hometown wastewater plant data, are a secondary Effluent (before filtration, see hereafter). The treatment stages of the plant are input mechanical, primary sedimentation, low charge biological stage, final sedimentation and finally a filtration step. The Population Equivalent Unit "PUE" of the plant is 18 000. The dimensions of the ozone reactor are presented in Table 18 and hydraulic data describing the plant in Table 19. Moreover, some components and pollutants in the water after sedimentation (filtration intake) are presented in Table 20.

Table 18 O_3R Dimensions

Item	Symbol	Value	Unit	Comment
O_3R Hydraulic Diameter	Φ_{hyd}	0.585	[m]	Vertical
O_3R Cross-Section	S_{O3R}	0.269	[m^2]	Horizontal
O_3R Diffusion Length	L_{O3R}	30.5	[m]	Vertical, Downstream/upstream
O_3R Diffusion Volume	V_{O3R}	8.21	[m^3]	-
CSTR/PFR Height	$h_{CSTR/PFR}$	0.564	[m]	Sector

Table 19 Hydraulic data of the wastewater plant

Design Parameter	Symbol	Unit	Value	Comment
Daily dry wastewater amount	$V°_{L/Day}$	[m^3/Day]	9000	0.5 [m^3/Day] per PUE
Average Flow	$V°_{Lav}$	[m^3/s]	0.104	24 hour/day Average
Average superficial velocity	$v°_{Lav}$	[m/s]	0.387	
Design residence time in O_3R, TBF #1 + TBF #2	Θ_{ResO3R}	[s]	42	Basis Design Flow $V°_{LDs}$
Average design residence time in Sector	$\Theta_{ResCSTR}$	[s]	0.83	
Design flow, dry weather	$V°_{LDs}$	[m^3/s]	0.179	Basis 14 hour/day
Design superficial velocity	$v°_{LD}$	[m/s]	0.665	Basis 14 hour/day
Minimum flow = 0.5*V°Lav	$V°_{Lmin}$	[m^3/s]	0.052	
Minimum superficial velocity	$v°_{Lmin}$	[m/s]	0.193	
Maximum design flow = 1.5* V°LDs	$V°_{Lmax}$	[m^3/s]	0.269	Wet Weather
Maximum Superficial Velocity	$v°_{Lmax}$	[m/s]	0.998	Wet Weather

Table 20 Components and pollutants, after final sedimentation, at intake filtration

Item	Abbreviation	Value	Unit
Dissolved Organic Carbon “DOC“	cDOC	10	[gC/m^3]
Potential of hydrogen	pH	≈ 8.0	[-]
Alkalinity	cAlk	≈ 3.5	[$mMHCO_3^-/CO_3^{2-}$]
Temperature	tWW	20	°C
Bromide concentration	cBr^-	0.3	[gBr^-/m^3] EAWAG
Bisphenol A “BPA“ concentration	cBPA	290	[$\mu g/m^3$] EAWAG

Table 21 contains the design data of the ozonation system. The ozone dose of 5.0 g-O_3/m^3 is based on the 0.5 g-O_3/g-DOC ratio, as recommended by EAWAG, Switzerland. The gas absolute pressure is measured at the discharge point of the free jet into the TWF. The value of $V°_{DW}$ depends upon the pressure P_{O3G} [Pa] at which the O_3G is made available at the gas suction flange of the hydro-injector, the lower this pressure, the larger $V°_{DW}$ [m^3/s]. The free jet bi-flux bubbly flow is generated by means of a hydro-injector, high velocity and the tube roughness.

Table 21 Ozone design data

Item	Abbreviation	Value	Unit
Ozone dose	c_{DO3}	5.0	[g-O_3/m^3]
Ozone carrier gas O_3CG	Vaporized liquid oxygen with 5% nitrogen		
Ozone concentration	c_{O3}	12	[w%] = % by weight
Ozone production rate	$M°_{O3}$	$0.89*10^{-3}$	[kg-O_3/s]
Ozone gas production rate	$M°_{O3G}$	$7.44*10^{-3}$	[kg-G/s]
Actual ozone gas volumetric rate	$V°_{O3G}$	$4.51*10^{-3}$	[m^3/s]
Gas absolute temperature	T_{O3G}	293.15	[K]
Gas absolute pressure	P_{O3G}	117'790	[Pa]
Ambiant pressure	P_{amb}	100'135	[Pa]
Ozone gas driving water flow	$V°_{DW}$	0.0061	[m^3/s]
	constant, = 3.42 [%] of $V°_{LDs}$		
Eddy Diffusivity, corrected for Taylor Range, considering part of the TKE is dissipated into heat			
generated by Φ_{Emax} = 4.9 [mm]	D_{Emax}	$2.11*10^{-6}$	[m^2/s],
$D_{Emin} \approx 2*Dm = 1.74*10^{-9}$ [m^2/s]	$D_{Emin} = D_{E\eta}$	$3.71*10^{-9}$	[m^2/s]
Average Eddy Diffusivity	D_{Eav}	$0.83*10^{-6}$	[m^2/s]

The average value D_{Eav} was calculated between the largest scale contributing to D_E, i.e., Φ_{Emax} = 4.9 [mm], and the Kolmogorov Length Scale η, where $D_E \approx 2*Dm$ [m^2/s]. The contribution from the neighbor bubbles to the actual D_E [m^2/s] acting inside the TBF will be analyzed farther in this document. The Eddy Diffusion D_E [m^2/s] for O_3 has been calculated according to section 16 **"Eddy Diffusion DE"** here above and estimated for our example to have a constant average value of $D_{Eav} = 8.38*10^{-7}$ [m^2/s], which is approx. 480 times faster than the molecular diffusivity for ozone $D_{mO3} = 1.74*10^{-9}$ [m^2/s] at 20 °C.

The hydrodynamic, diffusion and turbulence data in a TBF are presented in Table 22. All values in Table 22 are taken at the beginning of the free jet of Diff#1 (Fig. # 29 p. 57), corresponding to the level intake for free jet at a depth of -1.8 [m], if not otherwise specified. The value of Re_{L+G} considers a bi-flow of wastewater and ozone gas. The TEDR ε results from a total Δp = 186 [Pa], generated by the wall friction and BC head-loss. Moreover, the average kinetic ozone gas hold-up α_G is kinematic and based on superficial velocities as well as bubble slip velocity. They are approximately equal in both TBF.

Table 22 Basic/Initial, Hydrodynamic, Diffusion and Turbulence Data in TBF

Item	Abbreviation	Value	Unit
Isothermal process temperature	$T_P = T_{O3G} = T_L$	293.15	[K]
Reynold number of axial-average flow	Re_{L+G}	398 000	[-]
Henry constant of ozone at T_P	He_{O3}	$364*10^6$	[Pa]
Surface renewal mass transfer coefficient[1]	k_{mtE}	$8.50*10^{-3}$	[m/s]
Surface renewal rate	s	78.2	$[s^{-1}]$
Turbulent Energy Dissipation Rate "TEDR"	ε	0.0043	$[m^2/s^3]$
Kinematic viscosity at T_P	v_L	$1.0*10^{-6}$	$[m^2/s]$
Kolmogorov length scale	$\eta = (v^3/\varepsilon)^{1/4}$	$0.128*10^{-3}$	[m]
Universal Taylor scale	$\lambda = \pi*\eta/0.03$	$0.013*10^{-3}$	[m]
Average bubble Sauter diameter	Φ_{B32}	3.0	[mm]
Bubble slip velocity in contaminated water[2]	$v°_B{}^{\infty}$	0.235	[m/s]
Average kinetic ozone gas hold-up	α_G	2.41	[%]
Average distance between bubbles	d_{BBav}	4.9	[mm]
Average largest eddy diameter[3]	$\Phi_{Emax} \approx d_{BBav}$	4.9	[mm]

[1] according to Danckwerts [7] where $k_{mtE} = (D_{Eav}*s)^{0.5}$, non-corrected with performance factor k_{Perf} [-]
[2] $v°_B{}^{\infty}$ is equivalent to the bubble terminal ascending velocity, verified experimentally by running the pilot plant close to gas embolism
[3] with the assumption that eddy stretching between two bubbles leads to two eddies of size Φ_{Emax} where $\Phi_{Emax} < \lambda = 0.013*10^{-3}$ [m], hence within the Taylor Range "TLR".

Table 23 describes the layout and operation mode of the ozone reactor (O_3R) presented in Fig. # 29. The operation mode leading to a gas embolism ($v°_{Labs} = v°_B{}^{\infty}{}_{abs}$) must be avoided always. To avoid it, switching from DIFF#1 "off "to DIFF#2 "on" must take place before the embolism occurs.

Table 23 O_3R Layout and Operation Mode

Absolute velocities [m/s]	TBF #1	$V°_L$ [m^3/s]	$V°_G$ [m^3/s]	TBF #2	$V°_L$ [m^3/s]	$V°_G$ [m^3/s]
$v°_{Labs} > v°_B{}^{\infty}{}_{abs}$	*Co-Current*	*Down-Flow*	DIFF#1 "on"	-	*Up-Flow*	DIFF#2 "off"
$v°_{Labs} < v°_B{}^{\infty}{}_{abs}$			DIFF#1 "off"	*Co-Current*		DIFF#2 "on"
$v°_{Labs} = v°_B{}^{\infty}{}_{abs}$	Gas Embolism	Operation mode to be avoided, gas-holdup becomes very large. Switch to C*o-Current – Up-Flow* Mode				

Since the design superficial velocity $v°_{LD} = 0.665$ [m/s] > $2*v°_B{}^{\infty} = 0.235$ [m/s], switching to DIFF #2 "on" can be done at $0.5*v°_{LD} = 0.333$ [m/s]. The Residence Time Θ_{ResO3R} in TBF#2 will be equal or superior to 42 [s]. Fig. # 33 is established based on the data of our example and the equations found in Pope [15].

Experience shows that for typical ozone diffusion cases, this representation will apply. Indeed, since our confining system is well defined and “simple”, we can claim that the proposed approach to design is reliable as we are dealing with a turbulence situation within the yet mathematically proven Universal Range.

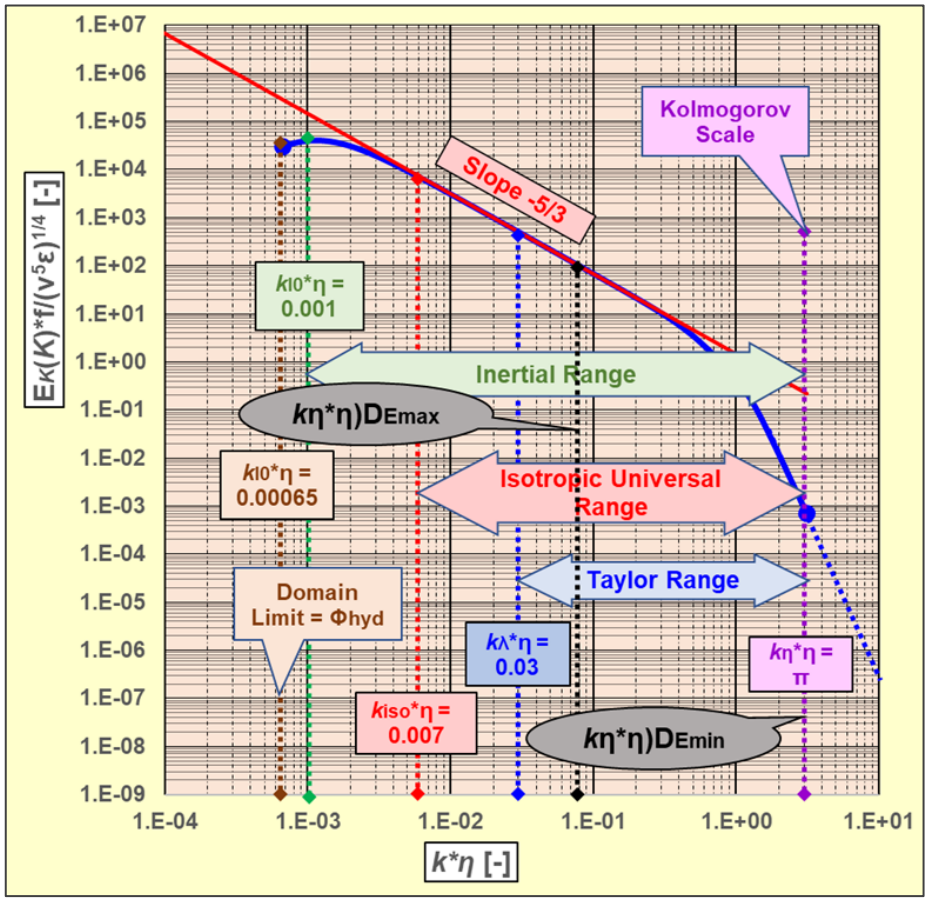

Fig. # 33 ***Turbulent Energy Cascade, Re_λ = 469 [-]***

We are also interested in having a clear picture of how D_E [m^2/s] fits into our example. The average distance between bubbles d_{BBav} = 4.9 [mm]. Moreover, at the design water flow, the superficial velocity $v°_{Lav}$ is 0.665 [m/s]. Hence, the design residence time in a CSTR $\Theta_{ResCSTR}$ = 0.85 [s]. We assume that diffusion takes place from a flat interface into a semi-infinite diffusion volume in water. We apply the integrated form of Fick’s Second Law of Diffusion with the Error-Function “Erf-f” [7].

Consider the left graph on Fig. # 34, with P = 1 [bar] at the top of the O_3R and P = 2.5 [bar] at the bottom of the O_3R. We see that a water layer equal to d_{BB} = 1 [mm] is saturated, i.e. c_{O_3} > 0 g-O_3/m^3, at both pressures with action of D_E [m^2/s]. For comparison, the pattern with D_m [m^2/s] after 10 [s] is also shown. The right graph on Fig. # 34 shows the c_{O_3} [g-O_3/m^3] within KS, assuming the value of D_m is $1.74*10^{-9}$ [m^2/s], which is conservative. We see that a diffusion length corresponding to Kolmogorov Length Scale $\eta = (v^3/\varepsilon)^{1/4}$ = 0.13 [mm] is saturated after an elapsed Time $\Theta_{elap} \approx 1$ [s], which equals more or less to the average design residence time in sector $\Theta_{ResCSTR}$ = 0.83 [s].

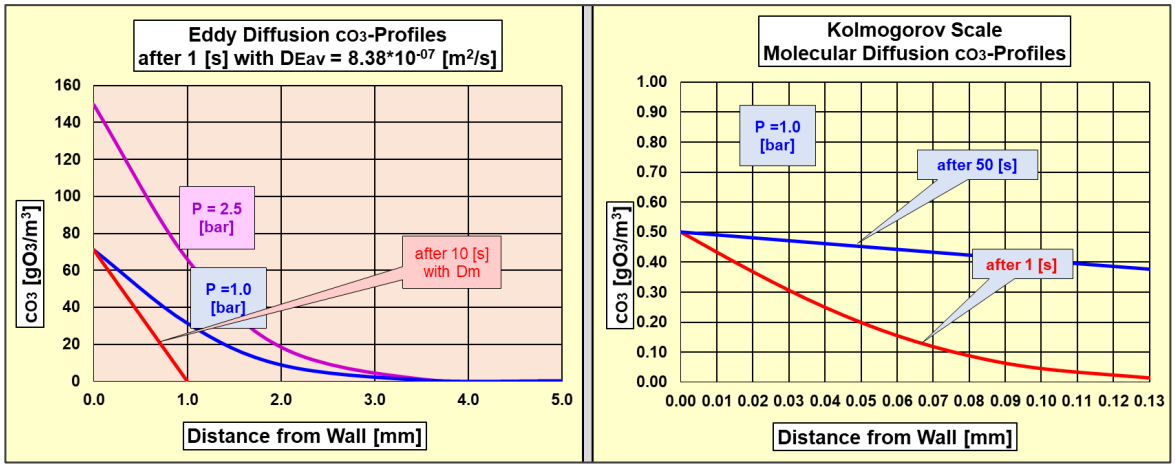

Fig. # 34 ***Eddy & Molecular Diffusion Profiles***

Considering that the actual $D_{E\eta}$ equals $3.71*10^{-9}$ [m^2/s], acting simultaneously with $D_m = 1.74*10^{-9}$ [m^2/s], means that homogeneity of c_{O3} [$g\text{-}O3/m^3$] will exist inside KS. These profiles are valid with the restriction that D_E [m^2/s] = constant and works on macroscopic pseudo-homogeneous and isotropic agitation level, similarly to D_m [m^2/s].

Now, we realize that a bubble and the water bulk volume around the bubble are spherical and not planar, meaning that dilution of concentration due to the increase of diffusion surface/volume must be considered. However, in a BC, each bubble is surrounded by other bubbles. We assume that in a HIT environment, the equilibrium mean position distribution of the bubbles inside the TBF is tetrahedral (Fig. # 35). This situation is true because in a fully turbulent “FT” homogeneous and isotropic dynamic environment, the push forces acting on the bubbles due to turbulent kinetic energy “TKE” exhibit equal statistical average amplitudes in all directions, as observed in the FT Pilot Plant (see Fig. # 8, p.15). Observations into the near-wall bulk of the flow confirm this assumption.

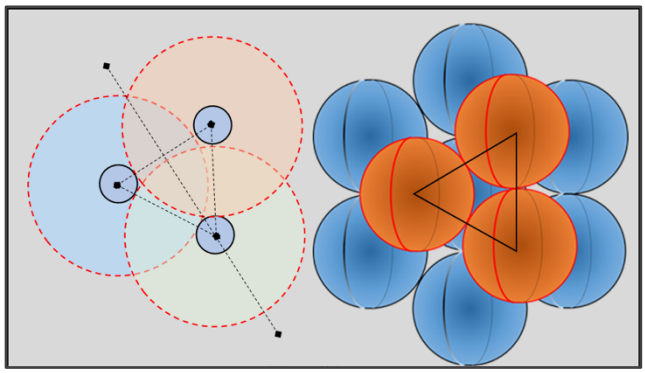

Fig. # 35 ***Tetrahedral Bubble Cluster***

According to the literature [55, 56], a sphere in a homogeneous tetrahedral packing can be surrounded by up to 12 neighboring spheres (Fig. # 35). This means that the diffusion water bulks of each bubble overlap with each other. Accordingly, the concentration profile from each bubble overlap. Finally, dilution of concentration is practically fully compensated.

Physical reality is that D_E [m^2/s] acts on a macroscopic homogeneous and isotropic dimensional level inside the Taylor Range "TLR", with D_E equal or less than D_{Emax} [m^2/s] resulting from eddies getting always smaller, down to the Kolmogorov Scale "KS". These smaller eddies contribute to homogenize the concentration c_{O3} [g/m^3] towards c_{O3av} [g/m^3] within the liquid diffusion bulk of influence of each bubble. The consequence of both above-described phenomena is that one can assume in each CSTR an average homogeneous ozone concentration c_{O3CSTR} [g-O3/m^3] = constant.

For a reactor design, an average $D_{Eav} < D_{Emax} = 2.11*10^{-6}$ [m^2/s] must be considered. Based on Pope [15] and Bakker [21], Fig. #38 can be drafted. It shows the profile of correction factor f_{TLR} [-] for TKE within the TLR.

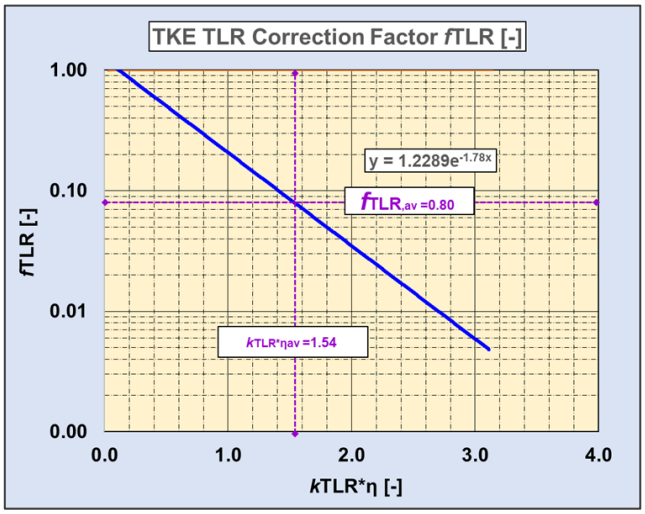

Fig. # 36 *Turbulent Energy Correction*

Eddy turnaround and decay times must also be addressed and quantified. Based on formulas presented in section 10 "**Turbulent and Fully Turbulent Water Flow TWF / FTWF"**, the values presented in Table 24 are obtained. The value of f_{TLR} is valid for a bubble Φ_{B32} = 3.0 [mm] and d_{BB} = 5.0 [mm] and the $\tau_{TE\kappa,max}$ corresponds to a Φ_{Emax} of 5.0 [mm]. Moreover, the value of $\tau_{TE\kappa,min}$ corresponds to $\eta = (v^3/\varepsilon)^{1/4}$ = 0.128 [mm].

Table 24 Other design data

Item	Abbreviation	Value	Unit
Turbulent diffusion correction factor	f_{TLR}	0.78	[-]
Eddy turnaround time maximum	$\tau_{TE\kappa,max}$	0.61	[s]
Eddy turnaround time minimum	$\tau_{TE\kappa,min}$	0.05	[s]
Eddy turnaround time average	$\tau_{TE\kappa,av}$	0.33	[s]
Average individual eddy decay time	$\tau_{DE\kappa}$	≈ 0.5	[s]

These times are of the order of magnitude of the residence time in CSTR $\Theta_{ResCSTR}$ = 0.85 [s]. Hence there is enough time in a CSTR for the process of energy dissipation in an eddy to fully take place and be reactivated by the continuously new generated turbulent energy.

We now address the chemical reaction process and the calculation program with the following assumptions, as per Fig. # 32, p.60. Chemical reactions of O_3 with, in this essay, dissolved organic matter "DOM" as dissolved organic carbon "DOC", Bromide and Bisphenol A, are qualified and calculated with the following assumptions:

- All chemical reactions take place principally in the HIT liquid bulk between the bubbles, hence all reactions happen in a HIT environment temporally simultaneously with each other and with their own rate;
- All chemical reactions are 2nd order.

Dissolved Organic Matter "DOM"

50 % of ozone transferred into the bulk liquid between the bubbles is transformed immediately, within 350 [ms], into mostly OH°-radicals by the DOM. These radicals then react immediately with DOC, according to Buffle [13], Nöthe et al. [57] and Wang and Chen [58].

Dissolved Organic Carbon "DOC"

The following values describe the reaction system designed in this essay :

- DOC, c_{DOC} = 10 [g-C/m^3];
- k''$_{O3/DOC}$ = 0.071 [m^{3}g^{-1}s^{-1}] for initial reactions [13, 52, 59];
- k''$_{O3/DOC}$ = 0.011 [m^{3}g^{-1}s^{-1}] for fast reactions [13, 52, 59].

We have considered the value of k''$_{O3/DOC}$ as the average between initial and fast reactions, based on reaction time scales presented by Buffle [13]. Therefore, k''$_{O3/DOC}$ = 0.041 [m^{3}g^{-1}s^{-1}] for the design program. DOC concentration remains practically constant, as has been demonstrated in many similar cases, as per Schaar [60], hence pseudo-first order reaction in O_3 with respect to DOC.

R_{CT} [-]

The typical variation of the value of R_{CT} [-] in secondary wastewater in Switzerland is shown in Fig. # 32, repeated here, as per Buffle [13]. The residence time in a sector $\Theta_{ResCSTR}$ = 0.83 [s]. However, it must be considered that each chemical process with O_3 and OH° will restart in each sector under the applicable intake and O_3-supply conditions, but last until the end of the O_3R, whose Θ_{ResO3R} = 42 [s]. Therefore, the variable R_{CT}-value to be selected shall be within the range delimitated by R_{CT} = 3.0*10^{-06} and 2.0*10^{-06}[-].

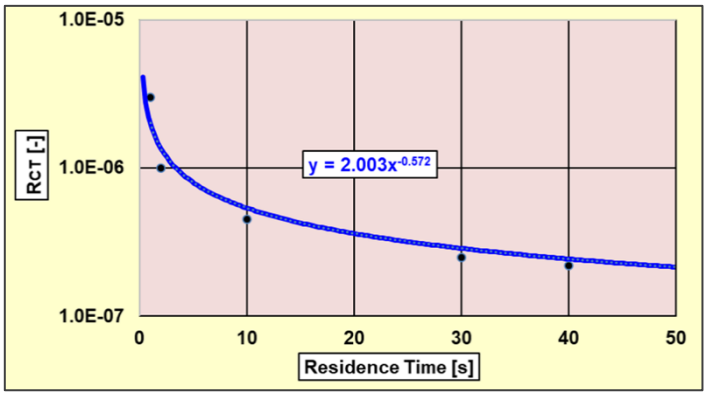

Fig. # 32 *Municipal Secondary Wastewater typical R_{CT}-values*

Bromate (BrO_3^-) Formation

The initial bromide concentration c_{Br^-} in the studied secondary wastewater is 300 [µg-Br^-/L], 0.3 [g/m^3]. The dual-oxidation process of Br^- with O_3 and OH° ends up with the formation of a new micropollutant, Bromate BrO_3^- which is considered carcinogenic. The selected simplified BrO_3^- Formation Process described here after in Fig. # 39 allows for an approximate determination of bromate formation in the case of the present example. This simplified diagram is proposed in many places in the literature and is the result of a consensus among specialists, for example in Morrison et al. [33], Rakness [61] and Elovitz et al. [51] .

In potable drinking water, the WHO recommends a maximum concentration c_{BrO3-} < 10 [µg/l] [62]. Since treated wastewater is discharged into lakes and rivers, which can be the source for potable-drinking water production, it is of the essence to have more-or-less a good quantitative idea of how much BrO_3^- is generated when treating a Secondary Wastewater Treatment Plant effluent SWW with Ozone, if the SWW contains a non-negligible amount of Bromide "Br^-". Such an approach in secondary wastewater is possible with the concept of exposures of Br^- to O_3 and OH°, characterized by the ratio R_{CT} [-] of both exposures (Equation 17-1), as already introduced here above and proposed by Von Sonntag and Von Gunten [52] and Buffle [13]. R_{CT} is generally determined based on OH°-scavenging with para-chlorobenzoic acid "pCBA" [13]. Its temporal profile depends on :

- the residence time Θ_{Res} [s] of the secondary wastewater inside the O_3-Reactor, i.e., each single sector in this particular example;
- the exposure dose of O_3;
- the quality for the dissolved organic matter "DOM" of the secondary effluent.

$$R_{CT}\,[-] \;=\; \frac{\int {}^{\circ}OH^{*}dt\,[ms]}{\int O_3{}^{*}dt[ms]} \qquad \text{(Equation 17-1)}$$

Unlike lake or river water, where DOM is generally of variable quality, literature tells that DOM of a municipal SWW treated in a low charge activated sludge process with a limited amount of industrial biologically refractory material is made of chemically similar constituents composing the Total/Dissolved Organic Carbon "TOC/DOC" [58]. The similarity in TOC constituents is a result of the biological transformation of the intake DOM into new DOM in intra- and extra-cellular processes in the activated sludge stage. Based on the analysis of molecular weight distribution, hydrophobicity and functional groups, the new DOM generated is more-or-less constant in composition.

The coming section is a trial which proposes a design method to estimate how much Bromate BrO_3^- could be generated in the O_3R described and designed in this document. We use the following specific features of the present example :

- the O_3R is hydrodynamically and hydraulically fully turbulent;
- the physical nature of the wastewater bubbly flow circulating in this O_3R is homogeneous and isotropic;
- the wastewater bubbly flow is plug-flow.

Hence, except for the narrow layer along the wall for the O_3R (Law of the Wall), it is assumed that the Main Flow Velocity in each sector of the O_3R of the smallest units identifiable in this design, i.e., the

Kolmogorov Scale “KS”, is constant within a narrow range of local variation of less than +/- 2 [%], corresponding to dynamic hold-up α_{Gdyn} [%] generated by the bubble column.

The slip velocity $v°_B^{\infty}$ [m/s] of the bubbles within the bubble column is considered as constant within a sector, but variable from sector to sector because of the increasing/decreasing pressure and material solubilization (O_2 and O_3). Hence, the residence times of the wastewater and bubbles are assumed to be constant within each sector for the design purpose. The ratio of OH°-exposure to O_3-exposure R_{CT} [-] has in a secondary wastewater a larger value as compared with natural water from a river or lake because of its higher DOM content (Fig. # 32) resulting into a stronger promotion of radicals OH°. Information from Morrison et al. [33] states that the R_{CT} value remains practically constant during the reaction of Br^- with O_3 and OH° under the existing conditions. Hence, it is assumed that this applies to each single sector of the O_3R (Fig. # 33).

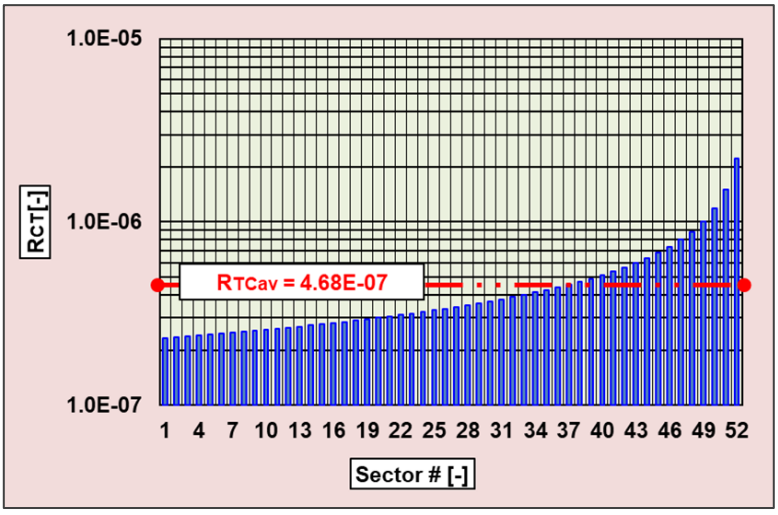

Fig. # 33 *R_{CT} per Sector*

To continue with this design approach, we assume that within a sector the concentration of dissolved O_3, and therefore of OH°, is constant. This assumption is justified by the fact that the transfer, turbulent diffusion D_E [m^2/s], and homogenization of O_3 from the gas phase O_3G to and inside the wastewater phase is a continuous and fast process within each sector, as per Fig. # 34 hereabove. These factors contribute to supply the sector continuously and rapidly with O_3 so compensating the negligible consumption of O_3 by the chemical reactions happening after the initial fast consumption. Hence, it is assumed that the oxidation of bromide “Br^-“ is a process with a much slower kinetic, essentially since the concentrations involved are much smaller. It is therefore acceptable to assume that the concentration of O_3, hence of OH°, remains practically constant in each sector during the process of BrO_3^- formation. The next simplification, as a consequence of the above stated facts, is that the second-rate chemical reactions can be transformed into first-rate chemical reactions with respect to O_3 and OH°. The converging scientific information of the literature [13, 52, 61, 63] proposes the following chemical processes for the formation of bromate BrO_3^- resulting from the reactions of bromide Br^- with O_3 and OH° in the presence of DOM in the wastewater (Fig. # 39). The whole reaction process of O_3 and OH° with Br^- can be described as consisting of 3 paths (Fig. # 39):

- the Direct Path involving only O_3;
- the Direct-Indirect Path involving O_3 and OH°;
- the Indirect-Direct Path involving OH°, O_3 and OH°.

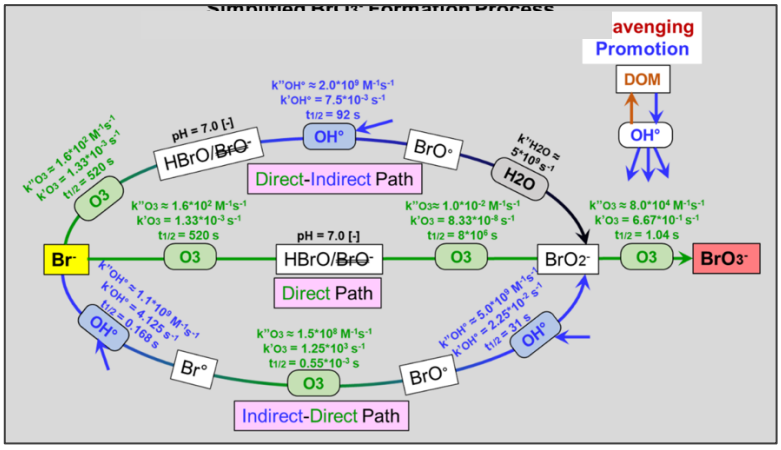

Fig. # 37 *Simplified Bromate Formation Process*

The second-rate and first-rate reaction constants are presented in Fig. # 37. It is also evident that the half-life times ($t_{1/2}$) of the first steps in each path are very long as compared with the residence time in each sector. This means that the process starts rather slowly in each sector. The values of BrO_3^- generated are given in the literature for the case of secondary wastewater [33, 64, 65]. The change of the concentration of DOM due to the action of O_3 and OH° is negligeable, only its quality changes due to a slight DOC drop, and some BOD formation. These data make evident that the generation of BrO_3^- within a sector is small with respect to Br^-. This also justifies the modification of all second-rate into first-rate kinetics.

It is therefore possible to apply the methods of parallel and consecutive first-rate chemical reactions. Considering the reaction rates and concentrations applicable to this design makes evident that the direct path gives in-between concentrations of BrO_2^- more than several hundred times smaller than in the Direct-Indirect and Indirect-Direct paths, making this path negligeable. The calculation can therefore proceed essentially along the paths Direct-Indirect and Indirect-Direct, where it also becomes evident that the oxidation of Br° by O_3 to BrO° along the Indirect-Direct Path is so fast that BrO° can practically be considered equal to zero during the process. We continue therefore the calculation by considering both paths as a two-step process, i.e., OH°- and O_3-oxidation processes of Br^- directly to BrO_2^-, followed with BrO_2^- conversion to BrO_3^- with O_3. The cumulated O_3- & OH°-exposures by which Br^- is oxidized are presented on Fig. # 38.

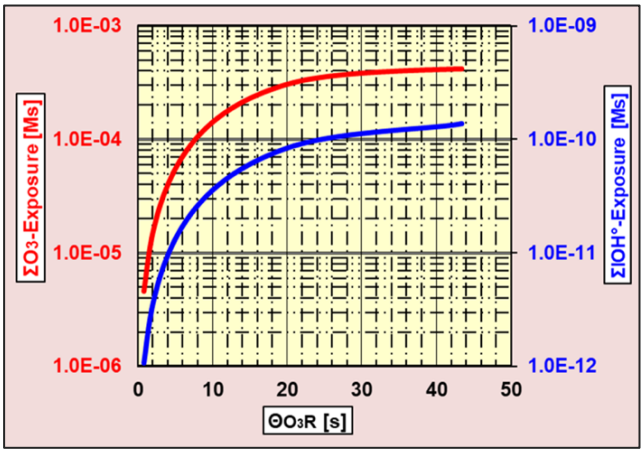

Fig. # 38 *O_3 & OH° cumulated exposures in the O_3R*

The proposed method of result calculation of BrO_3^- generated in very low value for the design situation in this O_3R is presented in Table 25. It is therefore of interest to understand quantitatively the influence of the parameters residence time [s], O_3-exposure [mg-O_3/L] and R_{CT} [-] on bromate BrO_3^- formation. This analysis leads to the results presented in Fig. # 41.

Table 25 Calculation example of bromate concentrations in O_3R

O_3-exposure [mg-O3/L]	Residence Time in O_3R [min]	Average residence time in Sector [s]	Average BrO_3^- concentration in sector [µg-$BrO3^-$/L]	BrO_3^- concentration in O_3R [µg-BrO_3^-/L]
0.46	0.72	0.83	0.0061	0.315

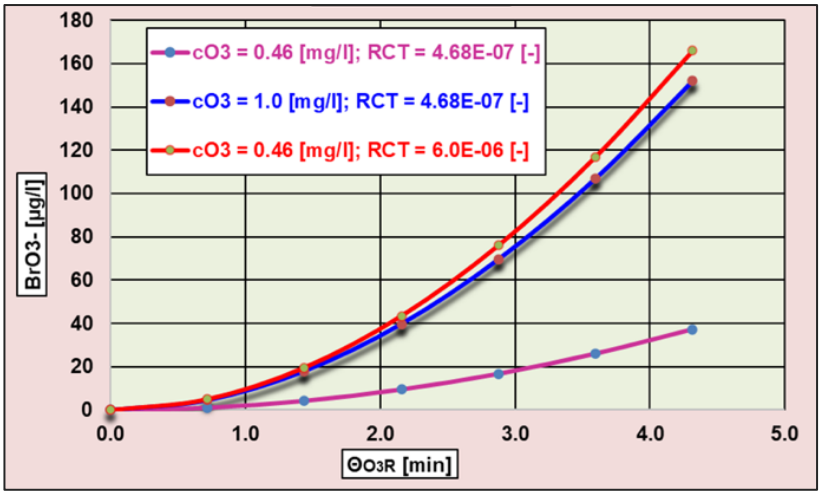

Fig. # 39 *Bromate formation profile*

According to Hoigné [54], Von Sonntag and Von Gunten [52], and Nöthe et al. [57] in a SWW with a ratio of c_{DO3}/DOC = 0.5 [g/g], the conversion of Br^- to $BrO3^-$ is less than 5 %, which in this case would amount to $c_{BrO3-} \approx 15$ [µg/l], supporting the results provided by our mathematical approach.

Bisphenol A “BPA”

The following values describe the reaction system designed in this essay :

- c_{BPA} = 290 [ng-BPA/L], 290 [µg/m^3];
- k’’$_{BPA/O3}$ [$M^{-1}s^{-1}$] = 17’000 [$M^{-1}s^{-1}$] [52]
- k''$_{BPA/OH°}$ [$M^{-1}s^{-1}$] = 7.0E+09 [$M^{-1}s^{-1}$] [52]

In this essay, BPA is used as an example organic micropollutant. Fig. # 40 presents the BPA concentration abatement profile versus residence time.

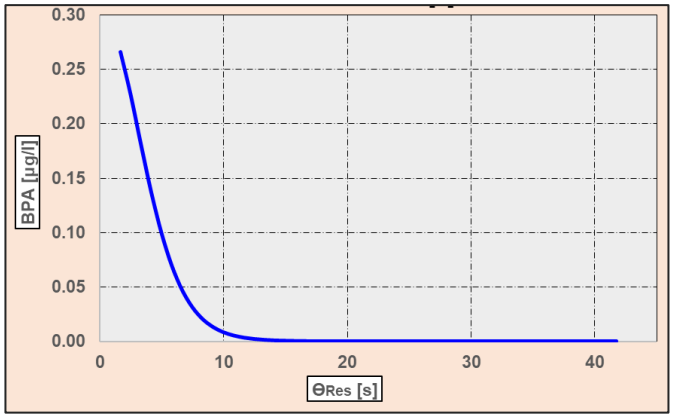

Fig. # 40 ***Bisphenol A (BPA) Profile***

Disinfection

Fig. # 41 shows the temporal profile of the dissolved ozone c_{O3L} [g-O3/m^3] in the TBF. c_{O3Lmax} is equal to 0.54 [g-O_3/m^3] after a reaction elapsed time Θ_{elap} of 13 [s] and the residual ozone c_{O3res} at the end of O3R is 0.12 [g-O_3/m^3]. This value corresponds to an ozone absorption efficiency η_{O3abs} = 97 [%] in O3R. The profile of the true cumulated disinfection CT [g-O_3*min/m^3] is also presented (Fig. # 41). At the output of the O_3R, the value of CT_{max} is 0.38 [g-O3*min/m^3] and the average value CT_{av} is 0.17 [g-O3*min/m^3].

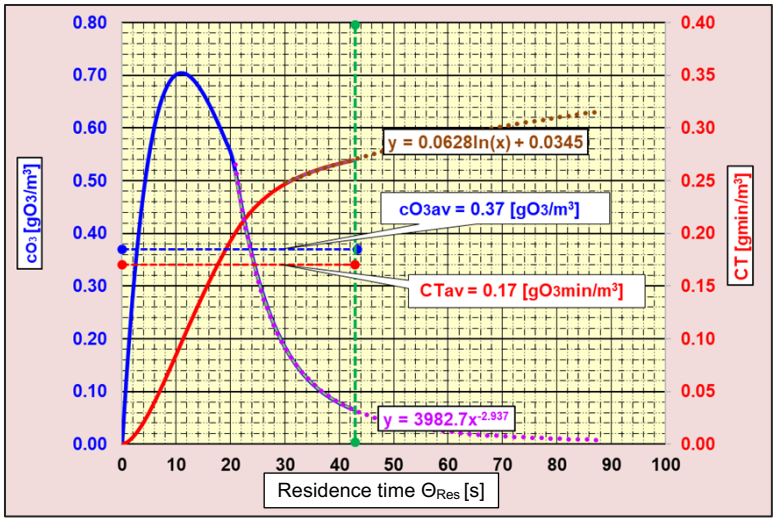

Fig. # 41 ***Residual Ozone Profile & cumulated CT in TBF***

According to Von Sonntag and Von Gunten [52] this value is sufficient for the inactivation of :

- more than 4 $\log_{10}$ for E. Coli;
- more than 4 $\log_{10}$ for Rotavirus;
- at least 3 $\log_{10}$ for G. Lamblia cysts.

The trendlines indicate that the residual ozone c_{O3} [g-O_3/m^3] should disappear after $\Theta_{Res} \approx 120$ [s] due to further consumption by the DOM, improving the disinfection to a CT-value of about 0.45 [g*min/m^3]. Evidently, this CT-value is not sufficient for inactivation of microorganisms protected by spores and oocysts, such as *B. Subtilis* Spores and *C. Parvum* oocysts. The question still revolves around the calculation of these CT-values. Assuming that these values were determined and measured in

homogeneous and turbulent laboratory set-ups and considering Fig. # 28 (see p. 53), we can reasonably consider that these data fit well into the proposed engineering design method. Molecular diffusion D_m [m^2/s] starts to prevail over eddy diffusion for mass D_E [m^2/s] at scales down from the Kolmogorov Size "KS" (distance < 0.13 mm), making the design approach conservative and safe.

Inactivation of the SARS-Covid-2 Virus by ozone in wastewater is of actual importance and is addressed hereafter. A good basis for the current knowledge is in the review by Bayarri et al. [5], which states "that CT = 0.1 - 0.4 g-O_3*min/m^3 may be needed to guarantee an inactivation of SARS-Covid-2 Virus of about 3-4 log_{10} in aerosols. Therefore, ozone, assuming it is acting similarly in wastewater, can be considered as a good candidate for effective SARS-Covid-2 Virus inactivation. What seems to be different with other viruses is that SARS-Covid-2 Virus is surrounded by a lipid envelope and an internal capsid, protecting it against direct action of a disinfectant on its genetic material, similarly to micro-organisms protected by spores or cysts. Its physical structure is similar to that of retroviruses. This fact could explain the large CT-value (0.6 g-O_3*min/m^3) for 99 [%] or 2 log_{10} inactivation in wastewater presented by IOA-EA_3G during the IOA-Webinar Series of July 8th,2021 [6]. Obviously, this value is much larger than the one discussed by Bayarri et al. [5], where no damage to the genome was detected. A lysis, mechanical damage to both the envelope and the capsid, seems to be sufficient for effective inactivation of SARS-Covid-2 Virus, similarly to bacterial inactivation. Based on these data, and using the correlation proposed by Von Sonntag and Von Gunten [52] an inactivation of SARS-Covid-2 Virus of approximately 80 [%] or 2 log_{10} can be expected in our PF-O_3R.

18. Dissolved Oxygen

This essay will lastly discuss dissolved oxygen and its impact on disinfection. To start this section, we provide a description of the oxygen molecule :

> *The O_2-molecule exists in a reduced form but is a rather strong oxidant. It is thermodynamically reactive, but kinetically unreactive. Oxygen and Water serve as opposite ends of a redox scale. The 4-electron oxidation of water to O_2 is reversed by the 4-electron reduction to H_2O. Along this pathway there is a possibility for the generation of the superoxide anion ($°O_2^-$), hydrogen peroxide (HOOH), or hydroxyl radicals (°OH). In biology these intermediates are generally undesirable.* [66]

This chemical process has been identified in pulp bleaching with oxygen, where lignin polymers were depolymerized into monomers if the exposure to O_2 for the delignification is not controlled correctly. The kinetics of the reactions with oxygen are rather fast since radicals are involved. Hence, the significant influence of excessive dissolved O_2 on disinfection cannot be overlooked.

The temporal profile of dissolved oxygen is presented in Fig. # 42, with an end value c_{O_2} of about 17 [g-O_2/m^3]. The initial value of c_{O_2} is approximately 8 [g-O_2/m^3]. The figure reflects the condition where the secondary effluent has a sufficient contact time with atmospheric air and undergoes aeration via discharge over the notched weir of the secondary sedimentation tank. This value is much larger the oxygen concentration prevailing in an aerobe activated sludge reactor for optimum biochemical oxygen demand (BOD) abatement, i.e., $c_{O_2} \approx 2$ [g-O_2/m^3]. There is plenty of information addressing the damage caused by an excessive level of dissolved O_2 to microorganisms. Based on the abovementioned facts, this high dissolved oxygen level will contribute to improve disinfection [67].

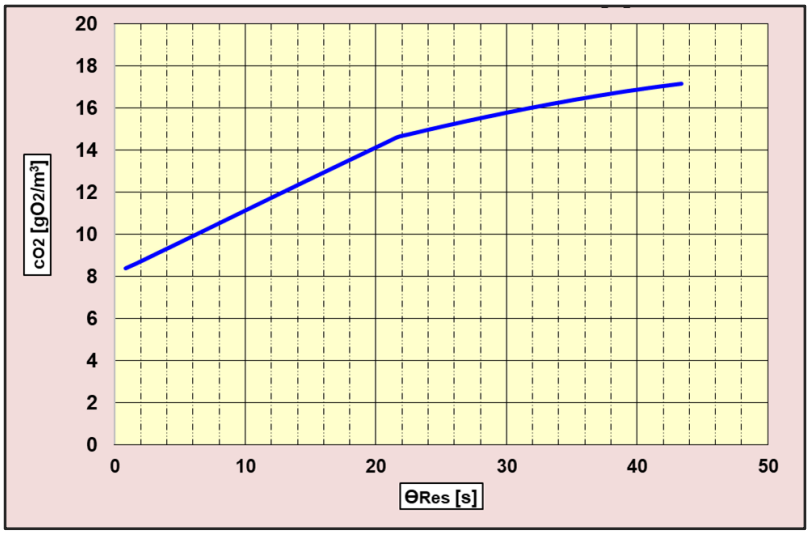

Fig. # 42 ***Residual Dissolved Oxygen***

19. Conclusion

By extensively reviewing established theories and experimental data documented in the literature regarding Fully Turbulent/Turbulent Water Flow (TWF) within geometrically simple systems such as straight pipe flow, researchers have discerned what is termed the "Universal Turbulent Flow Regime." Within this regime, the energy cascade of turbulent energy dissipation exhibits universality, meaning the relationship between "normalized energy" and "normalized eddy wave number" remains constant across all simple systems, i.e. equal. Most O_3Rs will fall in this regime. This observation therefore serves as a foundational principle for the initial stages of a precise engineering design of a T-O_3R.

Further investigation into systems with O_3-Gas bubbling into a PF-T-O_3R makes it possible to generate a homogeneous and isotropic O_3-Gas bubbly flow with simple means such as one or several turbulent gas-liquid bi-flux free jets. Moreover, it allows to propose an acceptable correlation for the determination of Eddy Diffusion D_E [m^2/s]. This fact provides the second basis for a good engineering design for T-O_3R. Moreover and assuming the values of the kinetics of the chemical reactions k" [$M^{-1}s^{-1}$] to be correct, supported by the fact that all pertinent data in the literature are converging, provides the third basis for a sufficiently precise Engineering Design for T-O3R. Summarizing, the proposed Engineering Design Method is applicable for a PF-T-O3R consisting of ozone diffusion chambers "O_3DCs" and Ozone Reaction Chambers "O_3RCs" connected in series.

The above presented facts and ideas support the findings experienced by the authors of much accelerated ozone overall reaction kinetics due to sufficiently full turbulence, homogeneity, and isotropy in a bubby flow in wastewater. Obviously, an ozone diffusion system implemented with a FTBF allows for shorter residence times and therefore smaller reactors with Plug-Flow pattern. Bromate generation, in this example based on actual data, is lower than the required norm of 10 µg/L for potable/drinking water. This fact is also confirmed by the value of the Damköhler Number Da_{II} based on mass transport and chemical reaction rates, which takes the value Da_{II} = 0.007 << 1. In this example, the CT-value is 0.28 [g-O_3*min/m^3] at the end of the O_3R and is thus more than enough for a 3- to 4-log inactivation of *G. Lamblia* cysts, according to Von Sonntag and Von Gunten [52]. However, this CT-value is not sufficient for the appropriate inactivation of the *B. Subtilis* spores and *C. Parvum* oocysts. In this case the O_3-dose must be increased and an additional FT-PF-Reaction Tank must be added downstream in order to guarantee proper disinfection. Adding another reaction tank offers more residence time & volume, which is sized based on the half-lifetime of O_3 prevailing in the water/wastewater.

This technology enables the operation of the ozone system nearly in real-time, offering the capability to efficiently adjust the O_3-Dose c_{DO3} to rapidly fluctuating quality and flow conditions of the Secondary Wastewater (SWW). In real-time DOM characterization of the SWW can be performed with UV-Signals at different wavelengths (220 to 320 [nm]) in order to offer a "Feed Forward Control". Moreover, the Feed Forward Control can be combined with a "Feedback Control" using the O_3-residual c_{O3L} [g-O_3/m^3] in the outlet flow of the ozonation reactor O_3R.

Large cities have sometimes very large Wastewater Treatment Plants WWTP. Some are made of only pre-treatment with sand- and oil-trapping stages and sedimentation with chemical addition, so rejecting

a Primary Wastewater Effluent PWE. Implementing an activated sludge stage with final sedimentation, where residence times can be as large as 24 [h] (low charge activated sludge), would require tremendous space which is mostly not available in dense urban areas. Approaches with pilot plant testing and preliminary projects based on ozone technology as second and final stage have been done with the participation of the authors for a few large cities in the world rejecting PWW and which do not have the space available for extension with activated sludge and final sedimentation. Such an ozonated PWW effluent presents the following characteristics:

- DOM quality transformation;
- DOM with Chemical Oxygen Demand (COD) resistant to biodegradation partly transformed into Biochemical Oxygen Demand (BOD), i.e., enrichment with DOM as food for the fauna;
- DOM with COD that is toxic to the fauna and flora of the receiving water body almost made inert;
- Disinfection;
- enriching the receiving body with oxygen since such ozone plants necessarily will operate with oxygen as Ozone Carrier Gas O_3CG.

One large City in North America is currently building such an ozone system.

20. Physical parameters, letters, symbols, units

Physical Parameters

a [m^2/m^3]	Specific Diffusion Area at the Gas-Liquid Interface
A [m^2]	Pipe Cross Area
c* [g/m^3]	Concentration of the Reactant Gas in the Liquid Phase in equilibrium with its concentration in the gas phase, in accordance with Henry's Law
c° [g/m^3]	Concentration of the Reactant Gas in the Liquid Phase
c_{alk} [mM HCO_3^-/CO_3^{2-}]	Alkalinity
c_{DO3} [g-O_3/m^3]	Ozone Dose
c_{BPA} [g/m^3]	Bisphenol A Concentration in wastewater
c_{Br-} [g/m^3]	Bromide Concentration in wastewater
c_{DOC} [g/m^3]	Dissolved Organic Carbon Concentration in wastewater
c_{O3G} [wt%]	Ozone Concentration in Carrier Gas
c_{O3L} [g-O_3/m^3]	Ozone Concentration in the water/wastewater
c_{O2L} [g-O_2/m^3]	Oxygen Concentration in the water/wastewater
c_D [-]	Bubble Drag Coefficient
c_Θ [g/m^3]	Variable Micropollutant Concentration over time
CT [g*min/m^3]	Ozone Exposure of Microorganisms for inactivation
d_{BB} [mm]	Distance between Bubbles in a homogeneous bubble column
d_C [m] or [mm]	System Confinement Distance
d_{Diff} [m]	Average Distance for Diffusion
Da_{II} [-]	Damköhler Number = Ratio of Chemical Reaction Rate to Mass Transfer Rate
D_B [m^2/s]	Bubble Dispersion Rate
D_E [m^2/s]	Eddy Diffusivity Coefficient for Mass
D_{Eav} [m^2/s]	Average Eddy Diffusivity Coefficient for Mass inside TBF
D_{EM} [m^2/s]	Eddy Diffusivity Coefficient for Momentum
D_m [m^2/s]	Molecular Diffusion Coefficient for Mass
D_{O3} [g-O_3/m^3]	Ozone Demand for the task to be achieved
e [mm]	Pipe Wall Roughness
E_κ [m^2/s^2]	Per Mass specific Turbulent Kinetic Energy of Eddy with Wavenumber *K*
$E_\kappa(\kappa)$ [m^3/s^2]	Per Wavenumber & Mass specific Turbulent Kinetic Energy of Eddy E(*K*)
$E_\kappa(\kappa)N$ [-]	Normalized Energy Spectrum
f [-]	Darcy Friction Factor
f_{ITR} [-]	TKE correcting factor for Integral Range

f_{TLR} [-]	TKE correcting factor for Taylor Range
g [m/s^2]	Gravitation
$h_{CSTR/PFR}$ [m]	Height of a Completely Stirred Tank Reactor and Plug-Flow Reactor
h_w [m]	Reactor Wetted Height
He_{O3} [Pa]	Ozone Henry Constant
He_{O2} [Pa]	Oxygen Henry Constant
k [m^2/s^2]	Turbulent Kinetic Energy TKE
k' [s^{-1}]	First Order Chemical Reaction Rate Constant
k'' [M^{-1} s^{-1}]	Second Order Chemical Reaction Rate Constant
k_{mt} [m/s]	Mass Transfer Coefficient
k_{mtE} [m/s]	Eddy Mass Transfer coefficient, Danckwerts Surface Renewal Mode
$k_{D/R}$ [s^{-1}]	Diffusion or Reaction Rate
k_{PERF} [-]	Reactor/Sector Kinetic Performance Factor
κ [m^{-1}]	Eddy Wave Number
κ_N [-]	Normalized Eddy Wavenumber
l_0 [m]	Largest Eddy in the Integral Range
l_{BS} [m]	Batchelor Length Scale
$l_{E\kappa}$ [m]	Eddy Wavelength
L_c [m]	Characteristic Length
L_{O3R} [m]	O_3R Diffusion Length
M [kg]	Mass of fluid inside the conduit
$M°_{O3}$ [kg-O_3/s]	Ozone Production Rate
$M°_{O3G}$ [kg-O_3/s]	Ozone Gas Production Rate
#B [-]	Number of Bubbles in bubble column
p [Pa]	Gauge Pressure or relative Pressure
$p_D(\Phi_B)$ [Pa]	Bubble Surface-deforming Stress
$p_\sigma(\Phi_B)$ [Pa]	Bubble Surface-reforming Stress
P [Pa]	Absolute Pressure = p + P_{amb}
P_{amb} [Pa]	Ambiant Pressure
P_{FJ} [m^2/s^3]	Production of Turbulent Kinetic Energy in Free jet
$R°$ [mole/m^2*s] or [g/m^2*s]	Mass Transfer Rate from the Gas Phase/Absorption Rate by the water/wastewater phase of the reactant
R_{CT} [-]	Ratio of Exposures to O_3 and °OH
Re_L [-]	Reynold Number of axial mean flow of water or wastewater
Re_B [-]	Reynold Number of the Bubble rising with its slip velocity in laminar/quiet water flow

r [mm]	Distance from the surface of the Bubble
s [s^{-1}]	Danckwers Model Surface Renewal Rate
S_B [m^2]	Surface of Bubble
S_{O3R} [m^2]	O_3R Cross-Section
t [°C]	Temperature
T [K]	Absolute Temperature
T_L [K]	Absolute Temperature of wastewater
T_{O3G} [K]	Absolute Temperature of Ozone Gas
T_P [K]	Absolute Temperature of Process
$u°_{E(\kappa)}$ [m/s]	Eddy Orbital Velocity
$u°_T$ [m/s]	Characteristic Turbulent Velocity Scale
v° [m/s]	Superficial Velocity = V°/A
$v°_L$ [m/s]	Wastewater or Water Superficial Velocity
$v°_G$ [m/s]	Ozone Gas Superficial Velocity
$v°_B^{\infty}$ [m/s]	Bubble terminal ascending Velocity, Slip Velocity
V_{O3R} [m^3]	O_3R Diffusion Volume
V° [m^3/s]	Fluid Volumetric Flowrate
V_B [m^3]	Volume of Bubble
$V°_{DW}$ [m^3/s]	Ozone Carrier Gas Driving Water Flow
$V°_L$ [m^3/s]	Wastewater Flow
$V°_{LD}$ [m^3/s]	Design Wastewater Flow
$V°_{O3G}$ [m^3/s]	Ozone Gas Volumetric Flow at operating Temperature T & Pressure P

Greek Symbols

α_{Gdyn} [%]	Dynamic Gas Hold-up in the bubble column
α_{WW} [-]	Correction Factor for Oxygen Mass Transfer in wastewater
β_{WW} [-]	Correction Factor for Oxygen Solubility in wastewater
δ [m]	Thickness of the Wall Layer, Buffer, Log & outer
Δp [Pa]	Wall Friction Head Loss
$\Delta\Phi_E$ [m] or [mm]	Eddy Diameter Increments for Design
ε [m^2/s^3]/[J/s*kg]	Mass Specific Turbulent Energy Dissipation Rate
ε_{BB} [m^2/s^3]/[J/s*kg]	Specific Energy Dissipation Rate of Turbulence needed for binary Bubble Breakage

ε_{BC} [m^2/s^3]/[J/s*kg]	Specific Energy Dissipation Rate of Turbulence acting inside a Homogeneous & Isotropic Bubble Column inside a Fully Turbulent water or wastewater flow
ε_{crit} [m^2/s^3]	Critical specific Energy Dissipation Rate of Turbulence where Bubble Surface Deformation starts
ε_{FJ} [m^2/s^3]/[J/s*kg]	Specific Energy Dissipation Rate of Turbulence acting inside a Free Jet
ε_{HI} [m^2/s^3]/[J/s*kg]	Specific Energy Dissipation Rate of Turbulence inside a Hydro-Injector
η [m]	Kolmogorov Scale
η_{O3abs} [%]	Ozone Absorption Efficiency in O_3R
Θ [s]	Time
Θ_{elap} [s]	Elapsed Time
Θ_{BB} [ms]	Bubble Breakage Time (binary splitting)
Θ_{Res} [s]	Hydraulic Residence Time
$\Theta_{ResCSTR}$ [s]	Flow Residence Time in a PFR/CSTR
λ [m]	Taylor Scale
λ_f [-]	Darcy Friction Factor
μ [kg/m*s]	Actual Fluid Viscosity (under existing pressure and temperature) = v * ρ
v [m^2/s]	Actual Fluid Kinematic Viscosity (under existing pressure and temperature)
v_E [m^2/s]	Eddy Viscosity (under the hydrodynamic conditions of the water flow)
v_L [m^2/s]	Kinematic Viscosity of water/wastewater
ρ [kg/m^3]	Actual Fluid Density (under existing pressure and temperature)
σ_L [N/m] or [kg/s^2]	Surface Tension of Water (under existing pressure and temperature)
σ_G [mm]	Standard Deviation of a Gaussian Probability Distribution of Φ_B [mm]
σ_{PDF} [-]	Standard Deviation of a Probability Distribution
φ_{FJ} [°]	Free Jet Angle
$\tau_{E\kappa}$ [s]	Time Scale related to a single Eddy with Wavenumber κ
$\tau_{TE\kappa}$ [s]	Eddy Turnaround Time with Wavenumber κ
$\tau_{DE\kappa}$ [s]	Eddy Decay Time with Wavenumber κ
Φ_B [m] or [mm]	Bubble Diameter
Φ_{B32} [m] or [mm]	Average bubble Sauter Diameter
Φ_{Bcrit} [mm]	Critical Bubble Diameter before Splitting can start
Φ_E [m] or [mm]	Eddy Diameter
Φ_{Eav} [m] or [mm]	Average Eddy diameter in the Liquid Bulk between the Bubbles of the TBF
Φ_{EDiff} [m] or [mm]	Eddy Diameter for Diffusion
Φ_{Emax} [m] or [mm]	Largest Eddy Diameter

Φ_{Emin} [m] or [mm]	Smallest Eddy Diameter, equal to the Kolmogorov Scale “KS”
Φ_{Pk} [m]	Scalar Patch Size
Φ_{hyd} [m] or [mm]	Hydraulic Diameter, square/cylindrical reactor
Φ_{FJ} [m]	Free Jet Diameter
Φ_{O3R} [m] or [mm]	Ozone Reactor Diameter
Φ_{P} [m] or [mm]	Pipe/Conduit (hydraulic) Diameter
ξ_B [-]	Gas Bubble Friction Coefficient in water/wastewater
$\sum$CSTR [-]	Number of CSTRs connected in series
Ω [s^{-2}]	Enstrophy

Lower Case Letters

abs	Absolute Value of Parameter
act	Actual
av	Average
B	Bubble
C	Turbulent energy Cascade
D	Deformation
D	Decay
Ds	Design
E	Eddy
G	Gas
h	Hydraulic
i	Initial
Int	Gas-Liquid Interface (at the bubble surface)
κ	Eddy Wavenumber
σ	Bubble Surface-restoring Surface Tension
L	Liquid/Water
m	Molecular
max	Maximum value
min	Minimum value
O_3	Ozone
res	Residual
S	Surface

T	Turbulent
0	Integral Scale
w	Bubble Wake

Abbreviations / Lower Case

BB	Bubble Breakage
BC	Bubble Column
BF	Bubbly Flow
BPA	Bisphenol A
BS	Batchelor Scale
BSE	Bubble Surface Energy
BOD	Biochemical Oxygen Demand
COD	Chemical Oxygen Demand
CRR	Chemical Reaction Rate
CSTR	Completely Stirred Tank Reactor
CC	Co-Current, gas and water flows in the same direction (up-flow or down-flow)
CS	Conduit Surface
CtC	Counter-Current, Gas Flow upwards, Water Flow Downwards
O_3D	Ozone Diffusion
DF	Water/wastewater Down-Flow Mode
DK	Diffusion Kinetics
DMTR	Diffusive Mass Transfer Rate
DO	Dissolved Oxygen
DO_3	Dissolved Ozone, i.e., ozone residual
2-D	2-Dimensional
3-D	3-Dimensional
DOC	Dissolved Organic Carbon
DOM	Dissolved Organic Matter
DOM_{sww}	Standard DOM Quality for Secondary/Tertiary Wastewater
DWF	Driving Water Flow
ED	Eddy Diffusion
EL	Entrance Length
FJ	Free-Jet

FM	Fully Mixed
FT	Fully Turbulent or Full Turbulence and Forced Turbulence
FTBF	Fully Turbulent Bubbly Flow
FTWF	Fully Turbulent Water Flow
GDF	Normal/Gaussian Distribution Function
GLIA	Gas-Liquid Interface Area
HHP	Hydraulic and Hydrodynamic Pattern
HI	Hydro-Injector
HIT	Homogeneous & Isotropic Turbulent/Turbulence
HLGR	Head Loss Generation Rate
HTBC	Homogeneous Turbulent Bubble Column
INR	Inertial Range
IUR	Isotropic Universal Range
ITR	Integral Range
KE	Mean Flow Kinetic Energy
KED	Kinetic Energy Dissipation
KS	Kolmogorov Scale
L	Laminar
MPs	Micro-pollutants
N	STP, Standard Conditions, i.e., T = 273.15 [K], P = 101.3 [kPa]
NT	Natural Turbulence
OH°	OH-Radical
O_3	Ozone Molecule
O_3G	Ozone Generator or Ozone Gas off the Ozone Generator
O_3CG	Ozone Carrier Gas
O_3CWF	Ozone Gas Carrier Water Flow
O_3R	Ozonation Reactor
O_3DC	Ozone Diffusion Chamber
O_3RC	Ozone Reaction Chamber
O_3RK	Ozone Reaction Kinetic
PCPs	Personal Care Products
PDF	Probability Distribution Function
PEC	Photosynthetic Enzymatic Complexes

PERF	Reactor Performance
PF	Plug-Flow or Piston
PFR	Plug-Flow Reactor
PUE	Population Equivalent Unit
PWE	Typical Primary Mixed Municipal-Industrial Wastewater Effluent
Re	Reynold Number
RANS	Reynold Averaged Navier-Stokes
RMS	Root Mean Square
RTD	Residence Time Distribution
Sc	Schmidt Number
Sh	Sherwood Number
SWW	Typical Secondary/Tertiary Mixed Municipal-Industrial Wastewater Effluent
T	Turbulent
TBF	Turbulent Bubbly Flow
TDD	Turbulent Dispersion Diffusion
TEC	Turbulent Energy Cascade
TEDR	Turbulent Energy Dissipation Rate
THI	Turbulent Kinetic Energy
TI	Turbulence Intensity
TKE	Turbulent Kinetic Energy
TKED	Turbulent Kinetic Energy Dissipation
TKE_w	TKE generated in the Wake of the Bubbles in a TBF
TLR	Taylor Range
TOC	Total Organic Carbon
TP	Operation Absollute Temperature and Pressure
TWF	Turbulent Water Flow
UP	Water/wastewater Up-Flow Mode
VOD	Vent Ozone Destructor
W	Water
We	Weber Number
WC	Water Column
WF	Water Flow to be ozonated
WW	Wastewater

Dimensionless Numbers of Interest

Fr	Bubble Froude Number, $Fr = v°_B{\infty}^2/g/\Phi_B$
Mo	Bubble Morton Number, $Mo = We^3/Fr*Re^4$, it characterizes the shape of the bubbles in the bubble column
Re	Reynold Number, $Re = v°\rho\Phi/\mu$, ratio of inertial to viscous forces
Re_B	Bubble Reynold Number, $Re = v°_B{\infty}\rho\Phi_B/\mu$
Sc	Schmidt Number, $Sc = v/D_m$, ratio of momentum to mass transfer
Sh	Sherwood Number, $Sh = k_{mt}Lc/D_m$, function of (Re, Sc), ratio of actual eddy to molecular diffusivity
We	Bubble Weber Number, $We = v°_B{\infty}^2\Phi_B\rho/\sigma$, ratio of inertial to surface forces

21. Bibliography

1. Gesuale G, Bellemare F, Liechti P-A, Fournier M, Payment P, Gagnon C, et al. (2010) Ozone: A Wastewater Disinfectant of the Future. Proceedings of the Water Environment Federation. 2010:4749-59.
2. Gaudy AF, Gaudy ET. (1980) Microbiology for environmental scientists and engineers. New York: McGraw-Hill.
3. Lazarova V, Liechti P-A, Savoye P, Hausler R. (2013) Ozone disinfection: Main parameters for process design in wastewater treatment and reuse. Journal of Water Reuse and Desalination. 3:337.
4. Kudela H. (2010) Turbulent flow. URL: http://www.itcmp.pwr.wroc.pl/~znmp/dydaktyka/fundam_FM
5. Bayarri B, Cruz-Alcalde A, López-Vinent N, Micó MM, Sans C. (2021) Can ozone inactivate SARS-CoV-2? A review of mechanisms and performance on viruses. J Hazard Mater.415:125658.
6. Martins RB, Castro IA, Pontelli M, Souza JP, Lima TM, Melo SR, et al. (2021) SARS-CoV-2 Inactivation by Ozonated Water: A Preliminary Alternative for Environmental Disinfection. Ozone: Science & Engineering.43(2):108-11.
7. Danckwerts PV. Gas-liquid reactions. New York: McGraw-Hill Book Co; 1970. Available from http://books.google.com/books?id=upxTAAAAMAAJ.
8. Soltermann F, Abegglen C, Tschui M, Stahel S, Von Gunten U. (2017) Options and limitations for bromate control during ozonation of wastewater. Water research.116:76-85.
9. Laufer J. The structure of turbulence in fully developed pipe flow. 1954.
10. Batchelor GK. (1953) The theory of homogeneous turbulence: Cambridge university press.
11. Hellström L, Zlatinov M, Cao G, Smits A. (2011) Turbulent pipe flow through a 90° bend.
12. Johnstone RE, Thring MW. (1957) Pilot plants, models, and scale-up methods in chemical engineering. New York: McGraw-Hill.
13. Buffle M-o. (2005) Mechanistic investigation of the initial phase of ozone decomposition in drinking water and wastewater. Diss ETH(16266).
14. Grassmann P. (1970) Physikalische Grundlagen der Verfahrenstechnik. Swiss Federal Institute of Zurich, Verlag Sauerländer Aarau und Frankfurt am Main.
15. Pope SB. (2001) Turbulent flows. Measurement Science and Technology.12(11):2020-1.
16. Tavoularis S, Saleh JM. Turbulent Flows, Chapter 31. Fluid Flow Handbook. New York: McGraw-Hill; 2002.
17. Fox RW, McDonald AT, Mitchell JW. (2020) Fox and McDonald's introduction to fluid mechanics. 10th edition / EMEA edition ed. Hoboken, NJ: Wiley.
18. Hinze J. (1959) Turbulence, an introduction to its mechanism and theory: McGraw-Hill Book Company Inc., New York. 586 p.
19. Mattioli F. Principles of Fluid Dynamics. Chapter 25 - The Reynolds Experiment. Department of Physics, University of Bologna 2013.
20. Hunt J, Morrison J. (2000) Eddy structure in turbulent boundary layers. European Journal of Mechanics - B/Fluids. 19:673–94.
21. Bakker A. (2002) Lecture 9 - Kolmogorov's theory applied computational fluid dynamics. Educational material Fluent Inc.
22. Roberts PJ, Webster DR. (2002) Turbulent diffusion. ASCE Press, Reston, Virginia; p. 7-47.
23. Cushman-Roisin B. Turbulent dispersion. The Mathematics of Marine Modelling: Water, Solute and Particle Dynamics in Estuaries and Shallow Seas: Springer; 2022. p. 167-196.
24. Bedrossian J, Blumenthal A, Punshon-Smith S. (2021) Almost-sure enhanced dissipation and uniform-in-diffusivity exponential mixing for advection–diffusion by stochastic Navier–Stokes. Probability Theory and Related Fields.179(3):777-834.

25. Bedrossian J, Blumenthal A, Punshon-Smith S. (2022) The Batchelor spectrum of passive scalar turbulence in stochastic fluid mechanics at fixed Reynolds number. Communications on Pure and Applied Mathematics.75(6):1237-91.
26. McDonough JM. (2007) Introductory lectures on turbulence: physics, mathematics and modeling.
27. Trettel B. (2018) Estimating turbulent kinetic energy and dissipation with internal flow loss coefficients.
28. Martínez-Bazán C, Montañés JL, Lasheras JC. (1999) On the breakup of an air bubble injected into a fully developed turbulent flow. Part 1. Breakup frequency. Journal of Fluid Mechanics.401:157-82.
29. Martinez C. (1998) Splitting and dispersion of bubbles by turbulence [Ph.D.]. United States -- California: University of California, San Diego.
30. Martínez-Bazán C, Montañés JL, Lasheras JC. (1999) On the breakup of an air bubble injected into a fully developed turbulent flow. Part 2. Size PDF of the resulting daughter bubbles. Journal of Fluid Mechanics.401:183-207.
31. Beckwith WF. (1963) Determination of turbulent thermal diffusivities for flow of liquids in pipes: Iowa State University.
32. Kamp A, Chesters A, Colin C, Fabre J. (2001) Bubble coalescence in turbulent flows: A mechanistic model for turbulence-induced coalescence applied to microgravity bubbly pipe flow. International Journal of Multiphase Flow.27(8):1363-96.
33. Morrison CM, Hogard S, Pearce R, Mohan A, Pisarenko AN, Dickenson ER, et al. (2023) Critical review on bromate formation during ozonation and control options for its minimization. Environmental Science & Technology.57(47):18393-409.
34. Eck B. (2013) Technische Strömungslehre: Springer-Verlag.
35. Luo J. (2004) Bubble dispersion and coalescence in turbulent pipe flow: Ph. D. Thesis, Dalhousie University, 2002.
36. Alexiadis A. (2007) Bubble dispersion patterns in bubbly-flow released from a porous plug into a gas-stirred ladle. Applied mathematical modelling.31(8):1534-47.
37. Shih T-H, Liou WW, Shabbir A, Yang Z, Zhu J. (1995) A new k-ϵ eddy viscosity model for high reynolds number turbulent flows. Computers & fluids.24(3):227-38.
38. Pellacani F. (2012) Development and validation of bubble breakup and coalescence constitutive models for the one-group interfacial area transport equation: Technische Universität München.
39. Nguyen C, Gonnermann H, Chen Y, Huber C, Maiorano A, Gouldstone A, et al. (2013) Film drainage and the lifetime of bubbles. Geochemistry, Geophysics, Geosystems.14(9):3616-31.
40. Glaeser H, Brauer H. (1977) Berechnung des impuls-und stofftransports durch die grenzflaeche einer formveraenderlichen blase.
41. Risso F. (2018) Agitation, mixing, and transfers induced by bubbles. Annual Review of Fluid Mechanics.50:25-48.
42. Pepper DW. (1970) Turbulent structure in the wake of sphere.
43. de Vries AWG. (2002) Path and wake of a rising bubble.
44. Cussler EL. (2009) Diffusion: mass transfer in fluid systems: Cambridge university press.
45. Sherwood TK, Pigford RL, Wilke CR. (1975) Mass transfer: McGraw-Hill New York.
46. Treybal RE. (1980) Mass transfer operations. New York.466:493-7.
47. Levenspiel O. (1998) Chemical reaction engineering: John wiley & sons.
48. Kraume M. (2004) Transportvorgänge in der Verfahrenstechnik: Springer.
49. Henkel J. (2010) Oxygen transfer phenomena in activated sludge: TU Darmstadt.
50. Elovitz MS, von Gunten U. (1999) Hydroxyl Radical/Ozone Ratios During Ozonation Processes. I. The Rct Concept. Ozone: Science & Engineering.21(3):239-60.
51. Elovitz MS, von Gunten U, Kaiser H-P. (2000) Hydroxyl Radical/Ozone Ratios During Ozonation Processes. II. The Effect of Temperature, pH, Alkalinity, and DOM Properties. Ozone: Science & Engineering. 22(2):123-50.

52. Von Sonntag C, Von Gunten U. (2012) Chemistry of ozone in water and wastewater treatment: IWA publishing.
53. Maizel AC, Remucal CK. (2017) The effect of advanced secondary municipal wastewater treatment on the molecular composition of dissolved organic matter. Water Res.122:42-52.
54. Hoigné J. (1998) Chemistry of aqueous ozone and transformation of pollutants by ozonation and advanced oxidation processes. Quality and treatment of drinking water II:83-141.
55. Aste T. (2005) Variations around disordered close packing. Journal of Physics: Condensed Matter.17(24):S2361.
56. Burtseva L, Werner F. (2015) Modeling of spherical particle packing structures using mathematical tessellation: Otto-von-Guericke-Universität, Fakultät für Mathematik.
57. Nöthe T, Fahlenkamp H, Sonntag Cv. (2009) Ozonation of wastewater: rate of ozone consumption and hydroxyl radical yield. Environmental Science & Technology.43(15):5990-5.
58. Wang M, Chen Y. (2018) Generation and characterization of DOM in wastewater treatment processes. Chemosphere.201:96-109.
59. Metcalf L, Eddy HP, Tchobanoglous G. (1991) Wastewater engineering: treatment, disposal, and reuse: McGraw-Hill New York.
60. Schaar HP. (2016) Ozonung von Kläranlagenablauf zur weitergehenden Abwasserreinigung: Technische Universität Wien.
61. Rakness KL. (2015) Ozone in Drinking Water Treatment: Process Design, Operation, and Optimization, Softcover Edition: American Water Works Association.
62. World Health Organization. (2022) Guidelines for drinking-water quality: incorporating the first and second addenda: World Health Organization.
63. Gottschalk C, Libra JA, Saupe A. Ozonation of water and waste water : a practical guide to understanding ozone and its applications. Weinheim, Chichester: Wiley-VCH ; John Wiley; 2010. Available from https://onlinelibrary.wiley.com/doi/book/10.1002/9783527628926.
64. Flanagan E. (2021) Ozone in water purification and bromate formation. Water Online.19.
65. Soltermann F, Abegglen C, Gotz C, Von Gunten U. (2016) Bromide sources and loads in Swiss surface waters and their relevance for bromate formation during wastewater ozonation. Environmental science & technology.50(18):9825-34.
66. Oxygen Reactivity 2010 [Available from: http://www.rsbs.anu.edu.au/O2/O2_1_Redox.htm.
67. Baez A, Shiloach J. (2014) Effect of elevated oxygen concentration on bacteria, yeasts, and cells propagated for production of biological compounds. Microbial cell factories.13:1-7.

22. List of additional references

Papers

1. Alexiadis A, Gardin P, Domgin JF. (2004) Spot turbulence, breakup, and coalescence of bubbles released from a porous plug injector into a gas-stirred ladle. Metallurgical and Materials Transactions B.35:949-56.
2. Bailey SC, Hultmark M, Schumacher J, Yakhot V, Smits AJ. (2009) Measurement of local dissipation scales in turbulent pipe flow. Physical review letters.103(1):014502.
3. Buehlmann PH. (2019) Balancing Bromate Formation, Organics Oxidation, and Pathogen Inactivation: The Impact of Bromate Suppression Techniques on Ozonation System Performance in Reuse Waters: Virginia Tech.
4. Chahed J, Colin C, Masbernat L. (2002) Turbulence and phase distribution in bubbly pipe flow under microgravity condition. J Fluids Eng.124(4):951-6.
5. Chen P. (2004) Modeling the fluid dynamics of bubble column flows: Washington University in St. Louis.
6. Colin C, Fabre J, Kamp A. (2012) Turbulent bubbly flow in pipe under gravity and microgravity conditions. Journal of Fluid Mechanics.711:469-515.
7. Dani A. (2007) Transfert de masse entre une bulle et un liquide : simulations numériques directes et fluorescence induite par nappe laser
8. Dani A, Guiraud P, Cockx A. (2007) Local measurement of oxygen transfer around a single bubble by planar laser-induced fluorescence. Chemical Engineering Science.62(24):7245-52.
9. Grodzinsky AJ. (2011) Fields, forces, and flows in biological systems: Garland Science.
10. Hondzo M, Al-Homoud A. (2007) Model development and verification for mass transport to Escherichia coli cells in a turbulent flow. Water resources research.43(8).
11. Khare M. (2016) Reactivity of hydroxyl radical: mechanistic insight into the reactivity with dissolved organic matter: Michigan Technological University.
12. Li W-T, Majewsky M, Abbt-Braun G, Horn H, Jin J, Li Q, et al. (2016) Application of portable online LED UV fluorescence sensor to predict the degradation of dissolved organic matter and trace organic contaminants during ozonation. Water Research.101:262-71.
13. Mazzotti M. (2015) Introduction to chemical engineering: chemical reaction engineering. ETH Swiss Federal Institute of Technology Zurich Separation Processes Laboratory, Zurich.
14. Murakawa H, Kikura H, Aritomi M. (2003) Measurement of liquid turbulent structure in bubbly flow at low void fraction using ultrasonic Doppler method. Journal of nuclear science and technology.40(9):644-54.
15. Peller JR, Mezyk SP, Cooper WJ. (2009) Bisphenol A reactions with hydroxyl radicals: diverse pathways determined between deionized water and tertiary treated wastewater solutions. Research on Chemical Intermediates.35:21-34.
16. Roudet M. (2008) Hydrodynamique et transfert de masse autour d'une bulle confinée entre deux plaques
17. Roudet M, Billet AM, Cazin S, Risso F, Roig V. (2017) Experimental investigation of interfacial mass transfer mechanisms for a confined high-reynolds-number bubble rising in a thin gap. AIChE Journal.63(6):2394-408.
18. Samstag M. (1996) Experimentelle Untersuchungen von Transportphänomenen in vertikalen turbulenten Luft-Wasser- Blasenströmungen. EUR(Luxembourg).
19. Schlünder E. (1977) On the mechanism of mass transfer in heterogeneous systems—in particular in fixed beds, fluidized beds and on bubble trays. Chemical Engineering Science.32(8):845-51.
20. Stöhr M, Schanze J, Khalili A. (2009) Visualization of gas–liquid mass transfer and wake structure of rising bubbles using pH-sensitive PLIF. Experiments in fluids.47:135-43.
21. Tyagi H, Liu R, Ting DS-K, Johnston CR. (2006) Measurement of wake properties of a sphere in freestream turbulence. Experimental thermal and fluid science.30(6):587-604.
22. Van Den Berg TH, Luther S, Mazzitelli IM, Rensen JM, Toschi F, Lohse D. (2006) Turbulent bubbly flow. Journal of Turbulence(7):N14.

Books

1. Acworth IN. (2003) The handbook of redox biochemistry.
2. APHA. (2017) Standard methods for the examination of water and wastewater. 23 ed: American Public Health Association, Washington, DC.
3. Batchelor GK. (1967) An Introduction to Fluid Dynamics: Cambridge University Press.
4. Daniels F, Alberty RA. (1975) Physical Chemistry: Wiley.
5. Degrémont. (1979) Water treatment handbook: John Wiley & Sons.
6. Fan LS, Tsuchiya K, Brenner H. (2013) Bubble Wake Dynamics in Liquids and Liquid-Solid Suspensions: Elsevier Science.
7. Henkel J. (2010) Oxygen transfer phenomena in activated sludge: TU Darmstadt.
8. Lide DR. (2004) CRC handbook of chemistry and physics: CRC press.
9. Mahan BH. (1975) University Chemistry: Addison-Wesley Publishing Company.
10. Metcalf L, Eddy HP, Tchobanoglous G. (1991) Wastewater engineering: treatment, disposal, and reuse: McGraw-Hill New York.
11. Montgomery JM. (1985) Consulting Engineers, Inc. Water Treatment Principles and Design:0.2-0.4.
12. Sawyer CN, McCarty PL, Parkin GF. (2003) Chemistry for Environmental Engineering and Science: McGraw-Hill Education.
13. Treatment OIW.) Application And Engineering AWWA Research Foundation, 1991. Lewis Publishers; p.
14. US EPA. (1999) Disinfection Profiling and Benchmarking Guidance Manual. Water Oo, editor: United States Environmental Protection Agency, Office of Water.
15. Weber WJ. (1972) Physicochemical processes for water quality control.
16. Wolf C. Inactivation of waterborne viruses by ozone: Kinetics and mechanisms. EPFL; 2019.